Distribution Agreement

In presenting this thesis or dissertation as a partial fulfillment of the requirements for an advanced degree from Emory University, I hereby grant to Emory University and its agents the non-exclusive license to archive, make accessible, and display my thesis or dissertation in whole or in part in all forms of media, now or hereafter known, including display on the world wide web. I understand that I may select some access restrictions as part of the online submission of this thesis or dissertation. I retain all ownership rights to the copyright of the thesis or dissertation. I also retain the right to use in future works (such as articles or books) all or part of this thesis or dissertation.

Signature:

Su Yang	Date

Age-dependent, region-specific mechanisms contribute to

Spinocerebellar Ataxia 17 pathogenesis

By

Su Yang
Doctor of Philosophy

Graduate Division of Biological and Biomedical Sciences
Biochemistry Cell and Developmental Biology

_____
Xiao-Jiang Li, M.D., Ph.D.
Advisor

_____
Gary J. Bassell, Ph.D.
Committee Member

_____
Anita H. Corbett, Ph.D.
Committee Member

_____
Yue Feng, Ph.D.
Committee Member

_____
Stephen R. Price, Ph.D.
Committee Member

Accepted:

_____
Lisa A. Tedesco, Ph.D.
Dean of the James T. Laney School of Graduate Studies

_____
Date

Age-dependent, region-specific mechanisms contribute to

Spinocerebellar Ataxia 17 pathogenesis

By

Su Yang
B.S., Nanjing University, 2008

Advisor: Xiao-Jiang Li, M.D., Ph.D.

An abstract of
A dissertation submitted to the Faculty of the
James T. Laney School of Graduate Studies of Emory University
in partial fulfillment of the requirements for the degree of
Doctor of Philosophy in
Graduate Division of Biological and Biomedical Sciences
Biochemistry Cell and Developmental Biology
2014

Abstract

Age-dependent, region-specific mechanisms contribute to

Spinocerebellar Ataxia 17 pathogenesis

By Su Yang

Spinocerebellar Ataxia 17 (SCA17), caused by an expansion of polyglutamine (polyQ) tract (> 42 repeats) in the N-terminus of TATA-box binding protein (TBP), belongs to a family of polyQ expansion-mediated neurodegenerative diseases. SCA17 is characterized by specific neurodegeneration in the cerebellum, despite the fact that mutant TBP is globally expressed. Aging is believed to be the primary risk factor for SCA17 and other polyQ expansion diseases, as symptoms associated with such diseases predominantly manifest during middle or late stages of life. However, how aging contributes to neurodegeneration remains unclear. To investigate aging-related molecular alterations and their involvement in SCA17 pathogenesis, we established SCA17 knock-in (KI) mice that inducibly express one copy of mutant TBP at different ages by tamoxifen-mediated Cre recombination. We find that mutant TBP, when expressed in aged mice, leads to accelerated onset of neurodegeneration and neurological symptoms, compared with young mice. Furthermore, the level of accumulated mutant TBP is higher in older SCA17 inducible KI mouse brains than younger ones, and correlates with age-related decline in chaperone activity. Mutant TBP reduces the expression of mesencephalic astrocyte derived neurotrophic factor (MANF), a protein that is enriched in the Purkinje cell layer of the cerebellum. Overexpression of MANF ameliorates mutant TBP-mediated toxicity both *in vitro* and *in vivo*. Lastly, we provided evidence that MANF increases protein kinase C (PKC) phosphorylation, which could underlie the neuroprotective effect. Taken together, these findings suggest that the age-related decline in chaperone activity affects polyQ protein functioning that is important for the viability of specific types of neurons.

Age-dependent, region-specific mechanisms contribute to

Spinocerebellar Ataxia 17 pathogenesis

By

Su Yang
B.S., Nanjing University, 2008

Advisor: Xiao-Jiang Li, M.D., Ph.D.

A dissertation submitted to the Faculty of the
James T. Laney School of Graduate Studies of Emory University
in partial fulfillment of the requirements for the degree of
Doctor of Philosophy in
Graduate Division of Biological and Biomedical Sciences
Biochemistry Cell and Developmental Biology
2014

Acknowledgement

First of all, I would like to thank my advisor Dr. Xiao-Jiang Li for his guidance and support during my time as a graduate student. He gave me a lot of scientific freedom to pursue whichever direction that I felt interested in, but he was also ready to help whenever I needed him. His mentorship helped me grow into a fledging scientist, for which I always feel gratitude. I would also like to thank my co-PI Dr. Shihua Li. She taught me a lot, from big scientific ideas to small tips to make experiments work. When I need help, she is always the first one that I could think of. My deep gratitude goes to my committee: Drs. Anita Corbett, Gary Bassell, Russ Price and Yue Feng, who were able to provide me with different scientific expertise and perspective. I benefited a lot from their suggestions, not only about science, but also concerning my career plan. I am also thankful to have worked in a lab filled with friendly and helpful lab members. Especially, I want to thank Dr. Shanshan Huang, who guided me into my thesis project, and shared all her experiences without any reservations.

I acknowledge all my friends (especially Jianxing Xiang, my classmate, labmate and ex-roommate) for their friendship. My graduate school life would be a lot more boring without them around. I owe my thanks to my parents and parents-in-law for their unconditional love, understanding and support. They always believe in me, even when I had doubt on myself. Last but certainly not least, I would like to thank my loving wife, Yanan Lu. We had a two-year long distance relationship when we were 8,000 miles apart. She sacrificed a lot so that we could stay together, and she is working really hard so that we could have a better future. She is the reason that I strive to be my best every day.

TABLE OF CONTENTS

FIGURES AND TABLES

Chapter 1: General Introduction

Chapter 2: Aging exacerbates SCA17 neuropathology by decreasing Hsc70

Chapter 1

General Introduction

1.1 The Polyglutamine Diseases

The polyglutamine (polyQ) diseases, including Huntington's disease (HD), spinal and bulbar muscular atrophy (SBMA), dentatorubral-pallidoluysian atrophy (DRPLA), and spinocerebellar ataxia (SCA) 1, 2, 3, 6, 7, and 17 (**Table 1-1**), are some of the most devastating hereditary neurodegenerative diseases. No effective treatments are currently available, and life expectancy after diagnosis normally ranges from 10 to 30 years, which profoundly affects the lives of the patients, physically, emotionally and economically.

The polyQ tract, encoded by a tandem repeat of CAG trinucleotide, is a domain commonly found in a number of proteins. The number of glutamines within a polyQ tract varies among different proteins and differs in healthy individuals. However, an abnormally expanded polyQ tract, depending on the protein in which it resides, leads to the polyQ diseases. Therefore, each polyQ disease is caused by polyQ expansion in a specific protein. However, several common features are shared among these diseases.

First, each of the diseases is caused by a CAG repeat expansion in the exon of a specific protein encoding gene. Thus, unlike some other neurodegerative diseases, such as Alzheimer's disease (AD) and Parkinson's disease (PD), the genetic cause for the polyQ diseases is clear and defined, which is advantageous in terms of studying disease pathogenesis and diagnosing patients. Moreover, all of the polyQ diseases are inherited in an autosomal dominant manner, with the exception of SBMA that is transmitted in an X choromosome -linked recessive manner. Therefore, the polyQ expansion within the pathogenic proteins is proposed to cause some gain-of-toxicity consequences, including altered transcription, mitochondrial dysfunction, oxidative stress, cellular transport defect, excitotoxicity, reduced synaptic plasticity and metabolic impairment. However, several

studies indicate that a partial loss-of-function could potentially contribute to disease pathogenesis as well. For example, a study of HD proposed that wild type huntingtin (htt) supported neuronal survival by enhancing BDNF vesicular transport, while mutant htt attenuated this function (Gauthier et al., 2004); a study of SBMA found mutant androgen receptor failed to regulate a subset of genes that are normally controlled by wild type androgen receptor (Lieberman et al., 2002); analysis of a SCA17 mouse model showed a reduced level of wild type TATA-box binding protein (TBP) when mutant TBP is present (Friedman et al., 2007), and expanded polyQ decreased *in vitro* binding of TBP to DNA (Friedman et al., 2008). Taken together, a combination of gain and loss-of-function could underlie the polyQ disease pathogenesis.

Second, all the polyQ diseases are late-onset, meaning that the disease symptoms in patients normally start to appear in the middle age. However, an inverse correlation between the length of CAG repeat and the age of onset has been established. In patients with the juvenile form of HD (age of onset less than 20 years), the average CAG repeat length in the mutant allele is around 60; whereas typical HD patients (age of onset between 21 and 50 years) have a mean repeat of 42 in the mutant allele (Wexler et al., 2004). A similar trend is also observed in SCA17 (Tsuji, 2004). Therefore, the CAG repeat length is the primary factor in determining age of onset of polyQ disease.

A third feature of the polyQ diseases is the presence of misfolded polyQ protein aggregates in patient brains. The cellular location of the aggregates depends on the protein context. For example, mutant htt aggregates were found both in the nucleus (DiFiglia et al., 1997) and neuropil (Gutekunst et al., 1999) of postmortem HD patient brains. In contrast, mutant TBP aggregates in SCA17 patient brains were predominantly

nuclear (Nakamura et al., 2001). A myriad of other proteins, such as ubiquitin and p62/SQSTM1, were present in these protein aggregates (DiFiglia et al., 1997; Nagaoka et al., 2004). Thus, a widely proposed mechanism explaining the polyQ mediated toxicity is that the polyQ protein aggregates sequester other proteins from their functional locations. However, whether these aggregates are the true culprits for the polyQ disease pathogenesis remains elusive. Notably, emerging evidence suggests that soluble mutant protein is more pathogenic than aggregated proteins in polyQ disease models (Nagai et al., 2007; Takahashi et al., 2008), suggesting that the aggregates could be the byproducts of cellular protective mechanisms.

Finally, an intriguing observation is that although mutant polyQ proteins are ubiquitously expressed throughout the body, only selective regions within the brain are significantly affected. In HD, the striatum and deep layer of cortex is the most vulnerable to mutant htt toxicity (Vonsattel et al., 1985). In SCAs, the cerebellum, especially the Purkinje neurons in the cerebellum, degenerates the most. Therefore, despite the fact that the expanded polyQ peptide alone is toxic (Marsh et al., 2000), the pathogenesis of polyQ diseases is highly protein context dependent. However, with the exception of TBP and androgen receptor, the exact biological functions of most polyQ proteins remain elusive. Thus, understanding the functions and interacting partners of polyQ proteins could provide insights into the region specific neurodegeneration in polyQ diseases.

1.2 Aging and polyglutamine diseases

Aging is a complicated biological process that affects almost any cells in a living organism. The main characteristic of aging is a chronic deterioration of physiological

integrity, which leads to abnormal functions and eventually death. Several hallmarks have been described for aging: (1) genomic instability, such as lesions in nuclear and mitochondrial DNA; (2) telomere attrition, meaning the constant shortening of telomere regions during repetitive cycles of DNA replication; (3) epigenetic alterations, including changes in DNA methylation, histone modification and noncoding RNAs; (4) loss of proteostasis, featured by declines in chaperone, ubiquitin-proteasome system (UPS) and autophagy activity; (5) deregulated nutrient sensing, which mainly concerns the insulin-AKT and mTOR pathways; (6) mitochondrial dysfunction, including increased production of reactive oxygen species (ROS) and impaired mitochondrial integrity; (7) cellular senescence, which is the phenomenon that cells cease to divide; (8) stem cell exhaustion, meaning the decreased proliferation of stem cell population; and (9) altered intercellular communication, such as abnormal inflammation responses (Lopez-Otin et al., 2013). Some of these hallmarks, such as genomic instability, telomere attrition and epigenetic alterations, are considered as the primary causes of aging, as they trigger the accumulation of damages over time, by means of altering protein expression or functions. Other hallmarks are the consequences of the primary causes, and are the culprits of aging phenotypes. Nonetheless, all these hallmarks are closely intertwined, which explains the complexity of aging, and the challenges to halt or reverse aging.

Aging is the primary risk factor for polyQ diseases, and polyQ disease symptoms mainly appear in the middle age. Accordingly, most of the hallmarks for aging have been observed in polyQ diseases as well. For example, altered histone modification and noncoding RNAs are proposed to contribute to HD (Lee et al., 2013); disruption of cellular protein folding is observed in polyQ disease models (Gidalevitz et al., 2006); the

IGF-1/AKT pathway is altered in HD patients (Humbert et al., 2002); mitochondrial damage is found in HD, SCA3 and SCA7 models (Damiano et al., 2010; Wang et al., 2006; Yu et al., 2009); neuronal inflammation, manifested by microglia activation, is present in both HD patients and animal models (Moller, 2010). Together, these results suggest the pathogenesis of polyQ diseases could share some similar mechanisms with natural aging. However, an important distinction between polyQ disease and natural aging is that the presence of mutant polyQ proteins could actively participate in the deterioration of above-mentioned molecular mechanisms. An example is that mutant htt triggers mitochondrial fragmentation by abnormally interacting with the mitochondrial fission GTPase dynamin related protein 1 (DRP1) (Song et al., 2011). Moreover, mutant polyQ proteins impair proteostasis by decreasing chaperone level (Friedman et al., 2007) and clogging the proteasome (Holmberg et al., 2004). Therefore, a positive feedback loop could underlie the late-onset nature of polyQ diseases. That is, during the aging process, cellular function gradually declines. Once the function drops below a certain threshold, the toxicity of mutant polyQ proteins can no longer be offset by normal cellular activities. Mutant polyQ proteins further damage such cellular activities to accelerate the aging process, which may contribute to the onset of polyQ diseases.

1.3 Protein homeostasis and polyglutamine diseases

The normal protein conformation is essential for a protein to execute its biological functions. Disrupted protein folding could lead to loss of protein functions, and also cause stresses to the cellular environment. In the case of polyQ proteins, the expanded polyQ tract renders them prone to aggregate. Pioneering work in 1994 showed that a

polyQ tract could form anti-parallel β-sheets held together by hydrogen bonds (Perutz et al., 1994), providing the first insight into polyQ protein aggregation. Later, expanded polyQ protein was found to aggregate into amyloid-like strucuture, revealed by electron microscopy (Scherzinger et al., 1997). Surprisingly, in contrast to the conventional models of nucleated growth polymerization of proteins, the aggregation nucleus of polyQ proteins is a monomer (Chen et al., 2002). These are some seminal studies that contribute to our understanding of polyQ protein aggregation pathway. However, many questions remain unanswered, with one of the most important questions being which form of polyQ protein is the most toxic: monomers, oligomers, or the final amyloid-like aggregates. Emerging evidence suggests that soluble forms of polyQ proteins are more pathogenic than aggregated forms. For example, microinjection of the soluble β-sheet monomer of expanded polyQ protein caused the highest level of cytotoxicity, compared to aggregates injection (Nagai et al., 2007); a live cell imaging study revealed that neuronal differentiated cells with soluble oligomers died faster than those with aggregates (Takahashi et al., 2008). Nonetheless, the exact nature of the aggregation pathway *in vivo*, and which protein species along this pathway in the main culprit of polyQ disease pathogenesis remain matters under investigation.

The presence of misfolded proteins constitutes a stressful environment that the cell has to overcome to maintain normal functions and survive. There are three major mechanisms employed by cells to cope with misfolded proteins: (1) chaperone system, which incorporates a large family of chaperone proteins that assist the proper folding and assembly of other proteins (Kim et al., 2013); (2) ubiquitin-proteasome system (UPS), which adds a poly-ubiquitin chain to the misfolded proteins, and targets the proteins to be

degraded by the proteasome (Li and Li, 2011a); (3) autophagy system, which utilizes the lysosomes to breakdown unwanted protein complexes and cellular components (Mizushima, 2007). Due to the close relationship with misfolded proteins, all three mechanisms have been extensively studied in polyQ diseases. Indeed, mounting evidence suggests that impairment of all three mechanisms can contribute to polyQ diseases. Various chaperone members, like Hsp70 and Hsp40, co-localize with polyQ protein aggregates, and overexpression of these chaperones can ameliorate cellular toxicity caused by mutant polyQ proteins (Cummings et al., 1998; Vacher et al., 2005; Wyttenbach et al., 2000). However, in terms of the protective mechanisms underlying chaperone overexpression, contradictory results exist. Some studies suggest increased level of chaperones could reduce polyQ protein aggregates (Cummings et al., 1998; Stenoien et al., 1999), while others argue that suppression of cellular toxicity by chaperone overexpression is independent of polyQ protein aggregates, but due to repressed caspase activation and altered transcriptional activities (Friedman et al., 2009; Zhou et al., 2001). Another thing worth noting is that although prominent rescue effects are seen in cellular models, the efficacy of chaperone overexpression in animal models is quite limited (Hansson et al., 2003; McLear et al., 2008), indicating in complicated biological systems, manipulation of a single protein homeostatic mechanism may not be sufficient to halt or reverse polyQ protein aggregation.

The chaperone system prevents polyQ protein aggregation by refolding misfolded proteins, whereas the UPS system employs a different approach - degrading the defective proteins. Ubiquitination is a common post-translational modification, in which a single, or a chain of ubiquitins is attached to the lysine residues of targeted proteins. Lysine 48-

linked polyubiquitin chain , which is linked by the 48th amino acid in ubiquitin, targets proteins to the proteasome to be destroyed (Komander and Rape, 2012). The proteasome is a cylinder-shaped protein complex composed of one 20S core and two 19S regulatory particles. The first line of evidence connecting the UPS system to polyQ disease is the presence of ubiquitin and the 20S proteasome core in the aggregates (Cummings et al., 1998; McLear et al., 2008). Moreover, mutant polyQ protein is polyubiquitinated, suggesting it can be targeted by the UPS (Kalchman et al., 1996; Thompson et al., 2009). Another important finding is that UPS activity is lower in neurons than in glia (Tydlacka et al., 2008), and lower in the neuronal synapses than in the cell bodies (Wang et al., 2008), which correlates well with the enrichment of polyQ aggregates in the neurons over glia, especially in the neuropils.

Autophagy is another celllular mechanism to degrade misfolded proteins. Unlike the UPS, which targets soluble misfolded proteins, authphagy mainly engulfs and breaks down aggregated forms of proteins in its acidic lumen. Three forms of autophagy exist: macroautophagy, in which a specific two-membrane vesicle named autophagosome fuses with lysosomes; microautophagy, in which proteins to be degraded are directly transferred into lysosomes through membrane invagination; chaperone mediated autophagy (CMA), in which specific proteins of interest are recognized by chaperones, and transported through lysosomes via the lamp2A receptor (He and Klionsky, 2009). Macroautophagy and CMA are the two forms mainly implicated in polyQ diseases. The first evidence to link autophagy to polyQ diseases is the observation that htt is localized in multi-vesicular structures resembling early and late macroautophagosomes (Sapp et al., 1997). An increased number of autophagic vacuoles has been found in HD models (Kegel

et al., 2000), yet whether this increase means autophagy activation or blockade remains controversial. Moreover, inhibition of autophagy by chemicals such as 3-methyladenine and bafilomycin increased mutant htt level and aggregates number, and decreased cell viability (Qin et al., 2003). On the other hand, activation of autophagy by means of blocking mammalian target of rapamycin (mTOR) pathway or overexpressing beclin-1 promoted mutant polyQ protein clearance and attenuated cell death (Nascimento-Ferreira et al., 2011; Ravikumar et al., 2004). CMA also contributes to the degradation of polyQ proteins, and expression of a fusion protein comprised of the polyQ binding peptide and Hsc70 binding motif led mutant htt to degradation through CMA (Bauer et al., 2010).

1.4 Neurotrophic factors and polyglutamine diseases

Neurotrophic factors (NTFs) are an important family of proteins regulating neuronal development, function and survival. Ever since the identification of the first NTF- nerve growth factor (NGF) in 1987 (Levi-Montalcini, 1987), the NTF family greatly expanded. Traditionally, the NTF family is further divided into three sub-families: (1) neurotrophins, including NGF, brain derived neurotrophic factor (BDNF), neurotrophin-3 (NT-3) and neurotrophin-4 (NT-4) (Huang and Reichardt, 2001); (2) glial cell line derived neurotrophic factors (GDNFs) (Airaksinen and Saarma, 2002); (3) neuropoietic cytokines, including interleukin-6 (IL-6), IL-11, IL-27, leukaemia inhibitory factor (LIF), ciliary neurotrophic factor (CNTF), cardiotrophin 1 (CT-1), neuropoietin and cardiotrophin-like cytokine (CLC) (Bauer et al., 2007). Recently, a new family of NTFs consisting of two members, cerebral dopamine neurotrophic factor (CDNF) and mesencephalic astrocyte derived neurotrophic factor (MANF), becomes an interesting

target for research. The unique feature of this NTF family is that homologues of vertebrate CDNF and MANF are found in invertebrates, including *Drosophila* and *C. elegans*, and *Drosophila* lines lacking functional MANF alleles showed larval lethality (Palgi et al., 2009), indicating some important functions that are conserved from invertebrates through vertebrates. Moreover, the distinctive structure of MANF (**Figure 1-1**) suggests that besides functioning extracellularly to trigger signaling pathways, like the classical NTFs, MANF could carry out important functions inside the cells as well, such as protection against ER stress (Lindholm and Saarma, 2010). The crystal structure of MANF revealed a well defined N-terminal domain belonging to the saposin family, which has lipid binding capacity (Parkash et al., 2009); on the other hand, C-terminal MANF is homologous to the SAP domain of Ku70, a well known inhibitor of apoptosis (Hellman et al., 2011).

Among all the NTFs, BDNF is the most extensively studied in polyQ diseases. BDNF is widely expressed in the central nervous system (CNS), and plays a critical role in neuronal growth, differentiation, plasticity and synaptic activity, predominantly through TrkB receptor, and to a lesser extent, through p75 receptor (Zuccato and Cattaneo, 2007). Reduced levels of BDNF have been found in the brain of various polyQ disease models (Duan et al., 2003; Takahashi et al., 2012; Zhang et al., 2003; Zuccato et al., 2001). The reason for BDNF reduction could be two-fold: (1) mutant polyQ proteins could impair BDNF transcription, leading to a reduced level of BDNF mRNA (Luthi-Carter et al., 2002; Zuccato et al., 2001; Zuccato et al., 2003); (2) wild type htt is proposed to regulate BDNF vesicle transport, which is attenuated in the presence of mutant htt (Colin et al., 2008; Gauthier et al., 2004). In either case, less amount of BDNF

would be released to targeted brain regions. However, despite the pro-survival nature of BDNF, increasing BDNF concentration in the brain by means of exogenous administration, adenoviral injection, or transgenic manipulation yielded only modest improvements over disease symptoms and pathology in HD models (Canals et al., 2004; Cho et al., 2007; Gharami et al., 2008), suggesting the pathogenesis of polyQ diseases is quite complicated, and BDNF therapy alone may not be sufficient to halt or reverse neurodegeneration.

Beside BDNF, other NTFs have also been implicated in polyQ diseases. For example, NGF levels were significantly lower in HD patients than in healthy subjects (Tasset et al., 2012); NT-3and NT-4 were able to prevent the death of striatal projection neurons in a HD mouse model (Perez-Navarro et al., 2000); CNTF was tested as a potential gene therapy for HD (Bloch et al., 2004); dysregulated NGF-TrkA signaling was associated with SCA17 (Shah et al., 2009). Moreover, vascular endothelial growth factor (VEGF), an angiogenic factor, ameliorated neurodeneration and ataxic phenotype in SCA1 mice (Cvetanovic et al., 2011). Taken together, these results suggest that NTFs constitute an important aspect of polyQ disease pathogenesis, and provide valuable perspective on developing effective therapeutic strategies for polyQ diseases.

1.5 Spinocerebellar Ataxia 17 (SCA17)

First identified in 1999, SCA17 is the latest addition to the family of polyQ diseases (Koide et al., 1999). SCA17 has been attributed to the polyQ expansion within TATA-box binding protein (TBP). The normal range of polyQ number is between 25 and 42 in human TBP (Rubinsztein et al., 1996), whereas disease symptoms can develop in

patients with as few as 47 repeats (Nakamura et al., 2001). There are two distinctions when comparing SCA17 to other polyQ disease in terms of polyQ tract: First, the polyQ length in normal TBP is longer than other normal polyQ proteins. For example, the polyQ number in normal htt ranges from 6 to 35. Thus, a polyQ tract long enough to become pathogenic in htt is well tolerated in TBP, again suggesting that the polyQ disease pathogenesis is highly protein context dependent. Second, the genomic sequence encoding the polyQ tract in TBP is not a pure repeat of CAG. Instead, several CAA codons disrupt the homogeneity of CAG repeats, with the most commonly seen sequence $(CAG)_3$ $(CAA)_3$ $(CAG)_n$ CAA CAG CAA $(CAG)_n$ CAA CAG (Gostout et al., 1993; Koide et al., 1999). This genomic structure could possibly explain the lack of CAG number instability in SCA17 (Reid et al., 2003), in contrast to what is frequently seen in HD and SCA1 (McMurray, 2010). This possibility is supported by a pedigree study finding an intergenerational increase of polyQ number, from a family who loses the CAA CAG CAA segment which separates the two CAG stretches in the TBP gene (Maltecca et al., 2003). Sequencing analysis performed on the patients of the third generation of this pedigree showed the structure of the repeat region was $(CAG)_3$ $(CAA)_4$ $(CAG)_{44}$ CAA CAG. Whereas the repeat number expanded to $(CAG)_3$ $(CAA)_4$ $(CAG)_{57}$ CAA CAG in the patient of the fourth generation.

In SCA17 patients, the most prominent neurodegeneration is seen in the cerebellum. Within the cerebellum, the Purkinje neurons, one of the largest neurons in the central nervous system and the only neurons projecting out of the cerebellum, are the most vulnerable (Bruni et al., 2004). However, diffuse cortical and brain stem atrophy, as well as subcortical white matter lesions are also revealed by brain magnetic resonance

imaging (Nakamura et al., 2001; Rolfs et al., 2003), which could explain the wild spectrum of disease features in SCA17 patients, including ataxia, dystonia, dementia, parkinsonism, psychiatric abnormalities and seizures (Koide et al., 1999; Manto, 2005; Nakamura et al., 2001). Indeed, SCA17 is alternatively named Huntington's disease-like 4 (HDL4), as its clinical features such as rapidly progressive dementia followed by concurrent chorea are also characteristic in HD (Stevanin and Brice, 2008; Toyoshima et al., 2004). Wild type TBP is found in mutant htt aggregates from post mortem HD brains (Huang et al., 1998), providing a potential explanation of clinical similarities between SCA17 and HD.

Presumably due to the critical functions of TBP, SCA17 is a very rare disease, with only a few cases reported in China, Japan, Korea, Germany, Italy and the northeast of England (Brusco et al., 2004; Craig et al., 2005; Koide et al., 1999; Nakamura et al., 2001; Wu et al., 2004). In addition, SCA17 is the most recently identified member of polyQ disease family. Therefore, our knowledge about SCA17 pathogenesis is still quite limited. However, two major advantages make SCA17 a valuable model for polyQ disease research: (1) of all the identified polyQ proteins, the size of TBP is the smallest, and the normal cellular function of TBP is well characterized (Burley and Roeder, 1996), which makes it ideal for understanding how polyQ expansion alters transcriptional activities; (2) several SCA17 models, ranging from stable cell line (Shah et al., 2009), *Drosophila* model (Ren et al., 2011), transgenic mouse model (Chang et al., 2011; Friedman et al., 2007; Friedman et al., 2008), transgenic rat model (Kelp et al., 2013) to knock-in mouse model (Huang et al., 2011) have been successfully generated. Obvious

neurodegeneration and motor impairment were found in all animal models, which greatly facilitates understanding disease mechanism and developing therapeutic strategies.

These models have provided insight into the cellular context of SCA17. Based on current findings, the chaperone system is closely related to toxicity caused by mutant TBP. Two research groups independently reported that mutant TBP shows enhanced interaction with nuclear transcription factor Y (NFY) subunit A, which binds to CCAAT sequences in the promoter region of a variety of chaperone proteins (Huang et al., 2011; Lee et al., 2012). This abnormal interaction impairs transcription medicated by NFY, leading to reduced expression of chaperones Hsp70, Hsp25, HSPA5 and HSPA8. Moreover, polyQ expansion reduced TBP dimerization, but enhanced the interaction between TBP and another general transcription factor TFIIB, which consequently resulted in downregulation of a small heat shock protein HSPB1. Conversely, overexpression of HSPB1 suppressed mutant TBP caused toxicity in mutant TBP cell lines (Friedman et al., 2007). These results provide an example of how altered transcription by mutant TBP contributes to SCA17 disease pathogenesis. However, a microarray study using brain samples of 8-week old SCA17 transgenic mice did not reveal global changes in gene expression, which was unexpected given that fact that TBP is a general transcription factor (Friedman et al., 2007). Interestingly, a truncated form of mutant TBP lacking its DNA binding domain retained the ability to sequester TFIIB, and transgenic mice expressing the truncated mutant TBP showed severe neurological symptoms (Friedman et al., 2008). Therefore, transcriptional dysregulation may not be the sole cause of mutant TBP toxicity.

1.6 TATA-box binding protein (TBP)

TBP is a general transcription factor that is involved in transcription by all three nuclear RNA polymerases (Nikolov and Burley, 1994). The importance of TBP is highlighted by the fact that homozygous TBP knockout embryos do not survive beyond the blastocyst stage (Martianov et al., 2002). Much attention has been paid to the role of TBP in RNA polymerase II-mediated transcription. During mRNA transcription, RNA polymerase II cannot bind to the promoter sequences by itself. Instead, a large protein complex termed the preinitiation complex (PIC) is required to guide RNA polymerase II to the transcription start site, unwind DNA, and position DNA into the RNA polymerase II active center (Lee and Young, 2000).

TBP is the core molecule in PIC. An *in vitro* assembly assay revealed that PIC formation is accomplished in the following order: upon binding to TATA box, TBP recruits approximately 13 TBP-associated factors (TAFs) to form TFIID complex, followed by coordinated association of TFIIA, TFIIB, non-phosphorylated RNA polymerase II, TFIIF, TFIIE and TFIIH (Burley and Roeder, 1996). TFIIH phosphorylates RNA polymerase II carboxy-terminal domain (CTD) during transcription initiation, which is essential for the progression of RNA polymerase II into the elongation phase (Helenius et al., 2011; Serizawa et al., 1995).

TBP within TFIID complex directly binds TATA-box, which is a highly conserved DNA sequence (TATAAA) typically located about 25 to 30 nucleotide upstream of the transcription start site in metazoans, and 40 to 100 nucleotides upstream of the transcription start site in the yeast *Saccharomyces cerevisiae*. In humans, nearly one third of potential promoter regions was predicted to contain a TATA-box (Suzuki et

al., 2001). TATA-box, together with some other sequence motifs, including the initiator element (Inr), the downstream promoter element (DPE) and the TFIIB recognition element (BRE), constitutes the core promoter, which is the minimal stretch of contiguous DNA sequence that is sufficient to direct accurate initiation of transcription by RNA polymerase II (Butler and Kadonaga, 2002). Each of these core promoter elements exists in some, but not all core promoters. Therefore, there are no universal core promoter elements.

The N-terminus of TBP is highly divergent, with little or no conservation among different species. The length of the polyQ tract, encoded by exon 2 of the TBP gene, also varies greatly in different organisms. For example, in human TBP, the normal polyQ number ranges from 25 to 42; in mouse TBP, less than 20 glutamines are present in the polyQ tract; whereas in the yeast *Saccharomyces cerevisiae* TBP (SPT15), no polyQ tract exists. The function of the N-terminus of TBP is also not well characterized. Deletion of the N-terminal domain of TBP did not lead to global changes in gene expression or cell proliferation in primary fibroblasts (Schmidt et al., 2003). Mouse fetuses carrying two copies of modified TBP alleles which encode TBP without the N-terminus died in midgestation from an apparent defect in the placenta, but could be rescued by rearing them in immunocompromised mothers (Hobbs et al., 2002), suggesting that the N-terminal domain of TBP may regulate the transcription of β2-microglobin (β2m), which is a molecule involved in antigen assembly and presentation.

On the other hand, the C-terminus of TBP is highly conserved in organisms ranging from human to mycetozoa, a group of slime molds (Hernandez, 1993). The C-terminal domain of TBP (**Figure 1-2**) carries out important functions involved in

transcriptional regulation, including DNA binding and transcriptionally related protein-protein interactions. A short stretch of basic amino acids, flanked by two copies of long imperfect repeat of 61 to 62 amino acids, enables the C-terminal TBP to fold into a saddle shaped tertiary structure, which binds the minor groove of DNA and induces DNA bending (Kim et al., 1993). Even at promoters without TATA-box, TBP is required for PIC to form. The presence of TBP at TATA-less promoters is achieved through direct or indirect binding with other sequence-recognizing factors such as TAFs (Pugh, 2000).

1.7 Summary of aims and results of the study

Based on the above review of different aspects of polyQ diseases, we know that the diseases are caused by ubiquitously expressed mutant proteins and display selective neurodegeneration in an age-dependent manner. In this study, by using SCA17 as a model, we aim to understand two fundamental questions in polyQ disease research: how aging contributes to polyQ disease pathogenesis, and how ubiquitously expressed mutant polyQ proteins lead to region-specific neurodegeneration (**Figure 1-3**).

The onset of symptoms in polyQ disease patients is usually in adulthood, despite the fact that mutant polyQ proteins are constitutively expressed. There are two possible explanations to the late-onset nature of polyQ diseases: one is that during aging, the long duration of protein expression allows misfolded proteins to accumulate and become toxic over time; the other is that aged neurons are more vulnerable to toxicity caused by misfolded proteins, when compared with neurons at an early stage. Distinguishing between these two possibilities is critical in determining therapeutic strategies to treat polyQ diseases: whether we should start treatment early to decrease mutant protein

accumulation, or we could improve cellular functions in aged neurons to reverse disease progression. However, accomplishing this goal is difficult using previous established mouse models, as mutant polyQ proteins are expressed throughout the life stages of the mice. We utilized our TBP105Q inducible knock in mice, in which mutant TBP is only expressed after tamoxifen injection. We injected tamoxifen into differently aged TBP105Q inducible knock in mice, and found older (14-month old) mice displayed earlier onset of SCA17 symptoms than younger (3-month old) mice, which correlated with a higher level of mutant TBP in older mouse brains, despite the fact that both age groups of mice expressed mutant TBP for the same length of time. We further identified Hsc70, a molecular chaperone, as a target negatively affected by aging. Overexpression of Hsc70 improved mutant TBP function and ameliorated SCA17 pathology. Taken together, these data supports the second possibility, which is that age related decline of chaperone activity makes neurons sensitive to insults caused by misfolded proteins.

The accumulation of mutant polyQ proteins is believed to cause neurodegeneration via some gain-of-function mechanisms. In agreement with this notion, mutant TBP showed enhanced interactions with TFIIB and NFY, and impaired their transcriptional activities (Friedman et al., 2007; Huang et al., 2011). However, these studies failed to address an important question: why mutant TBP is ubiquitously expressed in different tissues, yet causes selective neurodegeneration in the cerebellum, with the Purkinje neurons being the most vulnerable. Understanding the mechanisms behind the region-specific neuropathology is the key to developing effective treatments to SCA17. We identified mecensephalic astrocyte derived neurotrophic factor (MANF) as a protein enriched in the Purkinje cell layer of the cerebellum, whose enrichment is lost in

TBP105Q inducible knock in mice . Expanded polyQ reduced the binding of TBP to XBP1s, a transcription factor previously known to regulate MANF transcription, leading to MANF down-regulation, which suggests a partial loss of function could contribute to SCA17 pathogenesis as well. Overexpression of MANF ameliorated toxicity caused by mutant TBP both *in vitro* and *in vivo*, and the improvement is possibly due to enhanced PKC signaling mediated by MANF. Therefore, boosting MANF activity could be employed as a potential therapeutic strategy for the treatment of SCA17 and other types of SCAs.

Table 1 The polyglutamine diseases

PolyQ disease	Disease protein	Chromosome location	Normal CAG repeat	Pathological CAG repeat	Protein size (amino acid)	Subcellular lolalization	Affected brain region	Known/ putative protein function
HD	HTT	4p63.3	6-34	36-121	3144	Nucleus and cytosol	Striatum	Scaffolding protein
SBMA	AR	Xq12	6-38	40-62	906	Nucleus and cytosol	Spinal cord and brain stem	Hormone receptor
DRPLA	ATN1	12q13.31	7-34	53-88	1190	Nucleus and cytosol	Cerebellum	Transcription co-repressor
SCA1	Ataxin1	6p22.3	6-44	39-83	816	Nucleus and cytosol	Cerebellum	Transcription regulation
SCA2	Ataxin2	12q24.12	13-33	32-77	1313	Cytosol	Cerebellum	RNA metabolism
SCA3	Ataxin3	14q32.21	12-40	54-89	364	Cytosol	Cerebellum	Deubiquitinating enzyme
SCA6	CACNA1A	19p13.2	4-18	21-33	2505	Cell membrane	Cerebellum	Subunit of voltage gated Ca^{2+} channel
SCA7	Ataxin7	3p14.1	4-35	37-300	892	Nucleus	Cerebellum	Transcription regulation
SCA17	TBP	6q27	25-42	47-63	339	Nucleus	Cerebellum	Transcription factor

Abbreviations: HD, Huntington's disease; HTT, huntingtin; SBMA, spinal bulbar muscular atrophy; AR, androgen receptor; DRPLA, dentatorubral-palidoluysian atrophy; ATN1, atrophin 1; SCA, spinalcerebellar ataxia; CACNA1A, calcium channel, voltage-dependent, P/Q type, alpha 1A subunit; TBP, TATA-box binding protein.

Figure 1-1

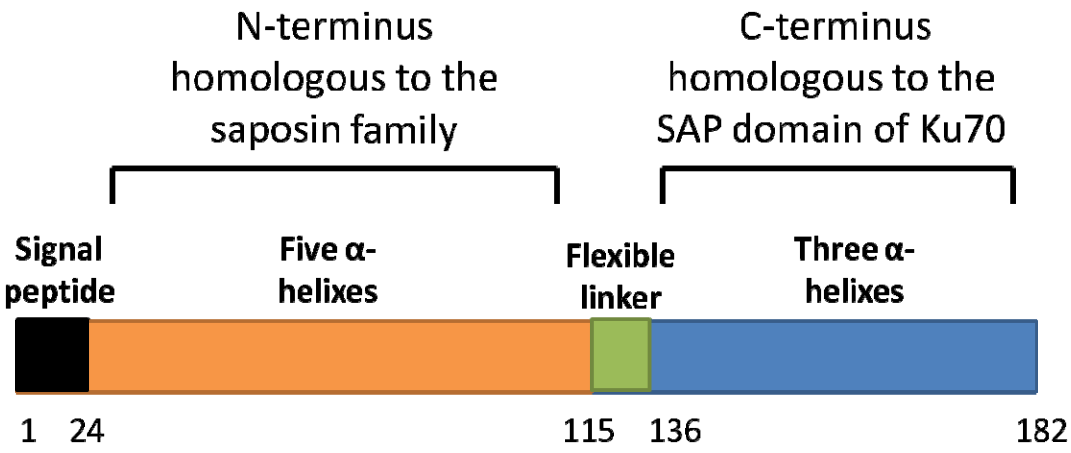
N-terminus
homologous to the
saposin family
C-terminus
homologous to the
SAP domain of Ku70
Signal
peptide
Five α-
helixes
Flexible
linker
Three α-
helixes
1
24
115
136
182

Figure 1-1 Schematic representation of human MANF.

The structure of human MANF is indicated by different colors. The first 24 amino acids (black) constitutes a signal peptide, which is cleaved off during exporting out of endoplasmic reticulum. The N-terminus of MANF (amino acid 25 to 115, orange) is composed of 5 α-helixes, and forms a structure homologous to the saposin family. The N-terminus and C-terminus of MANF are connected via a flexible linker region (amino acid 116 to 136, green). The C-terminus of MANF (amino acid 137 to 182, blue) is composed of 3 α-helixes, and resembles the SAP domain of Ku70, which is known to inhibit proapoptotic molecule Bax.

Figure 1-2

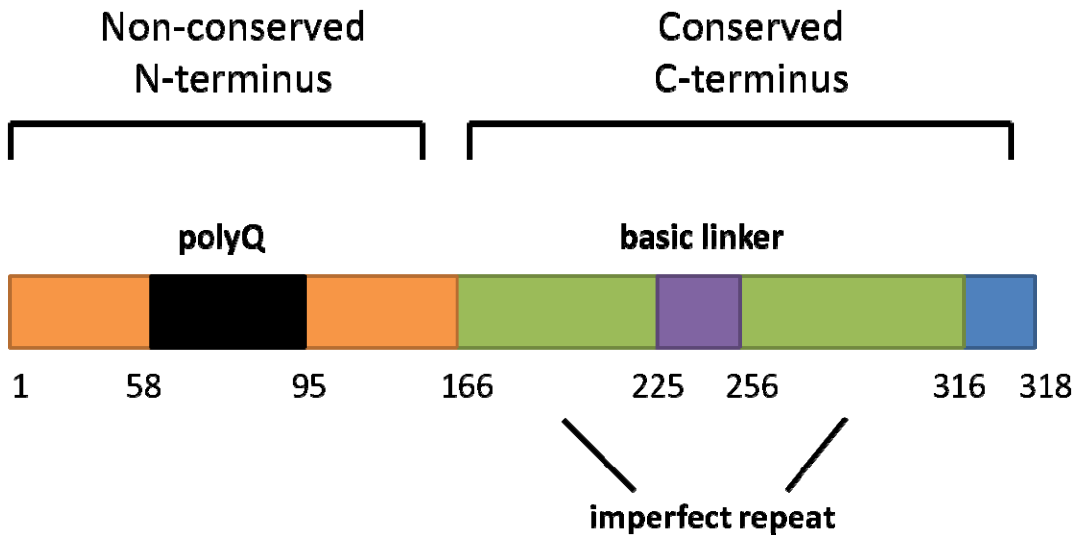
Non-conserved
N-terminus
Conserved
C-terminus
polyQ
basic linker
1
58
95
166
225
256
316
318
imperfect repeat

Figure 1-2 Schematic representation of human TBP.

The structure of human MANF is indicated by different colors. The non-conserved N-terminus of TBP (orange) contains a polyQ tract of 38 glutamines (25 to 42 glutamines in normal individuals), which is indicated in black. The C-terminus of TBP (blue) is highly conserved among different species. Two imperfect repeat domains (green) are separated by a lysine-rich basic linker (purple).

Figure 1-3

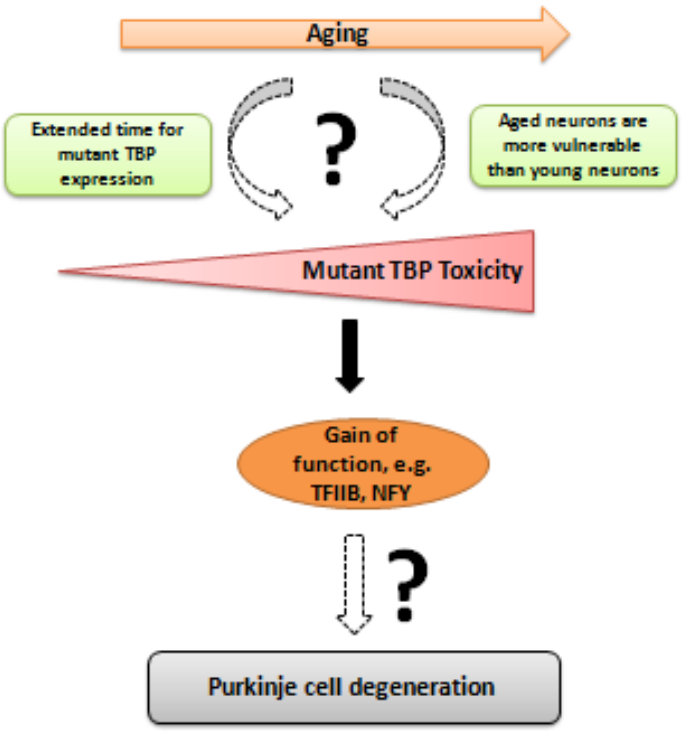
Aging
Extended time for mutant TBP expression
?
Aged neurons are more vulnerable than young neurons
Mutant TBP Toxicity
Gain of function, e.g. TFIIB, NFY
?
Purkinje cell degeneration

Figure 1-3 Previous knowledge about SCA17 pathogenesis and unanswered questions.

Mutant TBP toxicity gradually manifests during the aging process. However, whether the increase of toxicity with age is due to extended time for mutant TBP expression, or aged neurons are increasingly vulnerable to mutant TBP remains largely unknown. Mutant TBP is previously known to impair the functions of TFIIB and NFY by gain-of-function mechanisms. But why the ubiquitously expressed mutant TBP leads to specific Purkinje cell degeneration is still poorly understood.

Chapter 2

Aging exacerbates SCA17 neuropathology by decreasing Hsc70

This chapter includes work published as Su Yang, Shanshan Huang, Marta A. Gaertig, Xiao-Jiang Li, and Shihua Li (2014) *Neuron,* January 22; 81: 349-365. The majority of the work was done by Su Yang. Shanshan Huang helped with mouse breeding and experimental design. Xiao-Jiang Li and Shihua Li helped with experimental design and data analysis. Xiao-Jiang Li edited the manuscript for publication.

2.1 Abstract

Although protein misfolding-mediated neurodegenerative diseases have been linked to aging, how aging contributes to neurodegeneration remains unclear. Here we established spinocerebellar ataxia 17 (SCA17) knock-in mice that inducibly express one copy of mutant TATA-box binding protein (TBP) at different ages by tamoxifen-mediated Cre recombination. We find that more mutant TBP accumulates in older mouse brains, correlated with age-related decreases in Hsc70 and chaperone activity. Consistently, older SCA17 mice experienced earlier neurological symptom onset and more severe Purkinje cell degeneration. These data highlighted an important role of aging in the pathogenesis of SCA17, which could be broadly applicable to other polyQ diseases as well.

2.2 Introduction

Aging is a complex biological process and a known primary risk factor for neurodegenerative diseases caused by protein misfolding, such as Alzheimer's disease (AD), Parkinson's disease (PD), Huntington's disease (HD), and other polyglutamine (polyQ) expansion-mediated diseases, which frequently occur in the middle or late stages of life (Blennow et al., 2006; Collier et al., 2011; Duyao et al., 1993). The misfolded proteins are known to accumulate with age in neuronal cells, and this accumulation increases the level of toxic forms of proteins that can induce neurodegeneration. Aging is also linked to several pathological pathways, including mitochondria dysfunction (Passos and von Zglinicki, 2005), reactive oxygen species (ROS) damage (Afanas'ev, 2010), and protein homeostasis

disturbance (Akerfelt et al., 2010), which are implicated in neurodegenerative diseases (Federico et al., 2012; Gandhi and Abramov, 2012; Gidalevitz et al., 2006).

Because neurons are terminally differentiated cells that do not divide, it remains unclear whether aging-related factors promote the accumulation of mutant proteins in neurons versus the greater length of time proteins are expressed, or whether aged neurons are more vulnerable to misfolded proteins versus the cumulative effects of misfolded proteins with age. Understanding the mechanisms underlying age-dependent neurodegeneration is critical if we are to develop effective therapeutics for protein misfolding-mediated neurodegenerative diseases. For example, if aged neurons are more vulnerable than young neurons to misfolded proteins, reversing aging-related cellular dysfunction would be more effective than reducing the expression of polyQ proteins in treating these neurodegenerative diseases, especially since proteins with expanded polyQ repeats may still preserve critical function (Cattaneo et al., 2005).

Unfortunately, sorting out these important issues is difficult using current genetic mouse models of neurodegenerative diseases. This is because most of these mouse models express mutant proteins throughout life, making it difficult to distinguish between the cumulative effects of mutant proteins on neuronal cells over time versus a greater vulnerability of aged neurons to mutant proteins. To remedy this, we established an inducible mouse model of spinocerebellar ataxia 17 (SCA17) that allows for the expression of mutant proteins at different ages, enabling us to examine whether and how aged neurons are particularly affected. In SCA17, the polyQ expansion in TBP causes age-dependent neurodegeneration in the same manner as the other eight polyQ diseases, among them Huntington's disease (Orr and Zoghbi, 2007). These facts suggest that the neuronal toxicity

of mutant TBP and other polyQ disease proteins depends on aging-related factors. Because TBP is a well-characterized transcription factor, SCA17 makes an ideal model for investigating how polyQ expansion-mediated protein misfolding causes neuronal degeneration in an age-dependent manner.

Using our new SCA17 knock-in mouse model, we induced mutant TBP expression in mice at different ages. We found that SCA17 disease phenotypes in older mice progress much faster, along with decreases in chaperone activity and Hsc70 level, indicating that age-related decrease in chaperone function could cause the accumulation of mutant TBP, which leads to the late onset of SCA17 symptoms.

2.3 Materials and Methods

Antibodies and plasmids

Primary antibodies from commercial sources used include: 1C2 (Millipore/Chemicon, MAB1574), 1TBP18 (QED bioscience, 70102), calbindin (Millipore/ Chemicon), Hsc70 (Santa Cruz, 7298), Hsp90 (Cell Signaling, 4877), Hsp70 (Cell Signaling, 4872), Hsp40 (Cell Signaling, 4871), Actin (Sigma, A5060), p62/ SQSTM1 (Sigma, P0068), and LC3B (Sigma, L7543),. Rabbit polyclonal antibody EM192 against mouse TBP was generated as described before (Friedman et al., 2007). All secondary antibodies were purchased from Jackson Immunoresearch.

Mouse lines and tamoxifen injection

All mice were bred and maintained in the animal facility at Emory University under specific pathogen-free conditions in accordance with institutional guidelines of The Animal Care and Use Committee at Emory University. The TBP105Q floxed mice were generated as described before (Huang et al., 2011). To generate TBP105Q inducible knock-in mice, heterozygous floxed TBP105Q mice were crossed with CreER transgenic mice (The Jackson Laboratory, B6.Cg-Tg(CAG-cre/Esr1)5Amc/J), which express tamoxifen-inducible Cre throughout the body. Primers were used for genotyping of the presence of mutant TBP (forward: 5′-CCA CAG CCT ATT CAG AAC ACC-3′; reverse: 5′-AGA AGC TGG TGT GGC AGG AGT GAT-3′) and Cre (forward 5′-GCG GTC TGG CAG TAA AAA CTA TC-3′; reverse: 5′-TGT TTC ACT ATC CAG GTT ACG G-3′).

For injection of tamoxifen into the mice, tamoxifen (Sigma, T5648) was dissolved in 100% ethanol to 10 mg/ml; corn oil (Sigma, C8267) was added and mixed thoroughly before ethanol was evaporated using Vacufuge plus (Eppendorf). Tamoxifen, dissolved in corn oil, was injected intraperitoneally into mice at 0.1 mg per 1g body weight for 5 consecutive days.

Mouse behavior tests

The body weight of mice was measured every two days. The motor function of mice was assessed by rotarod test (Rotamex, Columbus Instruments) every six days. Prior to the initial test, mice were trained on the rotarod at the speed of 5 rpm for 10 minutes for 3 consecutive days. During the test, the rotarod was set to accelerate from 0 rpm to 40 rpm,

with the increment of 0.1 rpm per second. Each mouse was subjected to three trials, and the time it stayed on the rotarod was recorded automatically by the machine. The average time of three trials was used to evaluate the motor activity of the mice.

For foot printing assay, red ink was applied to the forepaws of tested mice, and black ink to the hindpaws. The mice were allowed to walk through a narrow tunnel with white paper placed at the bottom. Stride lengths were calculated by measuring the distances between forepaws of each step.

For the balance beam test, mice were trained for 2 days to walk the entire length of a 0.6 cm (approximately 1″) wide × 80 cm long wooden beam that was suspended 50 cm above the floor. On each trial the mouse was released onto the end of the beam and required to run down the entire beam and into the dark box. Each mouse was tested, and each session was the average of 3 trials. The time for a mouse to cross to the end was recorded.

Quantification of neuronal degeneration

Mouse brains were cut into 40 μm sagittal sections in a cryostat and mounted on glass slides. For Nissl staining, brain slices were immersed in cresyl violet solution overnight, dehydrated by alcohol, and cleared by xylene. For Golgi stain, mouse brains were incubated in 3% potassium dichromate in the dark for 4 days with daily changes, and then transferred to 2% silver nitrate in the dark for 2 days. Purkinjec cells were also labeled by an antibody to calbindin in immunofluorescent staining. Purkinje neuron images were taken by Olympus FV1000 confocal microscope. To quantify Purkinje neuron numbers in an unbiased manner,

NIH ImageJ software was used as described before (Bowman et al., 2007). Briefly, the "threshold" of calbindin-stained images (10X or 20X) was adjusted to highlight the soma of Purkinje neurons over background noise. The same setting has been applied to all images analyzed, and the number of Purkinje somas were counted. Molecular layer thickness of Purkinje cells was measured along the third, fourth and ninth folia half way down the preculminate, using the "spatial calibration" tool in Openlab software. To perform Sholl analysis, calbindin-stained images by confocal microscope were converted to 8-bit greyscale. NIH ImageJ software with "sholl analysis" plugins was used to count the number of neurite crossings, with the starting radius set to the radius of the Purkinje soma, and the ending radius set to the total length of Purkinje neurons.

Western blot, immunohistochemistry and immunoprecipitation

Methods for western blot and immunohistochemistry were described previously (Huang et al., 2011). For immunoprecipitation, transfected 293 cells were homogenized in NP-40 buffer (50 mM NaCl, 50 mM Tris-HCl pH8.0, 0.1% Triton X-100, 0.5% NP-40). Protein concentration was determined by BCA protein assay kit (Thermo Scientific, 23227), and 300 μg of protein was used for one experiment. The protein was first pre-cleared with protein A-agarose for 1 hour, and then incubated with primary antibody overnight. The next day, protein A-agarose was added into the mixture and kept for 1 hour incubation. The precipitated antibody-protein complexes were used for western blotting.

Luciferase protection assay

The method for luciferase protection assay and related reagents used in our study were adopted from a previous study (Thulasiraman and Matts, 1998). To prepare mouse brain lysate, mouse cortex and cerebellum tissues were homogenized in lysis buffer (0.25 M sucrose, 15 mM Tris-HCl pH8.0, 60 mM KCl, 15 mM NaCl, 5 mM EDTA, 1 mM EGTA, and 2 mM ATP) with a glass homogenizer. The homogenate was first centrifuged at 5000 RPM for 10 minutes at 4℃. The supernatant was collected and centrifuged again at 16000 RPM for 30 minutes at 4℃. The supernatant was saved for experiments. To perform luciferase protection assay, 20 μg of brain lysate was either added with 3 μl of the chaperone inhibitor PU-H71 (10 mM, Sigma) as a negative control or without any inhibitors. The lysate was kept at 37℃ for 90 minutes to allow PU-H71 to inhibit chaperone function. After that, the lysate was mixed with recombinant luciferase and other additions (cold mix, creatine phosphate, and creatine phosphokinase) for incubation at 42℃ for 40 minutes. Finally, the luciferase activity was determined by a microplate reader (Synergy H4, BioTek).

RNA isolation and reverse transcriptase PCR

RNA from mouse cortex and cerebellum was isolated by RNeasy Lipid Tissue Mini Kit (QIAGEN, 74804). RNA concentration was determined by Synergy H4 reader, and equal amount of RNA was used for cDNA synthesis with SuperScript III First-Strand synthesis system (Invitrogen, 18080-051). For semi-quantitative PCR, rTaq, reaction buffer and dNTP used are all from TaKaRa, and primers used are listed below.

For TBP, forward: 5'-TAC TCC ACA GCC TAT TCA GAA CAC C-3'; reverse: 5'-AAT GGA AGA GTT GTG GGG TCT GG-3'. For Actin, forward: 5'-TGA GAC CTT CAA CAC CCC AG-3'; reverse: 5'-GTG GTG GTG AAG CTG TAG CC-3'

Statistical analysis

For mouse behavioral analysis, each group consisted of at least 6 animals. For western blotting analysis, immunostaining, or other biochemical assays, data were generated from 3 or more experiments, and the results were expressed as mean ± SEM. Statistical significances were calculated based on either t-test, one-way ANOVA or two-way ANOVA. A P-value of <0.05 was considered significant.

2.4 Results

Generation of inducible SCA17 knock-in (KI) mice

We previously established floxed TBP105Q mice in which a transcription stop codon is used to prevent the transcription of mutant TBP (Huang et al., 2011). To induce the expression of mutant TBP in mice at different ages, we crossed floxed heterozygous TBP105Q mice with CreER transgenic mice that express a fusion protein containing Cre recombinase and an estrogen receptor ligand-binding site under the control of chicken β-actin promoter. Upon intraperitoneal injection of tamoxifen, an estrogen receptor ligand, this ligand can bind Cre recombinase fusion protein and cause it to enter the nucleus to act on the

loxP sites, resulting in removal of the stop codon and expression of mutant TBP (**Figure 2-1A**). For simplicity, the mice carrying both the floxed TBP105Q gene and CreER transgene are referred to as TBP105Q inducible KI mice. Littermates with other genotypes, including CreER transgenic mice, heterozygous TBP105Q floxed mice, and wild type mice, were used as control mice, as injection of tamoxifen in these mice does not lead to the expression of mutant TBP. Thus, tamoxifen can be injected into KI mice at different ages to permanently induce mutant TBP expression throughout the body.

We first injected tamoxifen in 3-month-old TBP105Q inducible KI mice for 5 consecutive days. Two months after the last injection, different tissues were collected for western blot analysis. Soluble mutant TBP in the cortex and liver of injected KI mice was seen in western blots probed with 1C2 antibody, which recognizes the expanded polyQ region. Immunoprecipitation of mouse TBP with the rabbit polyclonal antibody EM192 verified the existence of soluble mutant TBP in the cortex and liver (**Figure 2-1B**). Western blot probed with 1TBP18 antibody, which preferentially reacts with aggregated forms of mutant TBP, revealed SDS-insoluble mutant TBP aggregates in the stacking gel, which were from the cerebellum, cortex, and muscle of KI mice (**Figure 2-1C**). Immunohistochemistry with 1C2 antibody also verified the presence of mutant TBP in different brain regions in KI mice 2 months after tamoxifen injection at the ages of 3 or 14 months. Nuclear staining of mutant TBP was evident in the cortex, striatum, hippocampus, and cerebellum of these KI mice (**Figure 2-1D left panel**). Staining with 1TBP18 antibody revealed small mutant TBP aggregates in the nucleus under high magnification (100 X) (**Figure 2-1D right panel**). All these results confirm that tamoxifen injection can induce the expression of mutant TBP in the brain and peripheral tissues at different ages.

Aging exacerbates neurological phenotypes and Purkinje neuron degeneration in TBP105Q inducible KI mice

To study the impact of aging on SCA17 disease progression in our TBP105Q inducible KI mouse model, KI mice at 3, 9, and 14 months of age were injected with tamoxifen for 5 days, and then examined on a weekly basis for 3 months or until death. After tamoxifen injection, KI mice gradually developed characteristic SCA17 disease phenotypes, such as reduced body weight, impaired motor function, and hunched-back appearance. Some 14-month-old mice died starting from 40 days after tamoxifen injection, but none of the 3-month-old mice died within 3 months after injection. Because some mice had been sacrificed to examine brain pathology and TBP expression at different times after injection, the loss of body weight of these mice was used to reflect disease severity, as body weight can also be more reliably quantified than other behavioral phenotypes. Compared to the age-matched controls, older KI mice displayed a significant loss of body weight at an earlier time following tamoxifen-induced expression of mutant TBP; for example, 14-month-old KI mice started to lose their body weight significantly at 35 days after injection, whereas the 9-month-old group of KI mice showed a significant weight loss at 53 days after injection. On the other hand, 3-month-old KI mice showed no obvious body weight reduction until 113 days after injection (**Figure 2-2A**). Consistently, a hunched-back appearance of 3-, 9-, and 14-month-old KI mice was seen at 130, 75, and 60 days after tamoxifen injection, respectively (**Figure 2-2B**). We also analyzed rotarod performance to measure the motor function of KI mice. In agreement with the body weight loss result, 14-month-old KI mice had the worst performance, as the time they stayed on a rotating rod was significantly shorter than the age-matched controls, and this motor function deficiency started earlier (day 9 after

tamoxifen injection) than in 3- and 9-month-old KI mice (day 15 after injection) (**Figure 2-3A**). To further characterize the motor deficit, 1.5 months after tamoxifen injection, KI mice at different ages were subjected to balanced beam assay. The performance of 3-month-old KI mice was comparable to age matched controls, whereas 14-month-old KI mice spent significantly longer time to walk through the beam, suggesting an age-related decline in motor coordination and activity (**Figure 2-3B**). Ataxia is a definitive phenotype of SCA17 and results in gait abnormality. Using foot printing assay, we found that gait abnormality was most apparent in 14-month-old KI mice (**Figure 2-3C**), as stride length of 14-month-old KI mice was significantly decreased when compared with 3 and 9-month-old KI mice (**Figure 2-3D**).

Next, we wanted to correlate the phenotypes observed in KI mice with Purkinje neuron degeneration, a characteristic neuropathological feature seen in both SCA17 patients (Rolfs et al., 2003) and previously established SCA17 mouse models (Friedman et al., 2007; Huang et al., 2011). Compared with 16-month-old wild-type mice, immunostaining with an antibody to calbindin, a specific marker protein for Purkinje cells, revealed that the 14-month-old KI mice after 2 months of tamoxifen injection had the most severe Purkinje neuron loss, as the molecular layer thickness and dendritic branches were also significantly decreased; the 9-month-old KI mice had a modest level of degeneration, whereas the Purkinje neurons in the 3-month-old group remained largely intact (**Figure 2-4A, B, C**). These results were further confirmed by conventional Nissl and Golgi staining (**Figure 2-4D, E**). Western blotting analysis of the ratio of calbindin to actin in the cerebellum of KI mice at different ages also verified that the older KI mice showed greater loss of Purkinje cells after turning on the expression of mutant TBP by tamoxifen injection (**Figure 2-5A, B**). Because

the tamoxifen induction time was the same for KI mice at different ages, all these results unequivocally suggest that aging accelerates the disease progression and neurodegeneration in our SCA17 KI mouse model.

Aging promotes mutant TBP accumulation in TBP105Q inducible KI mice.

To assess whether aging influences the expression levels of mutant TBP, we used western blots to examine the levels of SDS soluble mutant TBP, because mounting evidence suggests that in polyQ disease models, soluble mutant protein is more pathogenic than aggregated proteins (Nagai et al., 2007; Takahashi et al., 2008). Three months after tamoxifen induction, there were higher levels of mutant TBP in the cortex and the cerebellum of 9- and 14-month-old KI mice than 3-month-old KI mice (**Figure 2-6A, B**). However, semi-quantitative RT-PCR showed similar amounts of mutant TBP transcripts in 3- and 9-month-old KI mice after tamoxifen injection (**Figure 2-6C, D**), suggesting that mutant TBP tends to accumulate in aged neurons at the protein level. Consistent with our previous transgenic mouse model (Friedman et al., 2007), there is a reduced amount of wild-type TBP protein in the presence of mutant TBP (**Figure 2-7A, B**). To rule out the possibility that the reduced wild-type TBP protein is due to only one functional allele of wild-type TBP in KI mice, we compared wild type TBP level in KI mice with or without tamoxifen injection. Wild type TBP was only decreased when mutant TBP was induced by tamoxifen injection in KI mice (**Figure 2-7C, D**), suggesting that the total amount of TBP is tightly regulated and expression of mutant TBP can down-regulate wild type TBP, presumably due to the critical functions of TBP.

Aging decreases chaperone activity and Hsc70 levels in mouse brain

There are three major cellular mechanisms to cope with misfolded proteins accumulated in the brain: the chaperone system, the ubiquitin-proteasome system (UPS), and the autophagy system (Gestwicki and Garza, 2012; Levine and Kroemer, 2008; Li and Li, 2011b). Several studies already implicate aging in impaired UPS activity in the central nervous system (Keller et al., 2000a; Keller et al., 2000b), but whether aging affects autophagy and chaperone function remains to be fully investigated. We first checked autophagy activity in the cortex and cerebellum of 3-, 12-, and 21-month-old wild-type mice by measuring the level of LC3B, a component of autophagosomes, and p62/SQSTM1, a polyubiquitin-binding protein degraded by autophagy. We saw no detectable differences of either LC3B or p62 between different ages (**Figure 2-8**), suggesting that autophagy activity in the brain is not significantly impacted by aging, at least under unstressed conditions.

We next focused on the chaperone system, which consists of a large family of proteins. To measure chaperone activity, we adopted an *in vitro* luciferase protection assay activity (Thulasiraman and Matts, 1998), in which brain lysate and recombinant luciferase were mixed together and incubated at a denaturing temperature (42ºC). At this temperature, the luciferase is thermally unstable and tends to misfold, whereas the chaperones in the brain lysates can prevent misfolding and maintain the luciferase activity. With chaperone inhibitor PU-H71 added into the mixture as a control, the specific chaperone activity could be quantified (**Figure 2-9A**). We found that the luciferase activity was significantly decreased with the lysates from aged cortex and cerebellum (**Figure 2-9B**), supporting the idea that chaperone activity declines during aging. We further explored which members of the

chaperones were responsible for this change. By individually checking each form of the major chaperones using western blotting analysis, we found that the protein levels of Hsc70 and Hsp90 were significantly decreased in the cerebellum of wild-type mice from 3 months to 21 months, whereas Hsp70 and Hsp40 levels remained stable **(Figure 2-9C, D).** Immunohistochemistry confirmed that Hsc70 level was reduced in the Purkinje cells of 18- and 24-month-old wild type mice compared with 6-month-old wild type mice (**Figure 2-9E**). Therefore, the age-related reduction of Hsc70 could explain the weakened luciferase protection and is also likely to accelerate mutant TBP accumulation in aged TBP105Q inducible KI mice.

2.5 Discussion

Although aging is a primary risk factor promoting neurodegeneration caused by misfolded proteins, differentiating the cumulative effects of misfolded proteins on neurons over time versus aging-related factors that may make neurons vulnerable to misfolded proteins has proved difficult. Using our SCA17 inducible KI mouse model, we provide convincing evidence that aged neuronal cells are more vulnerable to misfolded proteins and that this vulnerability is related to the age-dependent decline in chaperone activity.

Strong evidence for the above idea comes from SCA17 inducible KI mice expressing mutant TBP at the endogenous level for the same length of time: it is older KI mice that develop earlier and more progressive neurological phenotypes, as well as more severe degeneration of cerebellar Purkinje neurons. However, the protein levels are

determined not only by the time of synthesis, but also by degradation. We found that more soluble mutant TBP was present in older KI mouse brain than the younger KI mouse brains, suggesting that mutant TBP is more stable in older neurons. A decreased cellular capacity to clear misfolded proteins by the UPS is seen in different brain regions and different types of cells (Keller et al., 2000a; Keller et al., 2000b), which could account for the increased levels of mutant proteins. However, impaired UPS activity is unlikely to be the sole determinant of neurodegeneration, since other proteostatic mechanisms, such as chaperones and autophagy, are also involved in polyQ disease pathogensis, and the impact of aging on these two mechanisms has not been well defined.

An important finding in our study is that an age-dependent decrease in Hsc70 contributes to age-dependent neurodegeneration. Hsc70 is a constitutively expressed chaperone, which is different from other stress-induced chaperones, such as Hsp70 and Hsp40 (Brown, 2007; Kampinga and Craig, 2010; Liu et al., 2012). Although both constitutive and inducible types of chaperones are thought to have similar effects on protein refolding and protection against neuronal damage, how they are related to the aging-related neurodegeneration process remains unclear. We know that overexpression of Hsp70 or Hsp40 chaperones in cells and flies can reduce polyQ aggregation and toxicity (Chan et al., 2000; Cummings et al., 1998)**,** but has limited success in ameliorating the neurological symptoms of polyQ disease mouse models (Cummings et al., 2001; Helmlinger et al., 2004). We found that Hsc70, but not Hsp40 or Hsp70, is selectively reduced in the brain with age. When a cell ages, senescing signals arise, typically as a result of DNA damage due to oxidative stress or telomere shortening. Regulation of the expression of constitutive chaperones may be more sensitive to aging-related oxidative damage than other inducible

chaperones. The selective decrease of Hsc70 we see in the aged brain suggests that aging is more likely to affect the chaperoning function of unstressed neurons, which fits well with the slow and progressive decline of cellular function to cope with misfolded proteins in the aged brains. Hsc70 is also known to be involved in chaperone-mediated autophagy (CMA) by targeting proteins to lysosomes (Chiang et al., 1989). However, CMA activity is preserved in mice up to 12 months of age and could be upregulated by mutant polyQ proteins (Koga et al., 2011), so the decreased CMA function is unlikely to be involved in the neurotoxicity of mutant TBP in SCA17 KI mice younger than 12 months. In addition, mutant TBP is a nuclear protein whose turnover is unlikely to depend on the cytoplasmic CMA.

Figure 2-1

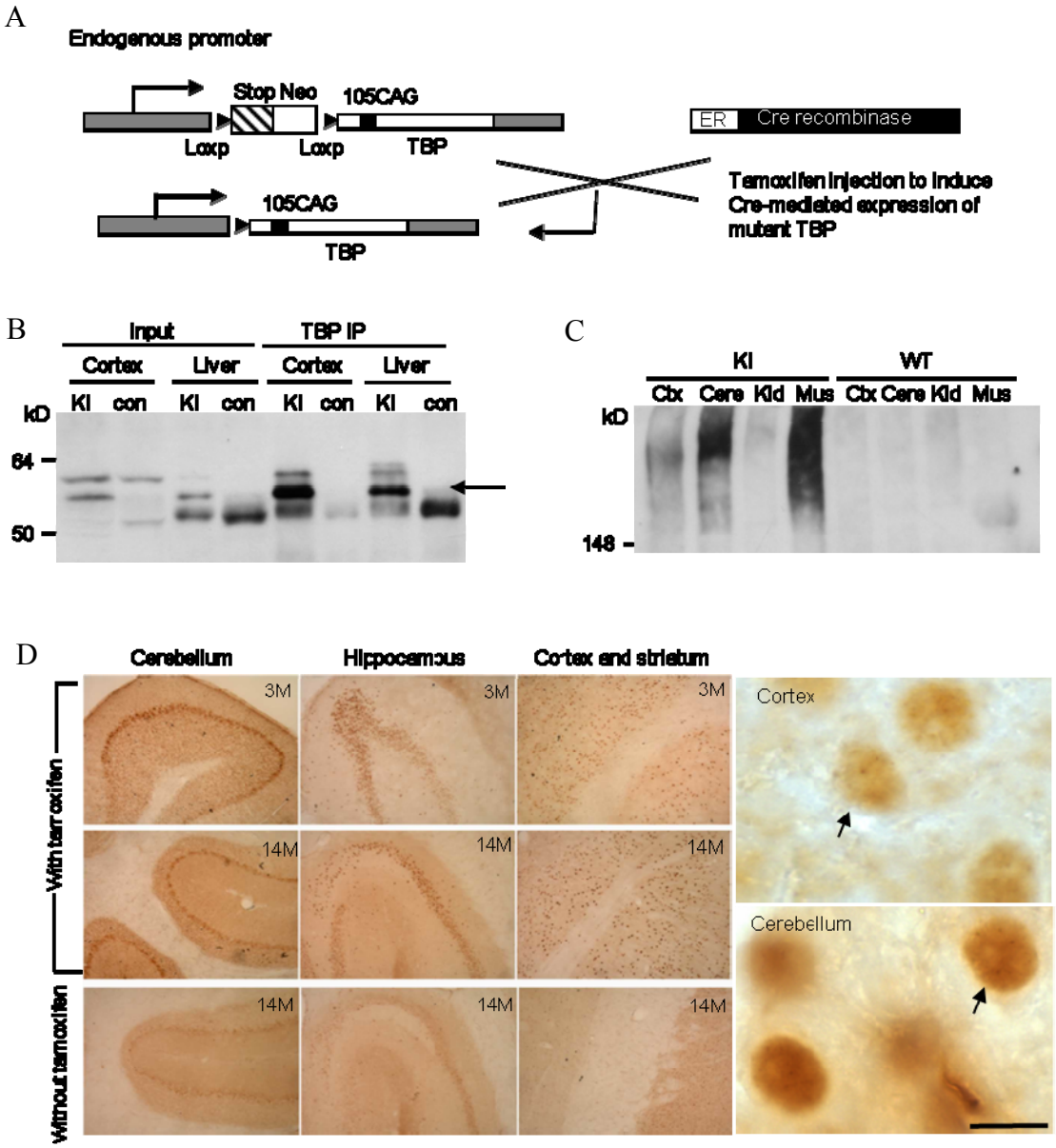
A
Endogenous promoter
Stop Neo
105CAG
Loxp
Loxp
TBP
ER
Cre recombinase
105CAG
TBP
Tamoxifen injection to induce Cre-mediated expression of mutant TBP
B
Input
TBP IP
Cortex
Liver
Cortex
Liver
KI
con
KI
con
KI
con
KI
con
kD
64
50
C
KI
WT
Cbx
Cere
Kid
Mus
Cbx
Cere
Kid
Mus
kD
148
D
Cerebellum
Hippocampus
Cortex and striatum
3M
3M
3M
14M
14M
14M
14M
14M
14M
With tamoxifen
Without tamoxifen
Cortex
Cerebellum

Figure 2-1 Charaterization of mutant TBP expression in TBP105Q inducible knock-in mouse model.

(A) A schematic illustration of expression of mutant TBP in TBP105Q inducible knock-in mice. (B) Western blotting analysis of immunoprecipitated TBP from the cortex and liver of wild-type (WT) and TBP105Q inducible knock-in (KI) mice after tamoxifen induction for two months. The rabbit polyclonal antibody EM192 was used to immunoprecipitate TBP, and the mouse monoclonal antibody 1C2 was used to visualize mutant TBP (arrow). (C) Mutant TBP aggregates in the stacking gel were clearly detected in the cortex (Ctx), cerebellum (Cere), and muscle (Mus) of TBP105Q inducible KI mice by anti-TBP (1TBP18), but not in the kidney (Kid). (D) 1C2 immunohistochemical study confirming mutant TBP expression in the cerebellum, hippocampus, cortex, and striatum of 3- and 14-month-old KI mice injected with tamoxifen. Small aggregates of mutant TBP were visualized in the nucleus under 100× magnification (arrows). Scale bars; 100 μm (left panel) and 5 μm (right panel).

Figure 2-2

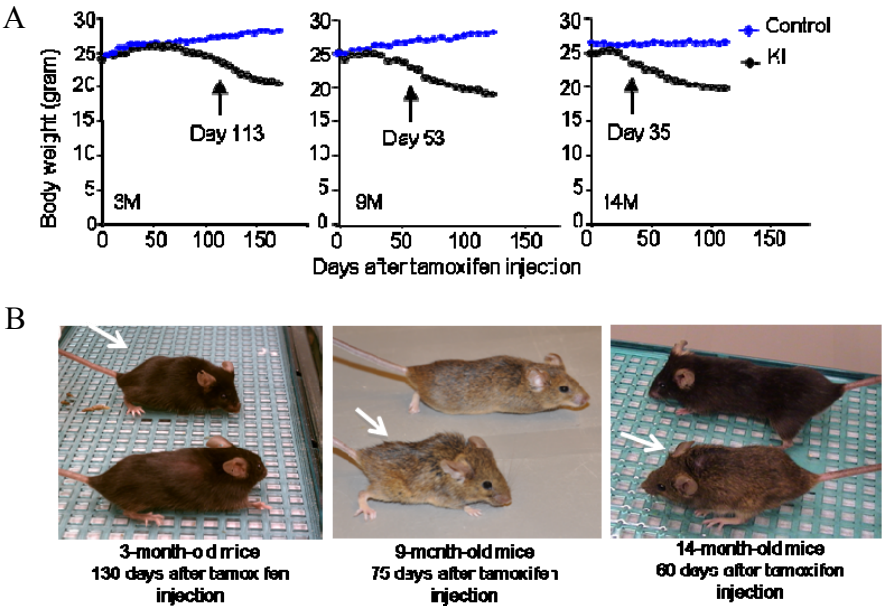
A
Body weight (gram)
Day 113
Day 53
Day 35
3M
9M
14M
Control
KI
Days after tamoxifen injection
B
3-month-old mice
130 days after tamoxifen injection
9-month-old mice
75 days after tamoxifen injection
14-month-old mice
60 days after tamoxifen injection

Figure 2-2 Characterization of body weight loss in TBP105Q inducible knock-in mouse model.

(A) TBP105Q inducible KI and control mice at 3, 9, or 14 months of age were injected with tamoxifen to induce the expression of mutant TBP. The older KI mice showed earlier onset of body weight loss (day 35 for 14-month, P=0.0374) than the younger KI mice (day 53 for 9-month, P=0.0125, and day 113 for 3-month, P=0.0438) after tamoxifen injection (n=9-11 each group, two-way ANOVA, P<0.0001). (B) Representative images of differently aged (3, 9, and 14 months) KI mice (white arrow) were taken at indicated days after tamoxifen injection.

Figure 2-3

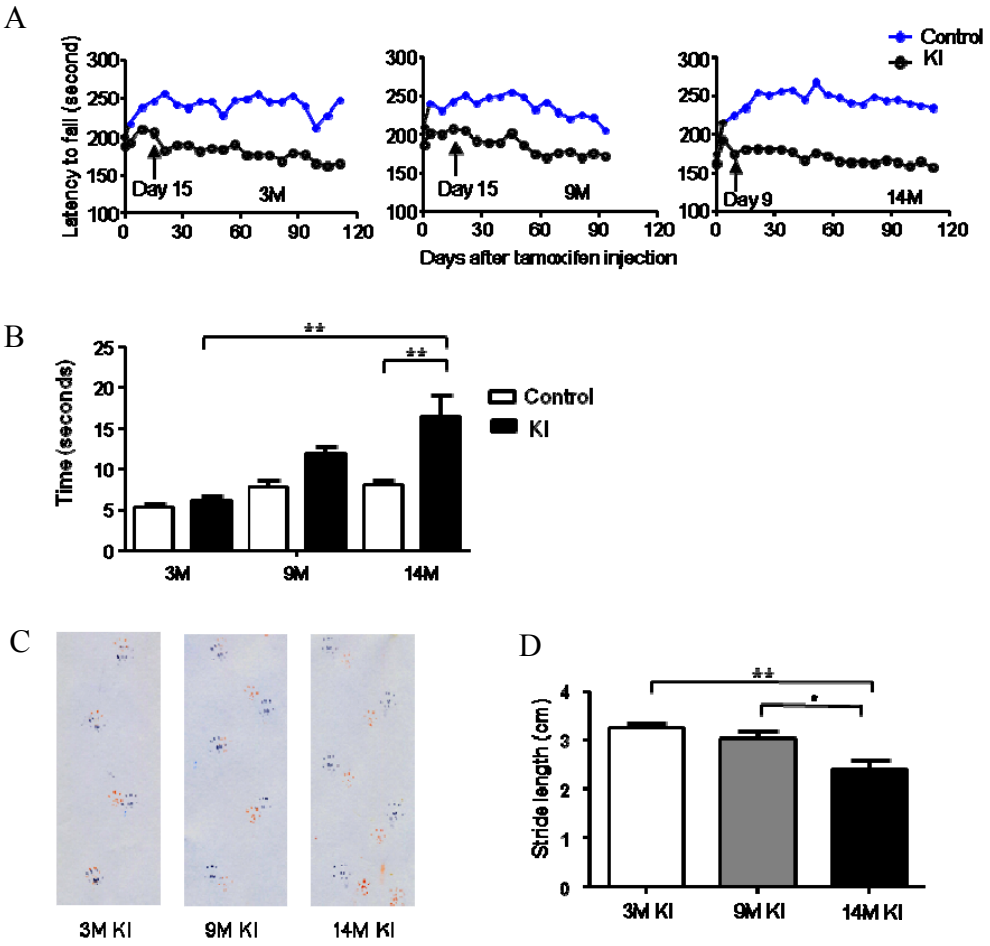
A
Latency to fall (second)
Day 15
3M
Day 15
9M
Day 9
14M
Control
KI
Days after tamoxifen injection
B
Time (seconds)
Control
KI
3M
9M
14M
C
3M KI
9M KI
14M KI
D
Stride length (cm)
3M KI
9M KI
14M KI

Figure 2-3 Characterization of motor impairment in TBP105Q inducible knock-in mouse model.

(A) Motor activity of mice injected with tamoxifen at 3, 9, and 14 months of age was analyzed by rotarod test. The older KI mice (day 9 for 14-month, P=0.0031) showed earlier onset of motor impairment than the younger KI mice (day 15 for 9-month, P=0.0298, and day 15 for 3-month, P=0.0217) after tamoxifen injection (n=9-11 each group, two-way ANOVA, $P < 0.0001$). (B) Motor coordination of mice was tested by balance beam walking assay 1.5 months after tamoxifen injection. The walking time of older TBP105Q inducible KI mice on the beam is significant longer than young KI mice (n=6; $^{**}P < 0.01$). (C, D) Foot printing assay of gait performance of TBP105Q inducible KI mice injected with tamoxifen at 3, 9, and 14 months of age to induce the expression of mutant TBP (n=6, $^{*}P<0.05$; $^{**}P<0.01$). Data are represented as mean ± SEM.

Figure 2-4

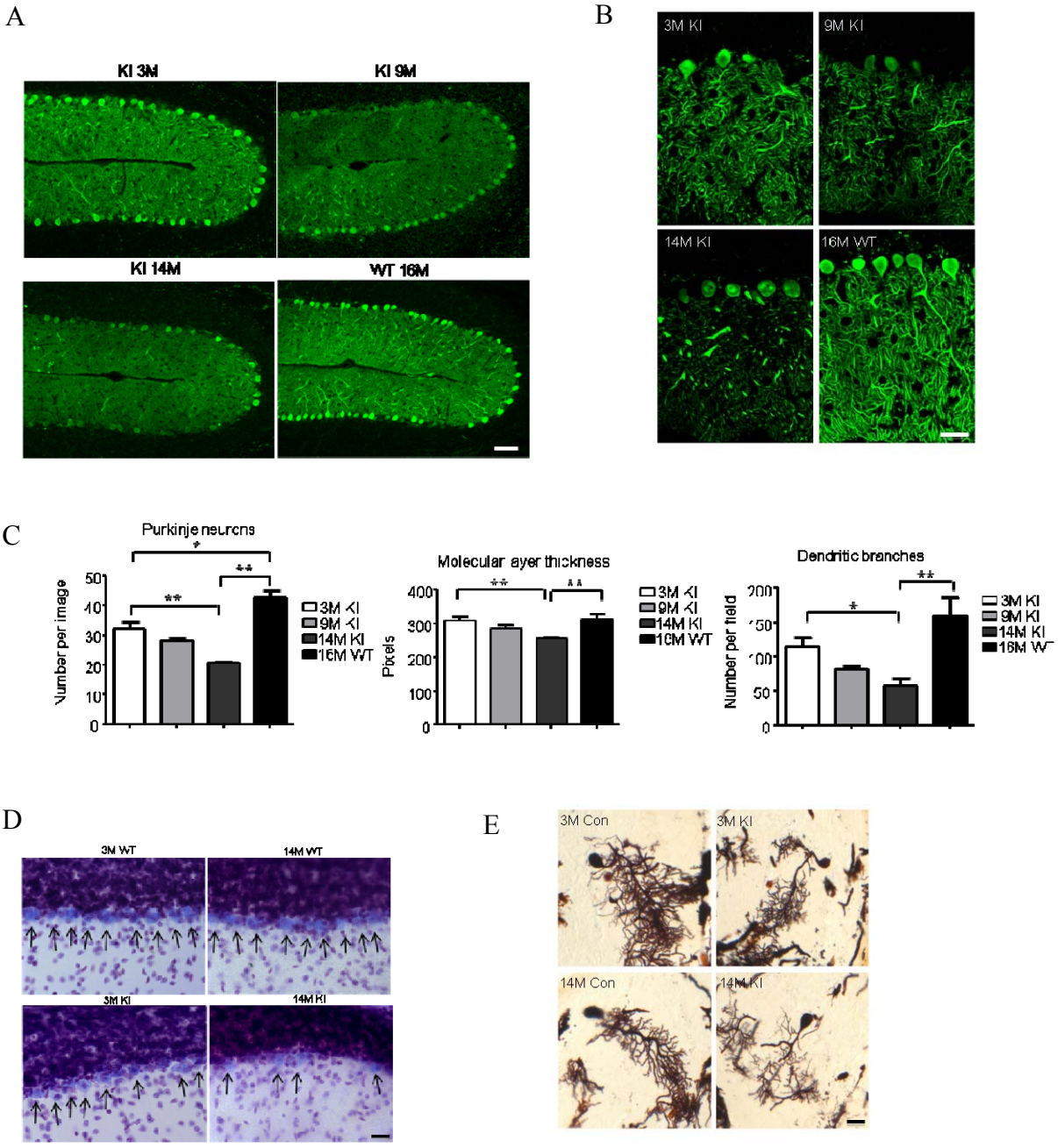
A
KI 3M
KI 9M
KI 14M
WT 16M
B
3M KI
9M KI
14M KI
16M WT
C
Purkinje neurons
Number per image
3M KI
9M KI
14M KI
16M WT
Molecular ayer thickness
Pixels
Dendritic branches
Number per field
D
3M WT
14M WT
3M KI
14M KI
E
3M Con
3M KI
14M Con
14M KI

Figure 2-4 Characterization of Purkinje cell degeneration in TBP105Q inducible knock-in mouse model.

(A, B) Degeneration of Purkinje neurons labeled by anti-calbindin in the cerebellum of KI mice injected with tamoxifen at different ages. WT mouse at 16 months of age served as a control. Scale bar: 50 μm. (C) Quantification of Purkinje neuron number, molecular layer thickness, and dendritic branches in TBP105Q inducible KI mice at different ages (n=6-8; $*P < 0.05$, $**P < 0.01$). (D) Nissl staining result of Purkinje cells from WT and TBP105Q inducible KI mice at 3 and 14 months of age. (E) Golgi staining result of Purkinje cells from differently aged KI mice and controls. Data are represented as mean ± SEM.

Figure 2-5

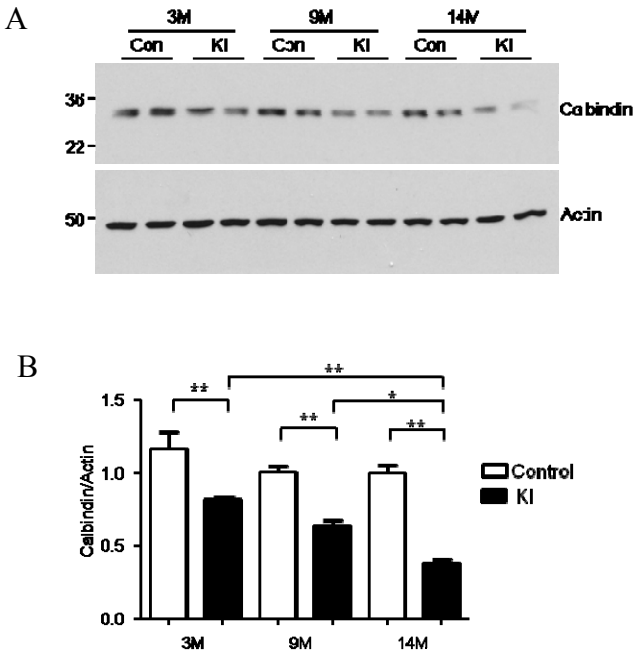
A
3M
9M
14M
Con
KI
Con
KI
Con
KI
36
22
50
Calbindin
Actin
B
Calbindin/Actin
1.5
1.0
0.5
0.0
**
**
**
*
**
Control
KI
3M
9M
14M

Figure 2-5 Loss of calbindin in the cerebellum of TBP105Q inducible knock-in mouse model.

(A) Western blotting (B) and quantitative analysis of calbindin protein level in the cerebellum of 3-, 9-, and 14-month-old TBP105Q inducible KI mice. Actin was used as a loading control (*$P < 0.05$, **$P < 0.01$). Data are represented as mean ± SEM.

Figure 2-6

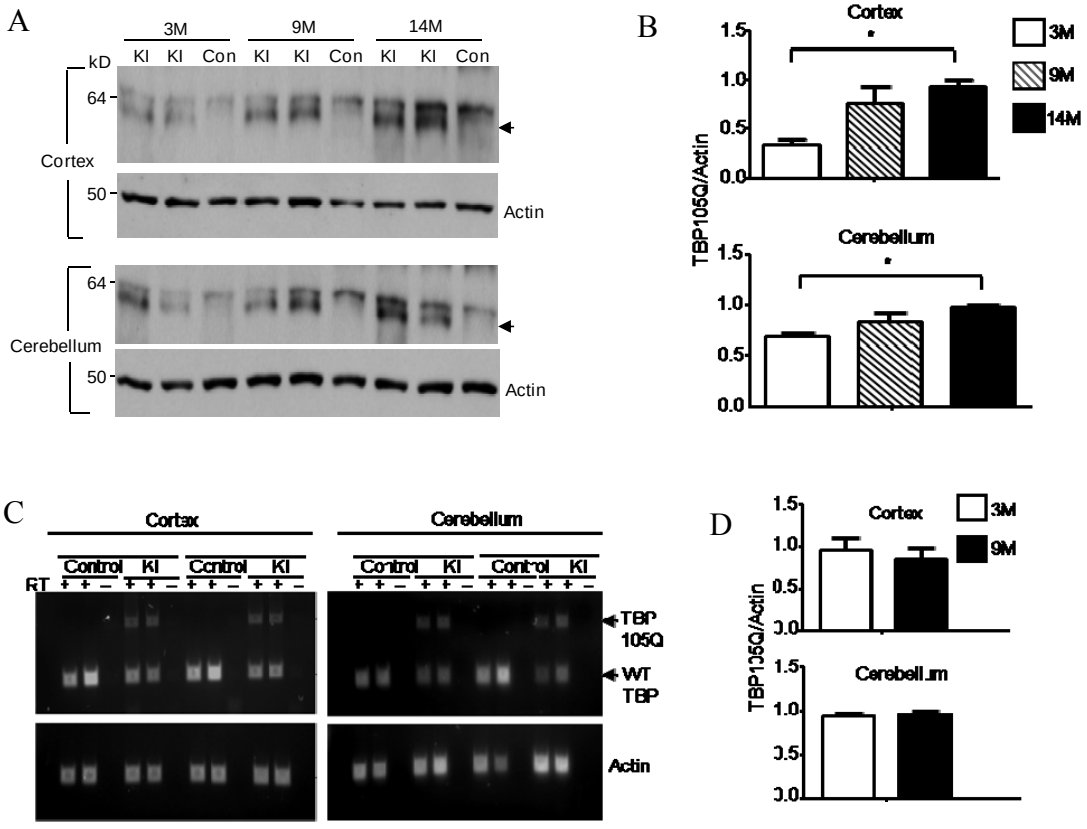
A
3M
9M
14M
kD
KI KI Con KI KI Con KI KI Con
64
Cortex
50
Actin
64
Cerebellum
50
Actin
B
Cortex
3M
9M
14M
TBP105Q/Actin
1.5
1.0
0.5
0.0
Cerebellum
C
Cortex
Cerebellum
Control KI Control KI Control KI Control KI
RT
TBP 105Q
WT TBP
Actin
D
Cortex
3M
9M
TBP105Q/Actin
Cerebellum

Figure 2-6 Age-related increase of mutant TBP in TBP105Q inducible knock-in mice.

(A) Western blotting analysis of soluble mutant TBP levels in the cortex and cerebellum of 3-, 9-, and 14-month old TBP105Q inducible KI mice. An age-related increase of soluble mutant TBP (arrow) was observed in KI mice. Control mice (Con) did not show mutant TBP expression. Actin was used as a loading control. (B) Quantification of the relative amount of TBP (the ratio of TBP to actin) on western blots (*$P < 0.05$). (C) RT-PCR revealed similar mRNA levels of mutant TBP in both the cortex and cerebellum of 3- and 9-month-old TBP105Q inducible KI mice. Actin was used as an internal control. (D) The ratio of mutant TBP to actin transcripts in RT-PCR is quantified. Data are represented as mean ± SEM.

Figure 2-7

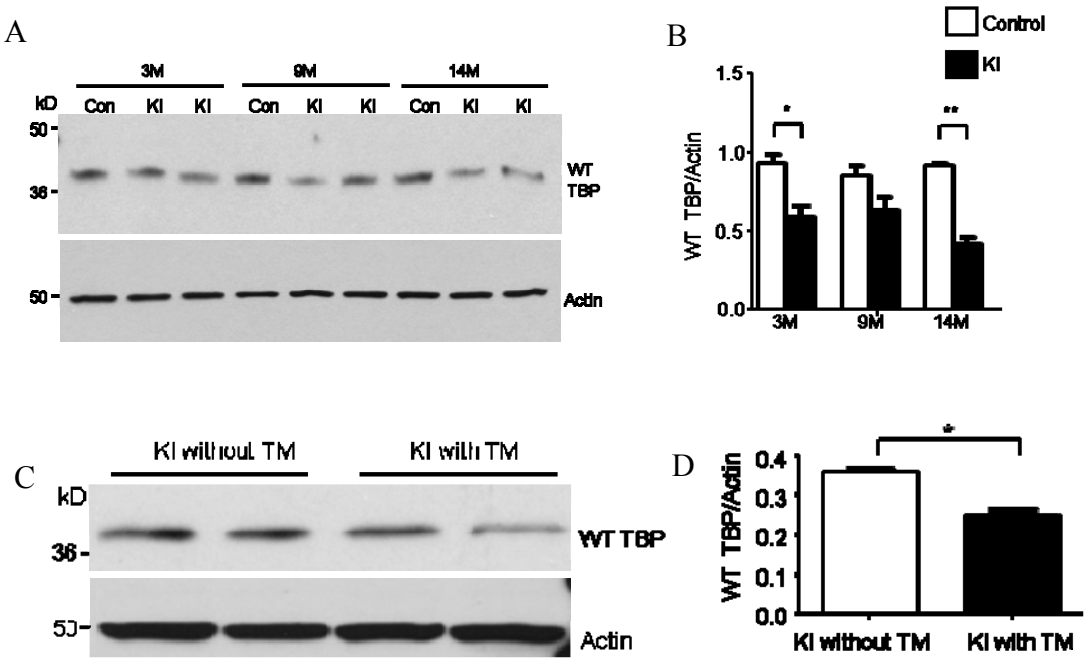
A
3M
9M
14M
kD
Con
KI
KI
Con
KI
KI
Con
KI
KI
50
36
WT TBP
50
Actin
B
Control
KI
1.5
1.0
0.5
0.0
WT TBP/Actin
*
**
3M
9M
14M
C
KI without TM
KI with TM
kD
36
WT TBP
50
Actin
D
*
0.4
0.3
0.2
0.1
0.0
WT TBP/Actin
KI without TM
KI with TM

Figure 2-7 Age-related decrease of wild-type TBP in TBP105Q inducible knock-in mice.

(A) Western blotting analysis of the expression of mouse endogenous wild-type TBP in the cerebellum of TBP105Q inducible KI and wild-type mice (WT) at 3, 9, and 14 months of age. (B) Quantitative analysis of WT TBP level on western blots by measurement of its ratio to actin (**P* < 0.05, ***P* < 0.01). (C) TBP105Q inducible KI mouse cerebellum with tamoxifen (TM) induction showing a reduction in WT TBP level. (D) The ratio of WT or TBP to actin is also quantified (* *P*<0.05). Data are represented as mean ± SEM.

Figure 2-8

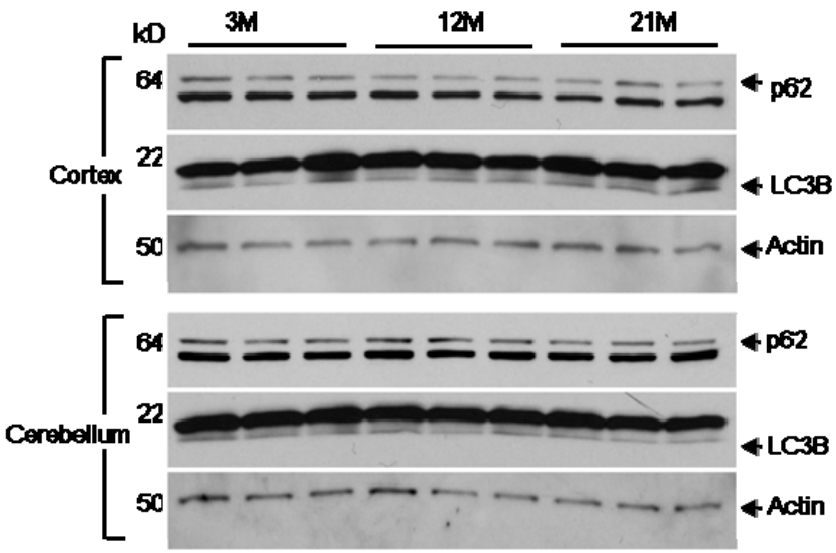
kD
3M
12M
21M
64
22
50
Cortex
p62
LC3B
Actin
64
22
50
Cerebellum
p62
LC3B
Actin

Figure 2-8 Autophagy activity in differently aged wild-type mouse brain.

Western blotting analysis of p62 and LC3B level in the cortex and cerebellum of 3-, 12-, and 21-month-old wild-type mice. No significant difference was found among three age groups.

Figure 2-9

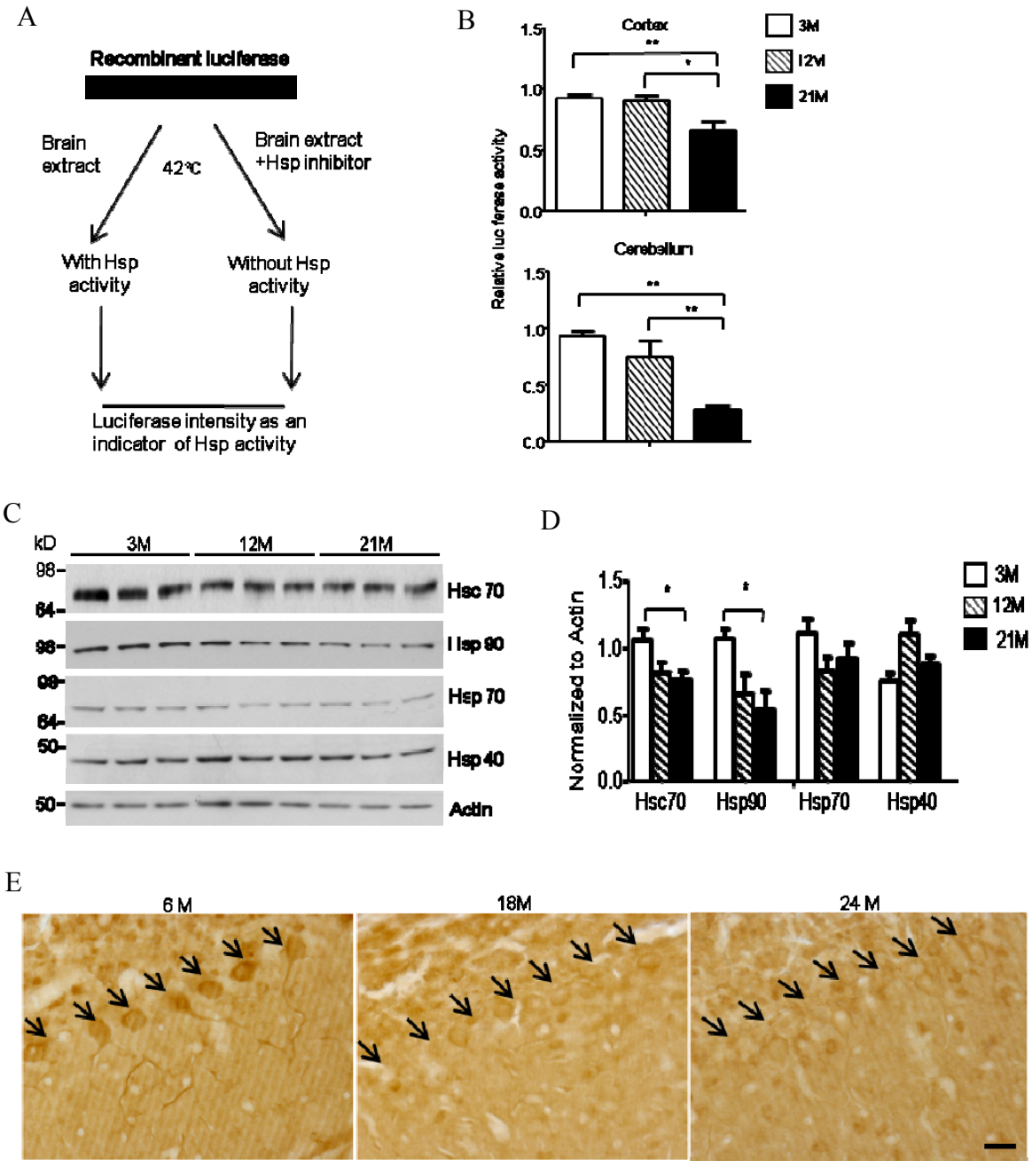
A
Recombinant luciferase
Brain extract
42℃
Brain extract +Hsp inhibitor
With Hsp activity
Without Hsp activity
Luciferase intensity as an indicator of Hsp activity
B
Cortex
Cerebellum
Relative luciferase activity
3M
12M
21M
C
kD
3M
12M
21M
Hsc 70
Hsp 90
Hsp 70
Hsp 40
Actin
D
Normalized to Actin
Hsc70
Hsp90
Hsp70
Hsp40
E
6 M
18M
24 M

Figure 2-9 Age-dependent decrease in chaperone activity and Hsc70 level in wild-type mouse brain.

(A) Luciferase protection assay was performed by incubating recombinant luciferase with lysates from either the cortex or cerebellum of 3-, 12-, and 21-month-old wild-type mice. Hsp inhibitor PU-H71 was added to the incubation to obtain Hsp-specific activity. (B) Decreased luciferase intensity was observed when brain lysates of 12- or 21-month-old mice were used, indicating an age-related decrease of chaperone activity in the cortex and cerebellum (*$P < 0.05$, **$P < 0.01$). (C) Western blot analysis of major chaperones using the cerebellum tissue from 3-, 12-, and 21-month-old wild-type mice. Actin was used as a loading control. (D) The relative levels of Hsp were normalized by actin for quantification. Hsc70 and Hsp90 showed a significant decrease with aging (*$P < 0.05$, **$P < 0.01$). (E) Hsc70 immunostaining showing age-dependent decrease in Hsc70 expression in Purkinje cells in wild type mice at different ages (6, 18, and 24 months). Arrows indicate Purkinje cells. Scale bar: 20 μm. Data are represented as mean ± SEM.

Chapter 3

Age dependent decrease of MANF contributes to region specific neurodenegeration in SCA17

This chapter includes work published as Su Yang, Shanshan Huang, Marta A. Gaertig, Xiao-Jiang Li, and Shihua Li (2014) *Neuron,* January 22; 81: 349-365. The majority of the work was done by Su Yang. Marta Gaertig helped with mouse breeding. Xiao-Jiang Li and Shihua Li helped with experimental design and data analysis. Xiao-Jiang Li edited the manuscript for publication.

3.1 Abstract

Mutant TBP is ubiquitously expressed in SCA17 patients, yet causes selective neurodegeneration in the cerebellum, with the Purkinje cells being the most vulnerable. The mechanism behind this region specific neuronal death remains largely unknown. We identified mesencephalic astrocyte derived neurotrophic factor (MANF) as a target that is specifically downregulated in the cerebellum of inducible TBP105Q inducible KI mice. Mutant TBP shows decreased association with XBP1s, an endoplasmic reticulum (ER) stress induced transcription factor, resulting in the reduced transcription of MANF. Overxpression of Hsc70 improves the TBP-XBP1s interaction and MANF transcription, and overexpression of MANF by lentiviral vector infection and transgenic mouse approach ameliorates mutant TBP–mediated Purkinje cell degeneration. These results suggest cerebellum specific reduction of MANF could lead to the pathogenesis of SCA17.

3.2 Introduction

Mutant TBP in aged neurons can selectively affect the expression of certain neuronal proteins to cause selective neurodegeneration. To identify such targets, a previous graduate student in our lab performed a microarray study using cerebellum tissues from mutant TBP transgenic mice. The microarray resulted showed that the mRNA level of nearly 200 transcripts have changed, either increased or decreased, in mutant TBP transgenic mice, as compared with wild-type TBP transgenic mice (Friedman et al., 2007). We examined the microarray result, and one interesting candidate was mesencephalic astrocyte derived neurotrophic factor (MANF), which is alternatively named arginine-rich, mutated in early stage tumors (ARMET). Mutations in the gene

encoding ARMET were found in various cancers, such as pancreatic, lung, breast, and prostate cancers (Shridhar et al., 1996a; Shridhar et al., 1996b; Shridhar et al., 1997), suggesting ARMET may play an important role in maintaining cell survival and proliferation. However, contradictory reports found a high frequency of genetic changes in ARMET encoding genetic sequence in primary head and neck, esophageal, lung and renal cell cancers, indicating those variations represent normal polymorphisms, rather than cancer causing mutations (Evron et al., 1997; Tanaka et al., 2000).

Nevertheless, emerging evidence argues that MANF plays a potential protective role on neuronal survival. Addition of MANF protein purified from astrocyte culture medium or bacterial source protected dopaminergic neurons in primary culture and a Parkinson's disease rat model (Petrova et al., 2003; Voutilainen et al., 2009), indicating like other classical neurotrophic factors, MANF is able to modulate neuronal survival extracellularly, through an unknown receptor. On the other hand, MANF is proposed to function inside the cell as well, since evidences suggest MANF is a soluble ER protein induced by the unfolded protein response (UPR), and is able to suppress apoptosis through its C-terminal domain, which is homologous to the SAP domain of Ku70, a well characterized inhibitor of proapoptotic Bcl-2 assoicated X protein (Bax) (Hellman et al., 2011; Mizobuchi et al., 2007).

The fact that MANF is a ER protein prompted people to study if the transcription of MANF is regulated in an ER stress related fashion. Indeed, an ER stress response element (ERSE) located around 150 bp upstream of the MANF transcription initiation site is known to play a critical role in regulating MANF transcription and is recognized by two transcription factors NFY and XBP1 (Mizobuchi et al., 2007). Interestingly, our previous

study found mutant TBP could impair NFY activity by enhanced association with NFY (Huang et al., 2011). Whether XBP1 functioning is also influenced by mutant TBP remains to be determined. XBP1 a transcription factor that is activated during ER stress and upregulates genes important for protein folding, maturation, and degradation (Lee et al., 2003). The activation of XBP1 involves an unconventional mechanism: an ER transmembrane kinase IRE1 splices a 26-nucleotide intron from XBP1 mRNA. This splicing event leads to a frame shift, which converts the biologically inactive XBP1u (unspliced) to its active form, XBP1s (spliced) (Yoshida et al., 2001).

In this chapter, we describe that MANF is downregulated in the cerebellum, especially in the Purkinje cell layer, in the presence of mutant TBP. Mutant TBP binds weakly to the transcription factor XBP1s and mediates less MANF transcription, which can be reversed by Hsc70 overexpression. Overexpression of MANF by lentiviral vector infection and transgenic mouse approach ameliorates toxicity caused by mutant TBP in Purkinje cells in SCA17 KI mice. These results demonstrate the decrease of MANF in the cerebellum could be a novel mechanism underlying SCA17 pathogenesis, and propose that increasing MANF activity is a potential therapeutic approach to treat SCA17.

3.3 Materials and Methods

Antibodies and plasmids

Primary antibodies from commercial sources used include: 1C2 (Millipore/Chemicon, MAB1574), 1TBP18 (QED bioscience, 70102), calbindin (Millipore/ Chemicon), Hsc70

(Santa Cruz, 7298), Actin (Sigma, A5060), MANF (LSBio, C53208, B2688; Abcam, ab67271), GFP (BD Living Colors, 632376), XBP1 (Santa Cruz, 7160), Flag (Cell Signaling, 2368), BDNF (Santa Cruz, 546), and HA (Cell Signaling, 2367).

XBP1u, and XBP1s plasmids were provided by Dr. David Ron. TBP13Q and TBP105Q plasmids were generated as described before (Friedman et al., 2007).

Mouse lines

To generate MANF transgenic mice, MANF cDNA linked with HA sequence was inserted into previously described vector containing prion promoter (Friedman et al., 2007). The vector was sent to Transgenic Mouse & Gene Targeting Core at Emory University for microinjection. Primers used for genotyping of transgenic MANF were forward: 5'-ATT GAC CTG AGC ACA GTG GAC CTG-3'; reverse: 5'-GTC ACT GTC ACC TTG TAC TCT GG-3'.

To generate germ-line knock-in (SCA17 KI) mice, heterozygous TBP105Q floxed mice were crossed with EIIa-Cre transgenic mice (The Jackson Laboratory, B6.FVB-Tg (EIIa-Cre) C5379Lmgd/J), in which Cre transgene under the control of the adenovirus EIIa promoter is expressed in germline cells that transmit the genetic alteration to progeny.

Cell culture, neurite outgrowth and MTS assay

Cell culture method has been described in Chapter 2

The neurite outgrowth assay and MTS assay of stably transfected TBP105Q PC12 cells have been described in previous studies (Friedman et al., 2007; Shah et al., 2009). Briefly, after plating the cells, MANF lentivirus (10^9/ml titer) was added into culture medium at 1:1000 dilution. For the neurite outgrowth assay, 1 day after infection, PC12 cells were treated with 100 ng/ml nerve growth factor in culture medium for 2 days. For MTS assay, 2 days after infection, PC12 cells were treated with 2 μM staurosporine in culture medium for 12 hours.

RNA isolation, reverse transcriptase PCR and real time PCR

Methods for RNA isolation and reverse transcriptase PCR have been described in Chapter 2.

For semi-quantitative PCR, primers used are lested below. For MANF, forward: 5'-ATG GAT CCA GGA TGT GGG CTA CGC-3'; reverse: 5'-ATG AAT TCC AGA TCA GTC CGT GCG-3'. For Actin, forward: 5'-TGA GAC CTT CAA CAC CCC AG-3'; reverse: 5'-GTG GTG GTG AAG CTG TAG CC-3'

For real time PCR, RealMasterMix 2.5× from 5 Prime was used. The PCR reaction was performed in Mastercycler realplex (Eppendorf). Primers used are listed below. For MANF, forward: 5'-ATT GAC CTG AGC ACA GTG GAC CTG-3'; reverse: 5'-TTC AGC

ACA GCC TTT GCA CAT CTC-3'. For Actin, forward: 5'-TCA CTG TCC ACC TTC CAG CAG ATG-3'; reverse: 5'-CTC AGT AAC AGT CCG CCT AGA AGC-3'

Promoter transcriptional activity assay

Mouse MANF promoter (-300 bp to 0 bp) was isolated from mouse genomic DNA by PCR with forward primer 5'-TAG GTA CCC CAA CAT GGC GAC C-3' and reverse primer 5'-ATC AAG CTT CCT CCT CAG CCG TCT C-3'. Promoter with XBP1 binding site deletion was created by PCR with the same forward primer and a different reverse primer 5'-ATC AAG CTT GAT GTT GCC CAG GAG C-3'. The isolated promoters were inserted into the pGL4.14 reporter construct (Promega) using HindIII and KpnI restriction sites. Lipofectamine (Invitrogen) was used to transfect the luciferase reporter together with other indicated plasmids into HEK293 cells. Two days after transfection, cells were collected, and luciferase reporter assay was performed using ONE-Glo Luciferase Assay System (Promega). Luciferase intensity was measured by Synergy H4 microplate reader.

Chromatin immunoprecipitation (ChIP)

HEK293 cells were transfected with TBP (13Q or 105Q) and XBP1s plasmids and collected 2 days after transfection. Cells were fixed with 1% formaldehyde for 10 minutes at 37℃, and transferred to SDS lysis buffer. DNA was sheared by 10 seconds × 10 sonication. After that, ChIP was performed according to the manual of ChIP assay kit (Millipore, 17-

295). Flag antibody (Cell Signaling, 2368) was used to pull down XBP1s. Primers used for semi-quantitative PCR are listed as follows. Forward: 5'-ACT CTC TAG GTC CCA GAC AGC AGC-3'; reverse: 5'-ATG GGC TGG AAC AGA AAC CTG AG-3'.

Viral vector and generation

To generate MANF lentivirus, MANF cDNA was used for PCR cloning with primers (forward: 5'-ATG GAT CCA GGA TGT GGG CTA CGC-3'; reverse: 5'-ATG AAT TCC AGA TCA GTC CGT GCG-3'). PCR product was in-frame fused with F2A-ECFP fragment and inserted into pFUGW lentiviral vector. Viral Hsc70 were expressed via adenoviral vectors. Lentiviral MANF and GFP viruses were produced at The Viral Vector Core at Emory University and adenoviral Hsc70 viruses were obtained from Vector Biolabs.

Stereotaxic injection and quantification of neuronal degeneration

For virus injection into the mouse cerebellum, mice were anesthetized with a 2.5% solution of Avertin (Sigma, T48402) at 0.15 ml per 10 g body weight intraperitoneally. The mice were then stabilized on a stereotaxic instrument (David Kopf Instruments). The location for injection was determined according to the distance from bregma: anterior-posterior=-6.3 mm, medial-lateral=±1.7 mm, dorsal-ventral = -1.5 mm. Small holes were drilled on the skull, and a 30-gauge Hamilton microsyringe was used to deliver the virus. The delivery speed was set to 200 nl per minute. The microsyringe was kept for 5 minutes

after injection, and retracted in 10 minutes. The wound was sutured, and Meloxican as well as penicillin/streptomycin was applied. After surgery the mice were placed on heated blankets to recover from anesthetic.

Methods for quantifying neuronal degeneration have been described in Chapter 2.

Statistical analysis

For mouse behavioral analysis, each group consisted of at least 6 animals. For western blotting analysis, immunostaining, or other biochemical assays, data were generated from 3 or more experiments, and the results were expressed as mean ± SEM. Statistical significances were calculated based on either t-test, one-way ANOVA or two-way ANOVA. A P-value of <0.05 was considered significant.

3.4 Results

Age-related decrease of mesencephalic astrocyte derived neurotrophic factor (MANF) specifically occurs in the cerebellum of TBP105Q inducible KI mice

To confirm our previous microarray result, we performed western blotting analysis using brain samples from differently aged TBP105Q inducible KI mice two months after tamoxifen injection. Interestingly, we found that MANF was significantly decreased in the cerebellum from 9- and 14-month-old KI mice, which is consistent with increased mutant

TBP with age following tamoxifen injection (**Figure 3-1A, B**). We also checked another neurotrophic factor, BDNF, but found its level was comparable with wild-type and KI mice (**Figure 3-1C, D**). These results suggest that MANF is selectively reduced by mutant TBP. Immunohistochemistry showed MANF was enriched in the Purkinje cell layer and was lost in 14-month-old KI mice (**Figure 3-2A**). However, MANF staining intensity in other brain regions, including the cortex, striatum, and brain stem, was indistinguishable between WT and 14-month-old KI mice (**Figure 3-2B**). We did the same immunostaining of a 12-month-old HdhQ150 knock-in mouse and saw a clear enrichment of MANF in the Purkinje cell layer (**Figure 3-2C**). All these findings indicate that mutant TBP can specifically downregulate MANF in Purkinje cells.

To investigate whether mutant TBP affects the mRNA level of MANF, we performed semi-quantitative PCR. We saw a decreased level of MANF transcripts in the cerebellum of KI mice in which mutant TBP was induced at 9 months of age, but no such decrease in the cortex or in the cerebellum of KI mice that started to express mutant TBP at 3 months (**Figure 3-3A**); the decrease was further verified by quantitative PCR via a real-time PCR assay (**Figure 3-3B**). Based on these results, we conclude that an age-related and tissue-specific reduction of MANF mRNA underlies the decrease of its protein expression.

Expanded polyQ disrupts the interaction between TBP and XBP1s and impairs the transcription of MANF

Since the MANF mRNA level is decreased in the presence of mutant TBP, we reasoned that mutant TBP could impair MANF transcriptional activity. However, no TATA box sequence is present in the MANF promoter region, indicating that TBP regulates MANF transcription via other transcription factors.

We hypothesized that mutant TBP affects XBP1s-mediated MANF expression in aged neurons. Although we have found that Hsc70 and Hsp90 decrease in the aged brain, Hsc70 has been reported to maintain the protein-DNA binding complex for gene transcription (Gehring, 2004; Li et al., 2008; Niyaz et al., 2001; Zeiner et al., 1999). Thus, we wanted to compare the effects of normal and mutant TBP on the binding of XBP1s to the MANF promoter and also wanted to know whether Hsc70 can influence this binding. To explore this, we needed to use cultured cells to express different TBP and Hsc70. We first performed chromatin immunoprecipitation (ChIP) of HEK293 cells that were transfected with XBP1s and TBP (either 13Q or 105Q) constructs (**Figure 3-4A**). Anti-Flag antibody was used to pull down flag-tagged XBP1s. DNA was recovered from the pull-down lysates and used as a template for semi-quantitative PCR of the MANF promoter. As compared with TBP13Q, TBP105Q significantly reduced the association of the MANF promoter with XBP1s (**Figure 3-4B, C**).

Earlier literature indicates that TBP and XBP1s are present in the same transcriptional complex (Hetz, 2012). We wanted to know whether mutant TBP shows altered association with XBP1s, which may account for the decreased association of XBP1s with the MANF promoter, and whether Hsc70 can improve the function of mutant TBP. To this end, HEK293 cells were transfected with XBP1s and TBP (either 13Q or 105Q) in the

absence or presence of Hsc70. Transfected XBP1s was then precipitated by anti-XBP1 antibody. Significantly less TBP105Q than TBP13Q was co-precipitated with XBP1s, suggesting that polyQ expansion impairs the interaction between TBP and XBP1s. Furthermore, overexpression of Hsc70 greatly increased the level of both TBP13Q and TBP105Q pulled down, indicating that Hsc70 facilitates the association between TBP and XBP1s (**Figure 3-5A, B**).

To functionally assess the effect of mutant TBP on the transcription of MANF, we generated a luciferase reporter that is expressed under the control of the MANF promoter (-300 ~ +2 nt). As a negative control, we also made a mutant promoter by deleting ERSE in the promoter (**Figure 3-6A**). HEK293 cells were transfected with the MANF reporter in combination with other constructs, and luciferase intensity was measured to quantify MANF transcription levels. As expected, the overexpression of XBP1s, rather than XBP1u, dramatically increased luciferase intensity, indicating XBP1s indeed stimulates MANF transcription **(Figure 3-6B**). We then compared the reporter activity when TBP13Q or TBP105Q was presented with XBP1s. Western blotting was used to quantify the expression level of the transfected proteins (**Figure 3-6C**). We found that the expression of TBP105Q yielded a lower level of transcription activity, which is consistent with its weaker association with XBP1s. Importantly, coexpression of Hsc70 significantly increased the reporter activity and eliminated the difference between TBP13Q and TBP105Q (**Figure 3-6D**).

To examine whether overexpession of Hsc70 can up-regulate MANF expression, we used our previously generated PC12 cell lines that stably express either TBP13Q or TBP105Q (Shah et al., 2009). We found that the endogenous level of MANF was decreased

in TBP105Q cells. However, transfection of Hsc70 resulted in a significant increase in MANF level (**Figure 3-7A, B**). The protective effects of Hsc70 on polyQ expansion-induced toxicity in different cellular and transgenic mouse models have been well established (Bauer et al., 2010; Jana et al., 2000; Jorgensen et al., 2007; Novoselova et al., 2005). Similarly, the TBP105Q cell line showed impaired neurite outgrowth in response to nerve growth factor (NGF), but Hsc70 overexpression could significantly reverse this neurite outgrowth deficit (**Figure 3-7C, D**). Also, overexpression of Hsc70 via adenoviral vector in the cerebellum of KI mice reduced the degeneration of Purkinje cells and increased the levels of MANF in Purkinje cells (**Figure 3-7E, F**). Taken together, these findings suggest that chaperone activity is critical for maintaining the normal function of mutant TBP and that the age-dependent decrease in its activity leads mutant TBP to lose its normal function and alters gene expression important for neuronal survival.

MANF overexpression ameliorates mutant TBP toxicity *in vitro* and *in vivo*

If a decreased MANF level in the cerebellum contributes to Purkinje cell degeneration in SCA17 mice, overexpression of MANF should alleviate this pathological change. To test this hypothesis, we generated a lentiviral MANF vector, in which mouse MANF is linked with ECFP through a F2A sequence and is expressed under the control of the ubiquitin promoter (**Figure 3-8A**). When translated, the F2A peptide can be self-cleaved to separate MANF and ECFP, and ECFP fluorescence could be an indicator of MANF expression. We first infected HEK293 cells with MANF lentivirus and detected robust expression of both MANF and ECFP via western blotting (**Figure 3-8B**). We then infected

stable PC12 cell lines that express either TBP13Q or TBP105Q. After NGF stimulation, we found that MANF overexpression could significantly increase the numbers of TBP105Q cells containing long neurites versus control cells (**Figure 3-9A, B**), which suggests that MANF rescues the neurite outgrowth defect caused by mutant TBP. The PC12 cells expressing mutant TBP are also sensitive to apoptotic stimuli, such as staurosporine treatment (Shah et al., 2009). MTS assay showed that MANF overexpression was able to significantly improve the survival of TBP105Q PC12 cells (**Figure 3-9C, D**).

Next, we performed stereotaxic injection of lentivirus expressing MANF into the cerebellum of 12-month-old TBP105Q inducible KI mice. MANF lentivirus was injected on the right side of the cerebellum, and the lentivirus expressing GFP alone was injected into the left side as a control. One month later, the injected mice were subjected to tamoxifen treatment to express mutant TBP for another 1.5 months before being examined. Immunofluorescence staining of the cerebellum revealed the expression of ECFP and GFP, which was used to locate the site of virus infection, and calbindin staining was used to visualize Purkinje cells (**Figure 3-10A**). In wild-type mice, both lentiviral MANF- and GFP-infected sides showed a comparable density of Purkinje neurons (**Figure 3-10B**). In the KI cerebellum, however, we saw a severe loss of Purkinje neurons caused by mutant TBP in the lentiviral GFP-infected side, and importantly, the lentiviral MANF infected-side had a significant increase in the number of Purkinje neurons (**Figure 3-10A, B)**, further confirming the protective effect of MANF on mutant TBP toxicity.

Transgenic MANF expression alleviates ataxic gait and Purkinje cell neurodegeneration in SCA17 knock-in mice.

Injected MANF lentivirus can only infect a limited area of the cerebellum so that it was difficult to see behavioral changes of SCA17 mice after injection. We generated a MANF transgenic mouse model, in which the prion promoter was used to drive the expression of MANF that is tagged with human influenza hemagglutinin (HA) at the C-terminus (**Figure 3-11A**). Western blot (**Figure 3-11B**) and immunohistochemistry (**Figure 3-11C**) with anti-HA tag antibody confirmed that transgenic MANF was widely expressed in the brain of transgenic mice. Using TBP105Q loxp mice, we recently obtained knock-in mice (SCA17 KI) that expressed mutant TBP105Q from germline and displayed ataxic gait, manifested by significantly shorter strides and poor coordination between forepaws and hindpaws at the age of 6-months. We crossed MANF transgenic mice with these SCA17 KI mice and generated (KI/MANF) mice that express both mutant TBP and transgenic MANF. At 6 months of age, KI/MANF mice showed significant improvement in clasping phenotypes (**Figure 3-12A, B**) and in foot-printing phenotype (**Figure 3-12C**) as compared with SCA17 KI mice. Quantification of stride lengths in foot-printing assay and walking time during balance beam test verified a significant improvement of motor function and coordination of KI/MANF mice (**Figure 3-12D. E**). Western blotting results revealed an upregulation of calbindin levels in the SCA17 KI mouse cerebellum expressing transgenic MANF (**Figure 3-13A, B**). In agreement with this result, immunofluorescent staining showed that transgenic MANF was also protective on Purkinje neuron survival, as a significantly higher density of Purkinje neurons was seen in the cerebellum of KI/MANF mice compared with SCA17 KI mice (**Figure 3-13C, D, E**). In addition, the thickness of molecular layer and dendritic

complexity was also improved in KI/MANF mice **(Figure 3-13F, G**). It should be noted that a similar amount of mutant TBP was seen in both SCA17 KI and KI/MANF mice (**Figure 3-13A**), suggesting that the rescue effect of MANF was not due to a reduced level of mutant TBP but resulting from improving MANF function.

3.5 Discussion

In neurodegenerative diseases caused by polyQ expansion, the disease proteins are not necessarily expressed more in the neurons that are particularly affected. For example, in Huntington's disease, the disease protein huntingtin is in fact expressed at a lower level in the striatum, the region that is preferentially affected in HD, than in other brain regions (Fusco et al., 1999). This phenomenon is observed in SCA17, as the level of TBP is significantly lower in the brain, when compared with its level in the testis, small intestine and pituitary (Perletti et al., 1999). Thus, other cell type-specific and aging-related factors must be involved in the selective neurodegeneration.

We identified MANF as a cell type-specific target for Purkinje cell degeneration in SCA17. MANF is a newly discovered, non-canonical neurotrophic factor. Unlike other classical neurotrophins, such as NGF, BDNF, and NT-3, which mainly function by binding to their respective receptors in the cell membrane, MANF is believed to exert its neuroprotective effects both extracellularly, through binding to an as-yet-unidentified receptor (Voutilainen et al., 2009), and intracellularly, by inhibiting apoptosis (Hellman et al., 2011). We provide several lines of evidence to support the idea that MANF is involved in the

selective Purkinje cell degeneration in SCA17**.** First, MANF is enriched in Purkinje cells, and its expression is reduced in TBP105Q inducible KI mouse cerebellum. Second, as a neuronal protective factor, the overexpression of MANF can alleviate Purkinje cell degeneration in SCA17 KI mouse brains. Third, the expansion of polyQ repeats reduces TBP binding to XBP1s and decreases the association of XBP1s to the promoter of MANF, resulting in decreased expression of MANF. Because TBP level is strictly regulated and the increased levels of mutant TBP can reduce the level of normal TBP, both the lower level of normal TBP and the dysfunction of mutant TBP can contribute to the decreased level of MANF via a similar mechanism of loss of function reported in other polyQ diseases (Lim et al., 2008; Nedelsky et al., 2010), resulting in impaired function of MANF in neuronal cells.

Hsc70 is found to interact with co-chaperones to maintain the conformation and interactions of protein complexes, such as DNA binding protein complex (Gehring, 2004; Li et al., 2008; Niyaz et al., 2001; Zeiner et al., 1999). Indeed, we found that overexpression of Hsc70 can improve the association of mutant TBP with XBP1s and increase the transcription activity of the MANF promoter. Thus, a lower level of Hsc70 may impair the function of mutant TBP on the expression of MANF. Because MANF is enriched in Purkinje cells, this decrease can affect Purkinje cells in particular and contributes to the selective neurodegeneration in SCA17.

Figure 3-1

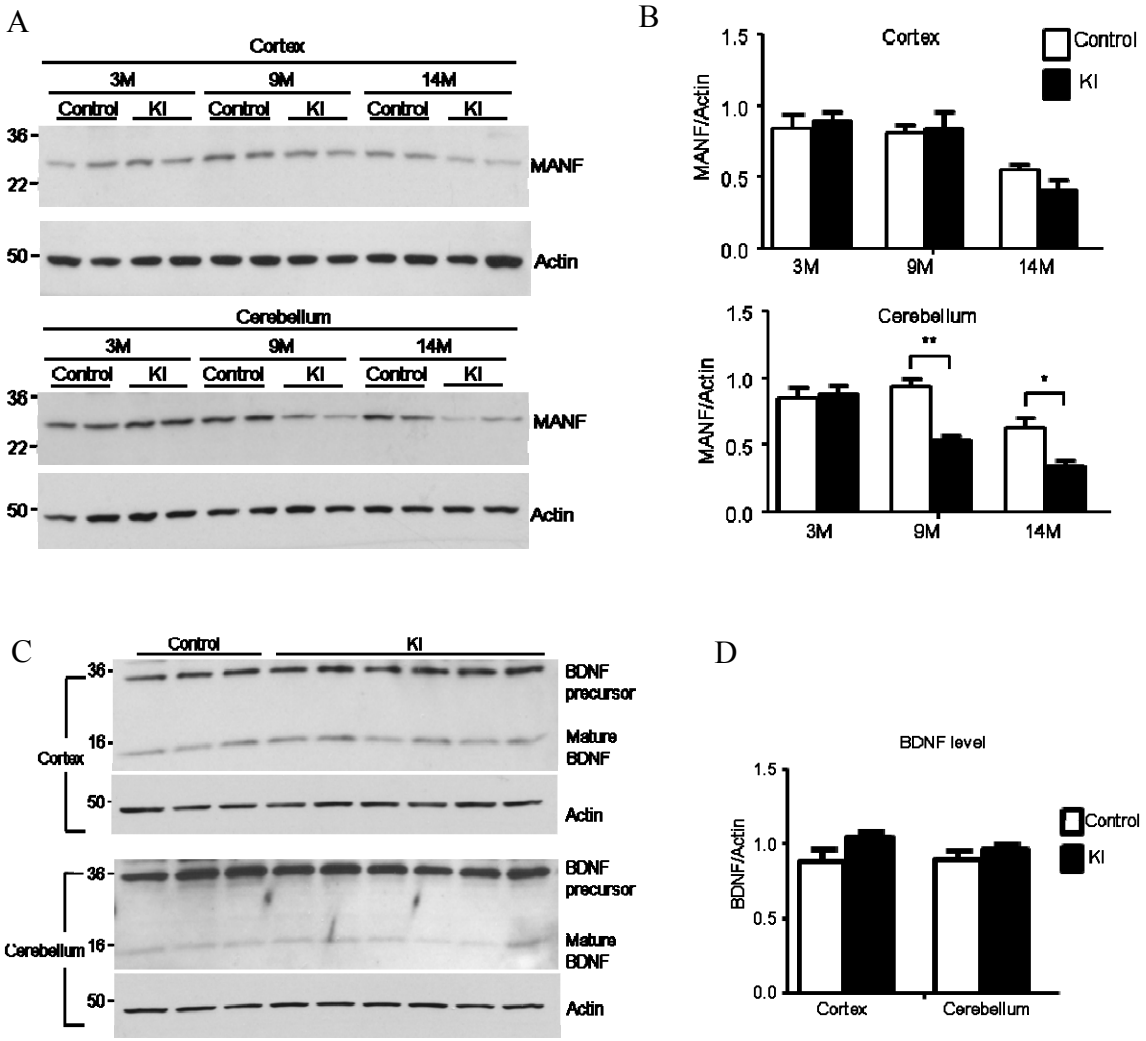
A
Cortex
3M
9M
14M
Control
KI
36
22
50
MANF
Actin
Cerebellum
B
Cortex
Control
KI
MANF/Actin
1.5
1.0
0.5
0.0
3M
9M
14M
Cerebellum
**
*
C
BDNF precursor
Mature BDNF
Actin
Cortex
Cerebellum
16
D
BDNF level
BDNF/Actin

Figure 3-1 Age-dependent decrease of MANF occurs specifically in the cerebellum of TBP105Q inducible knock-in mice.

(A) Western blotting analysis of MANF protein level in the cortex and cerebellum of 3-, 9-, and 14-month-old control and TBP105Q inducible KI mice. (B) Quantification of the ratio of MANF to actin showing that only the cerebellum in TBP105Q inducible KI mice, starting at 9 months, had a significant decrease of MANF compared with the control cerebellum (*P < 0.05, **P < 0.01). (C) Western blotting and quantitative analysis of BDNF level in the cortex and cerebellum of TBP105Q inducible KI mice. (D) The ratios of BDNF to actin on western blots showed no significant differences between KI and control mice. Data are represented as mean ± SEM.

Figure 3-2

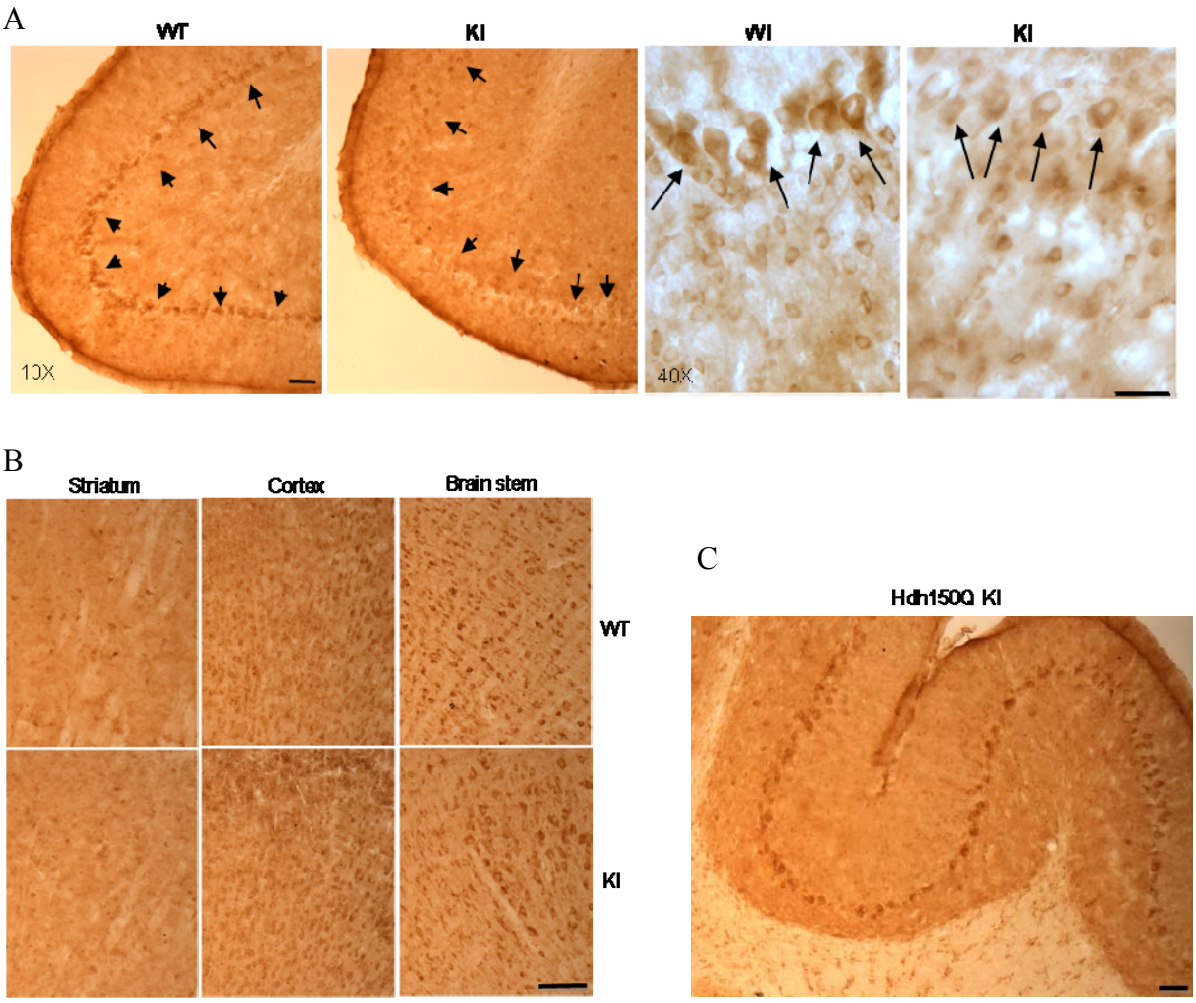
A
WT
KI
WI
KI
10X
40X
B
Striatum
Cortex
Brain stem
WT
KI
C
Hdh150Q KI

Figure 3-2 MANF is enriched in the Purkinje cell layer and the enrichment is lost in TBP105Q inducible knock-in mice.

(A) Immunohistochemical study showing the enrichment of MANF in Purkinje neurons of WT cerebellum, and this enrichment is lost in the cerebellum of 14-month-old TBP105Q inducible KI mouse. (B) No obvious changes in MANF immunostaining intensity were seen in the striatum, cortex, and brain stem between KI mice and WT mice at 14 months of age. (C) The enrichment of MANF in the Purkinje cell layer of cerebellum remains in a Huntington's disease knock-in (HdhQ150) mouse at the age of 12 months. Scale bars: 40 μm.

Figure 3-3

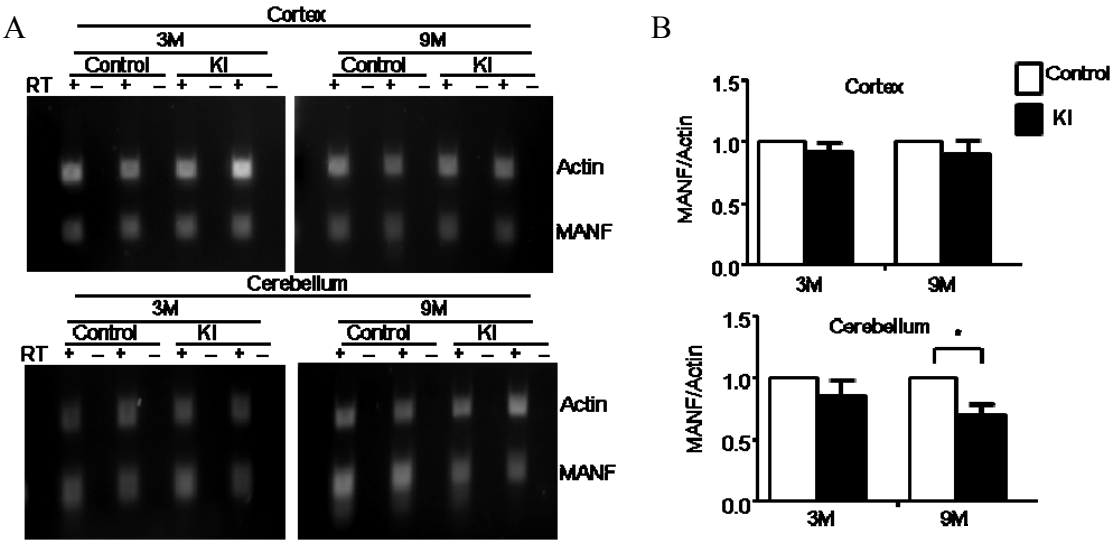
A
Cortex
3M
9M
Control
KI
Control
KI
RT
+ – + – + – + – + – + – + –
Actin
MANF
Cerebellum
3M
9M
Control
KI
Control
KI
RT
+ – + – + – + – + – + – + –
Actin
MANF
B
Control
KI
Cortex
MANF/Actin
1.5
1.0
0.5
0.0
3M
9M
Cerebellum
*
MANF/Actin
1.5
1.0
0.5
0.0
3M
9M

Figure 3-3 Reduced MANF mRNA level in the cerebellum of TBP105Q inducible knock-in mice.

(A) RT-PCR revealed a decrease in MANF mRNA level, which is specific to the cerebellum of KI mice at an old age (9-month). Actin was used as an internal control. (B) Real-time PCR was used to confirm the RT-PCR result. Relative abundance of MANF was calculated with the value from the control mice set to 1, and actin served as an internal control (*P < 0.05). Data are represented as mean ± SEM.

Figure 3-4

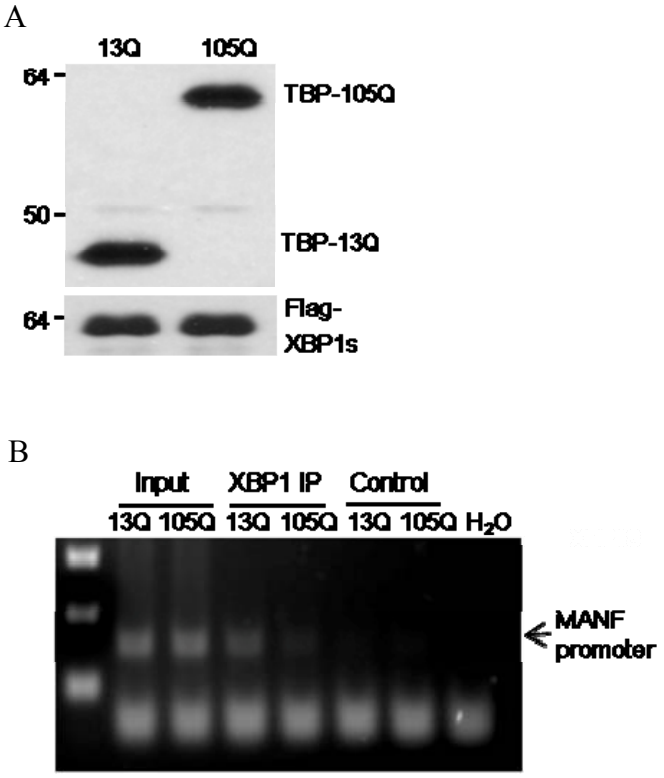
A
13Q
105Q
64
TBP-105Q
50
TBP-13Q
64
Flag-
XBP1s
B
Input
XBP1 IP
Control
13Q 105Q 13Q 105Q 13Q 105Q H2O
MANF
promoter
C
IP/Input
0.8
0.6
0.4
0.2
0.0
**
13Q
105Q

Figure 3-4 Reduced occupancy of XBP1s on MANF promoter in the presence of mutant TBP.

(A) Western blotting analysis confirmed the expression of respective proteins (TBP13Q, TBP105Q, and XBP1s) in cells used for ChIP assay. (B) Semi-quantitative PCR result using lysates from chromatin immunoprecipitation with anti-Flag (ChIP, left panel). Control was beads only without anti-Flag. (C) Quantitative analysis of PCR result showed that more MANF promoter was pulled down in cells transfected with TBP13Q than with TBP105Q (right panel, $^{**}P<0.01$). Data are represented as mean ± SEM.

Figure 3-5

A

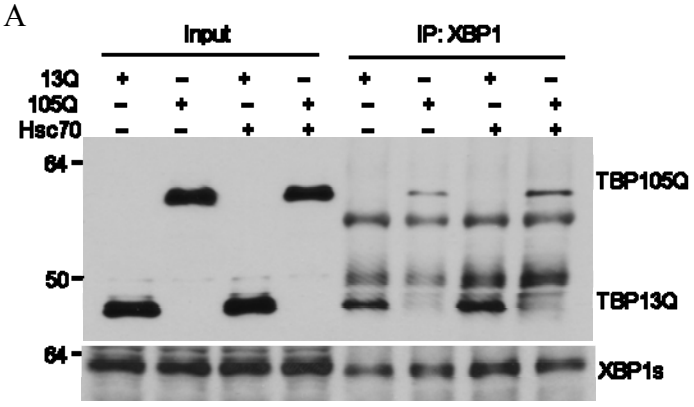
Input
IP: XBP1
13Q
105Q
Hsc70
64
50
64
TBP105Q
TBP13Q
XBP1s

B

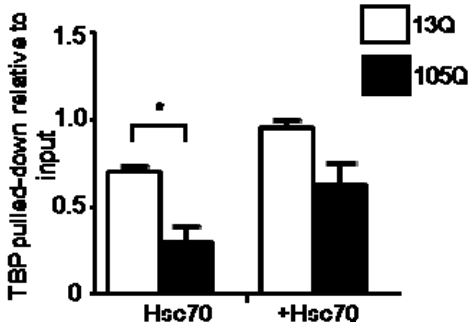
TBP pulled-down relative to input
1.5
1.0
0.5
0
*
13Q
105Q
Hsc70
+Hsc70

Figure 3-5 Expanded polyQ impairs the binding between TBP and XBP1s

(A) Coimmunoprecipitation of transfected XBP1s with TBP in the presence or absence of Hsc70. Equal amount of XBP1s was pulled down by XBP1 antibody in each sample, whereas less TBP105Q was pulled down with XBP1s. Overexpression of Hsc70 increased the precipitated amount of TBP (both 13Q and 105Q). (B) The relative amounts of TBP precipitated with XBP1s (*$P < 0.05$). Data are represented as mean ± SEM.

Figure 3-6

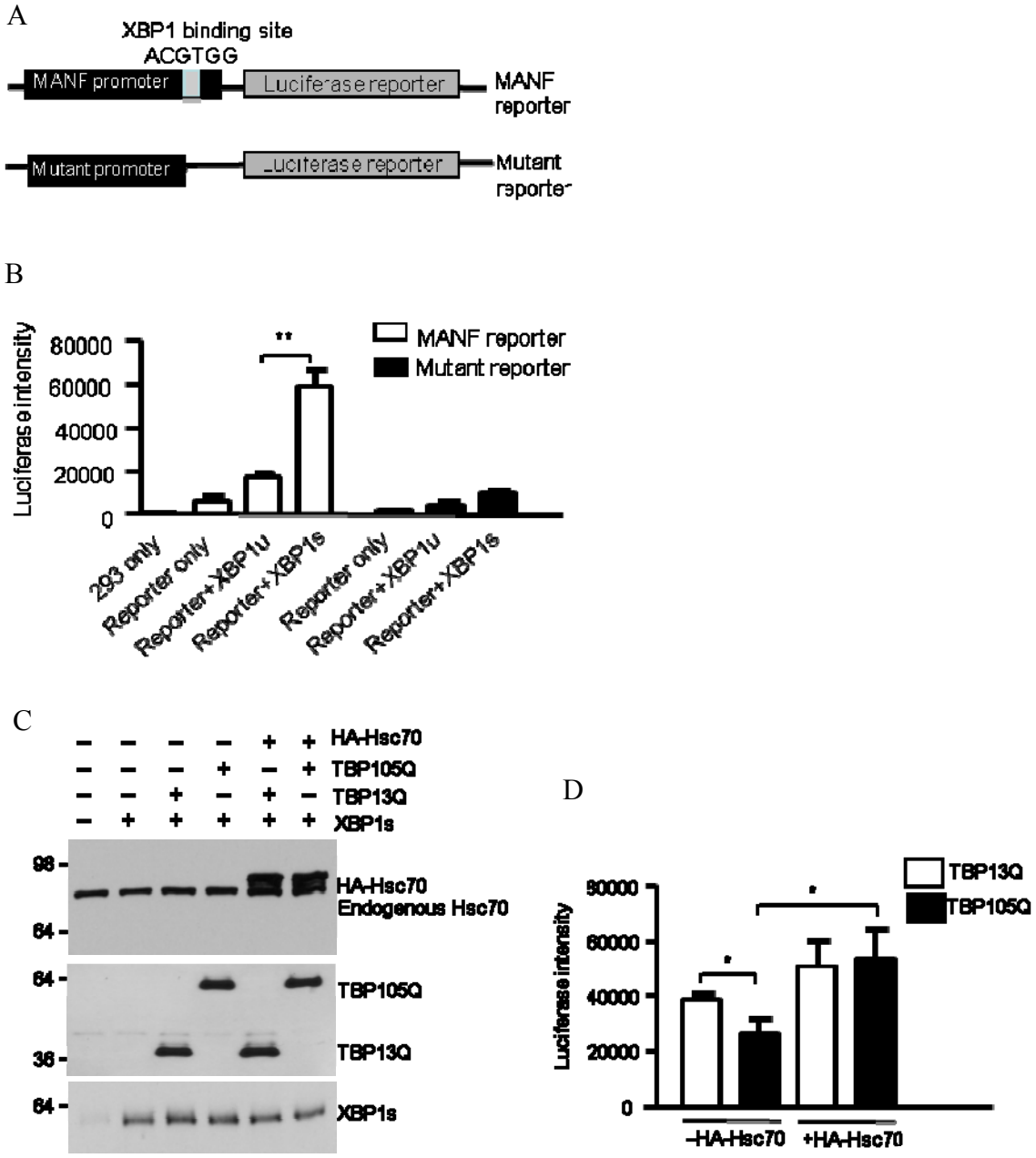
A
XBP1 binding site
ACGTGG
MANF promoter
Luciferase reporter
MANF reporter
Mutant promoter
Luciferase reporter
Mutant reporter
B
Luciferase intensity
80000
60000
40000
20000
0
**
MANF reporter
Mutant reporter
293 only
Reporter only
Reporter+XBP1u
Reporter+XBP1s
Reporter only
Reporter+XBP1u
Reporter+XBP1s
C
HA-Hsc70
TBP105Q
TBP13Q
XBP1s
98
64
HA-Hsc70
Endogenous Hsc70
64
TBP105Q
36
TBP13Q
64
XBP1s
D
TBP13Q
TBP105Q
Luciferase intensity
80000
60000
40000
20000
0
*
*
-HA-Hsc70
+HA-Hsc70

Figure 3-6 Luciferase assay showed that mutant TBP impairs XBP1s mediated MANF transcription.

(A) Schematic map of luciferase constructs for reporter assay.(B) Luciferase activity of transfected HEK293 cells showed that XBP1s, but not XBP1u, greatly increased luciferase intensity. (C) Western blotting verifying the co-expression of TBP, Hsc70, and XBP1s with the MANF promoter reporter. (D) Overexpression of Hsc70 significantly rescued the impaired luciferase activity by TBP105Q (*$P< 0.05$). Data are represented as mean ± SEM.

Figure 3-7

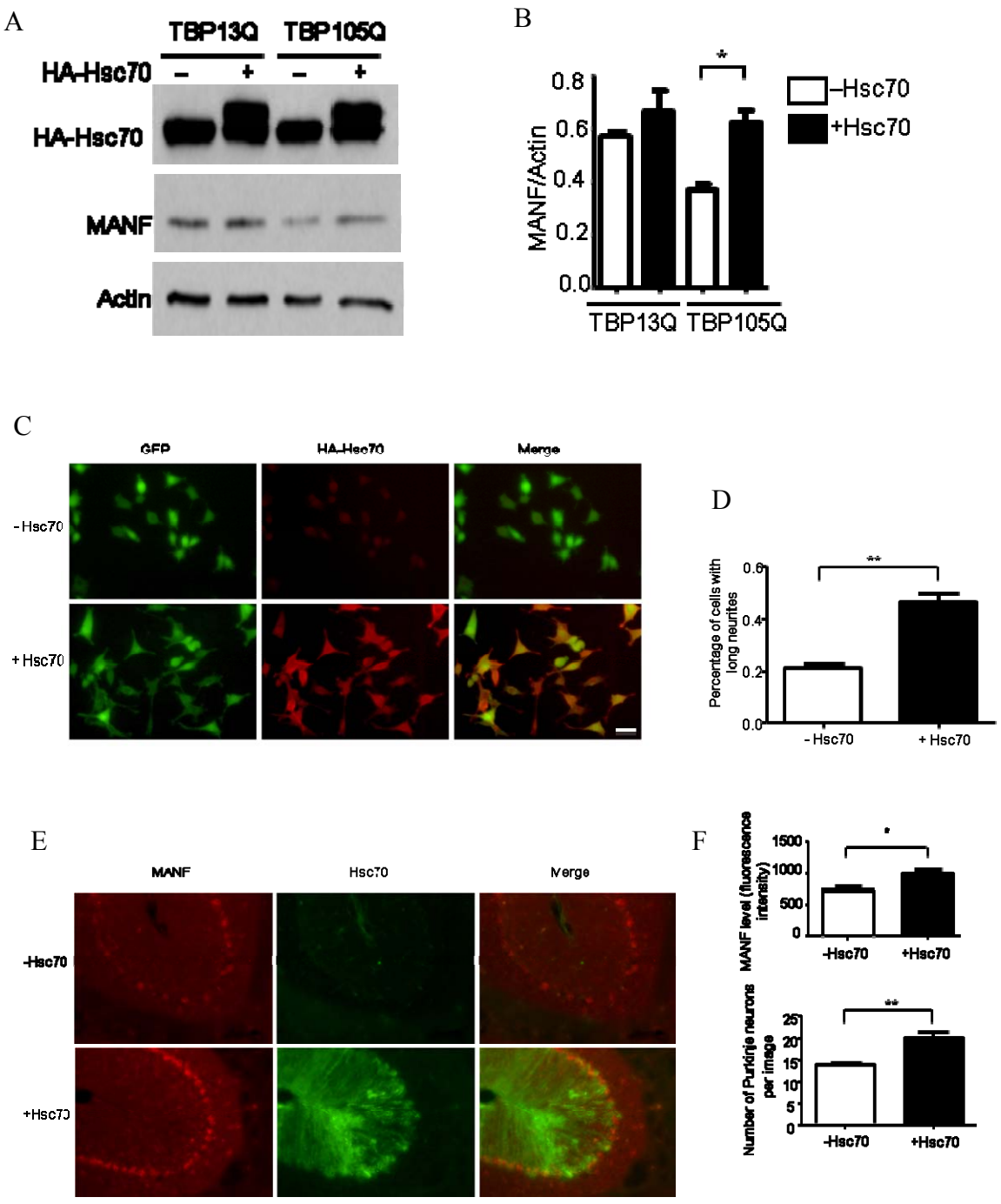
A
TBP13Q
TBP105Q
HA-Hsc70
– + – +
HA-Hsc70
MANF
Actin
B
MANF/Actin
0.8
0.6
0.4
0.2
0.0
*
–Hsc70
+Hsc70
TBP13Q TBP105Q
C
GFP
HA-Hsc70
Merge
- Hsc70
+ Hsc70
D
Percentage of cells with long neurites
0.6
0.4
0.2
0.0
**
- Hsc70
+ Hsc70
E
MANF
Hsc70
Merge
-Hsc70
+Hsc70
F
MANF level (fluorescence intensity)
1500
1000
500
0
*
-Hsc70
+Hsc70
Number of Purkinje neurons per image
25
20
15
10
5
0
**
-Hsc70
+Hsc70

Figure 3-7 Hsc70 overexpression rescues MANF reduction in the presence of mutant TBP.

(A) Western blot analysis of MANF expression levels in TBP stably transfected cells that were transfected with (+) or without (–) HA-tagged Hsc70. (B) The ratios of MANF to actin on the blot are also presented (* $P<0.05$). (C) Representative images (20X) showing that overexpression of Hsc70 increased the neurite outgrowth of TBP105Q PC12 cells in response to NGF. Scale bar: 10 μm. (D) The percentage of PC12 cells containing neurites longer than two cell body diameters (n=10, ** $P<0.01$) (E) Immunofluorescent staining images (20X) of SCA17 KI cerebellum infected (+) or uninfected (–) with Hsc70 adenovirus. (F) Quantitative assessment of MANF fluorescence intensity and the number of Purkinje cells in SCA17 KI cerebellar sections (n=9, * $P<0.05$, ** $P<0.01$). Data are represented as mean ± SEM.

Figure 3-8

A


Lentiviral MANF vector
Ubiquitin promoter
MANF
F2A
ECFP

B

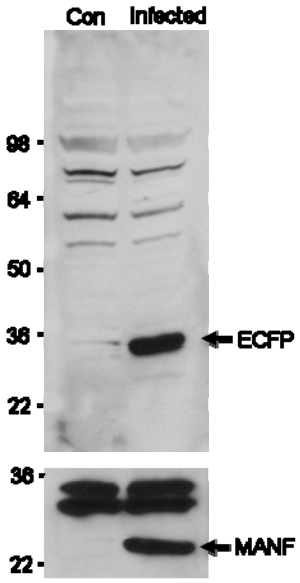
Con
Infected
98
64
50
36
22
ECFP
36
22
MANF

Figure 3-8 Generation of lentiviral MANF vector

(A) Schematic map of lentiviral MANF vector. (B) Western blotting analysis of HEK293 cells infected with lentiviral MANF for two days (Infected) confirming the expression of both MANF and ECFP. Uninfected HEK293 cells (Con) were used as a negative control.

Figure 3-9

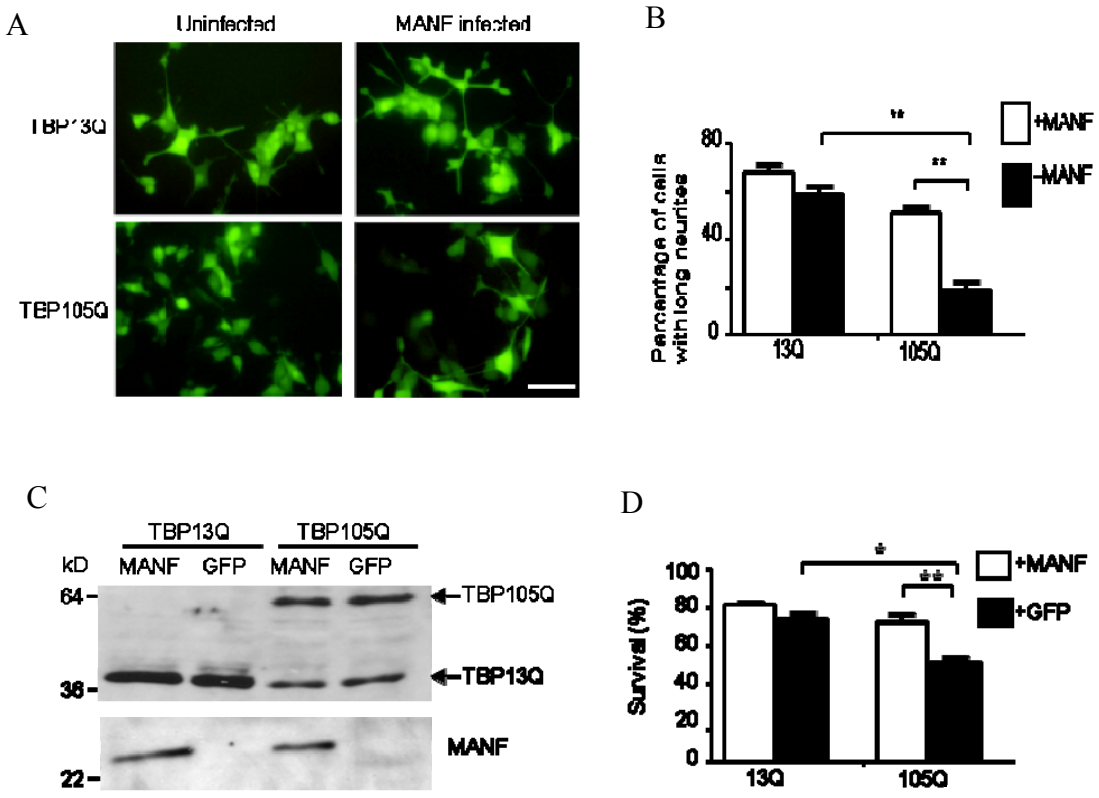
A
Uninfected
MANF infected
TBP13Q
TBP105Q
B
+MANF
-MANF
Percentage of cells with long neurites
80
40
0
13Q
105Q
**
**
C
TBP13Q
TBP105Q
kD
MANF
GFP
MANF
GFP
64
36
22
TBP105Q
TBP13Q
MANF
D
+MANF
+GFP
Survival (%)
100
80
60
40
20
0
13Q
105Q
*
**

Figure 3-9 MANF overexpression by lentiviral infection ameliorates mutant TBP toxicity *in vitro*.

(A, B) PC12 cells stably expressing either wild-type TBP (TBP13Q) or mutant TBP (TBP105Q) were infected with lentiviral MANF or uninfected. Fluorescent imaging (A) and quantitative analysis (B, n=15, $^{**}P < 0.01$) showed that MANF significantly increased the percentage of cells with long neurites. Scale bar: 10 μm. (C) Western blot analysis of PC12 cells stably expressing either wild-type TBP (TBP13Q) or mutant TBP (TBP105Q), which were infected with lentiviral MANF or GFP. (D) MTS assay showed a significant increase in the survival of PC12 cells (versus non-staurosporine-treated cells) expressing mutant TBP when infected with lentiviral MANF compared to lentiviral GFP ($^{*}P < 0.05$, $^{**}P < 0.01$). Data are represented as mean ± SEM.

Figure 3-10

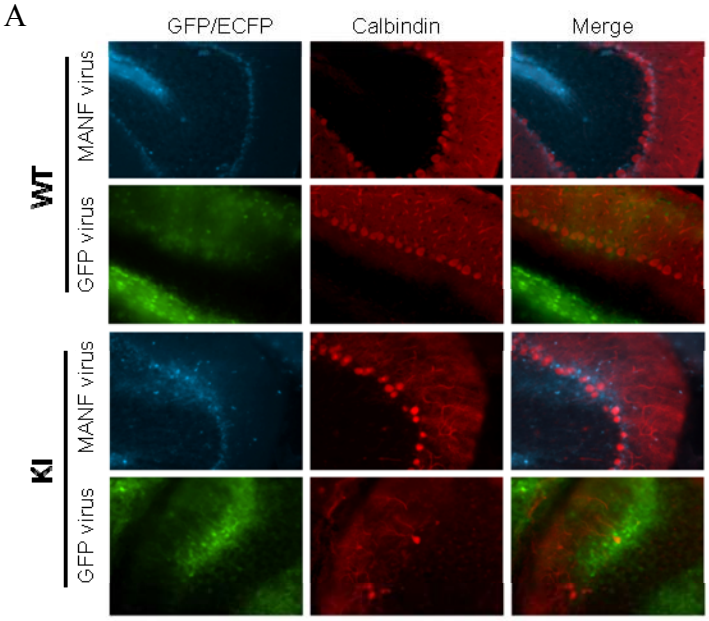
A
GFP/ECFP
Calbindin
Merge
WT
MANF virus
GFP virus
KI
MANF virus
GFP virus

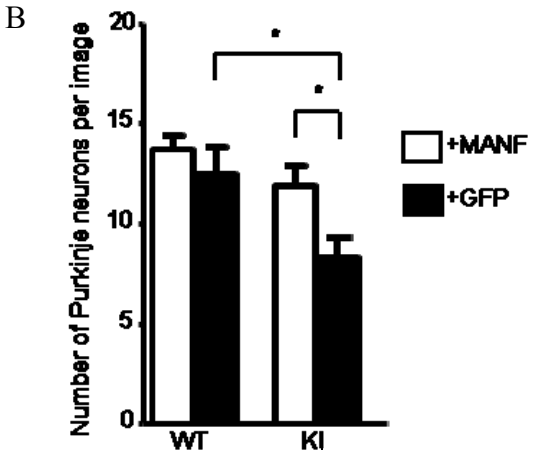
B
Number of Purkinje neurons per image
20
15
10
5
0
WT
KI
+MANF
+GFP
*
*

Figure 3-10 MANF overexpression by lentiviral infection ameliorates mutant TBP toxicity *in vivo*.

(A) One-year-old WT and TBP105Q inducible KI mice were injected with MANF lentivirus on the right side of the cerebellum and with lentiviral GFP on the left side. Fluorescence of GFP or ECFP was used to locate the region infected by lentivirus. Calbindin staining showed that MANF overexpression rescued the loss of Purkinje neurons caused by mutant TBP. Scale bar: 50 μm. (B) Quantitative assessment of the number of Purkinje cells labeled by anti-calbindin per image field (20x, n=9, $*P < 0.05$). Data are represented as mean ± SEM.

Figure 3-11

A

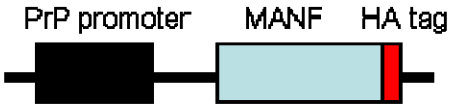

B

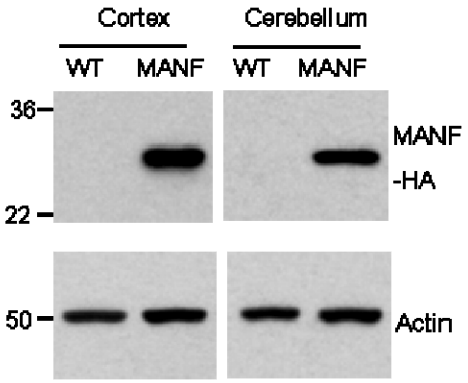

C

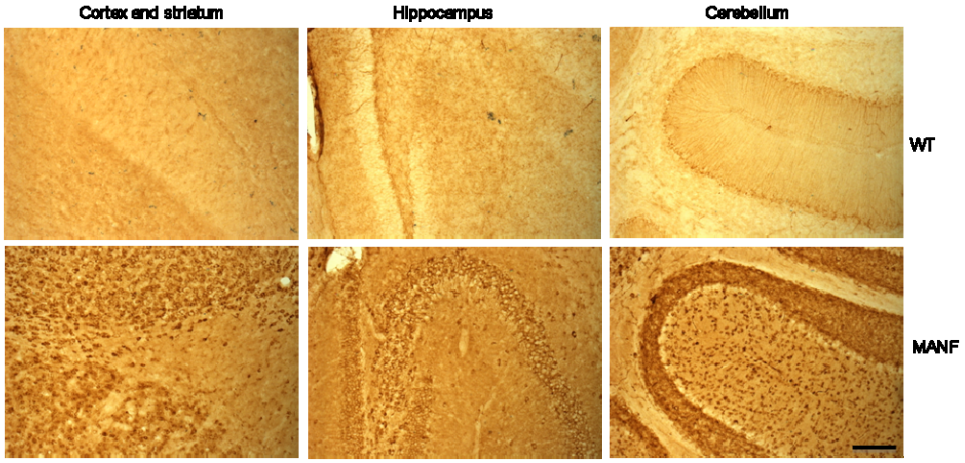

Figure 3-11 Generation of MANF transgenic mouse model.

(A) Schematic map of transgenic MANF construct. (B) Anti-HA Western blotting verified the expression of transgenic MANF-HA in the brain cortex and cerebellum in MANF transgenic mouse. (C) Immunohistochemistry using HA antibody confirmed ubiquitous expression of HA tagged MANF in different brain regions of TG mice, such as the cortex, striatum, hippocampus and cerebellum. The brain of wild-type (WT) mice showed negative staining result. Scale bar: 50 μm.

Figure 3-12

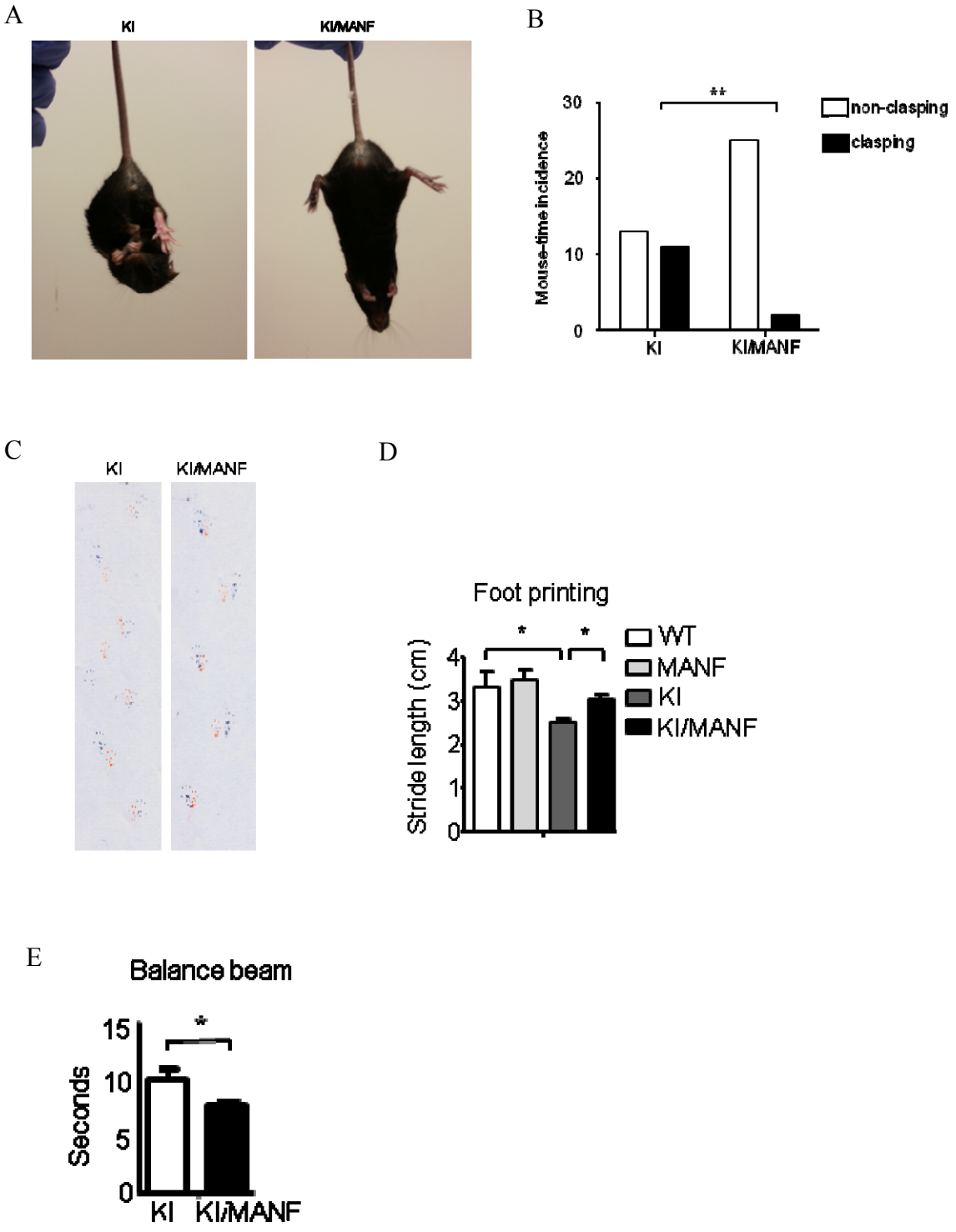
A
KI
KI/MANF
B
**
non-clasping
clasping
Mouse-time incidence
30
20
10
0
KI
KI/MANF
C
KI
KI/MANF
D
Foot printing
*
*
WT
MANF
KI
KI/MANF
Stride length (cm)
4
3
2
1
0
E
Balance beam
*
Seconds
15
10
5
0
KI
KI/MANF

Figure 3-12 Improvement of behavioral phenotypes in SCA17 KI mice with MANF overexpression.

(A) Photos of SCA17 KI mice showing the clasping phenotype, which was not seen from KI/MANF mice. (B) Quantification and analysis of the clasping phenotypes using Chi-square test (**$P < 0.01$). (C) Gait of SCA17 KI and KI/MANF mice was assessed using foot-printing assay. (D) KI/MANF mice show longer stride lengths in foot-printing test and (E) shorter walking time in balance beam assay than SCA17 KI mice, indicating an improvement in gait performance and motor coordination (n=6 each group, *P<0.05). Data are represented as mean ± SEM.

Figure 3-13

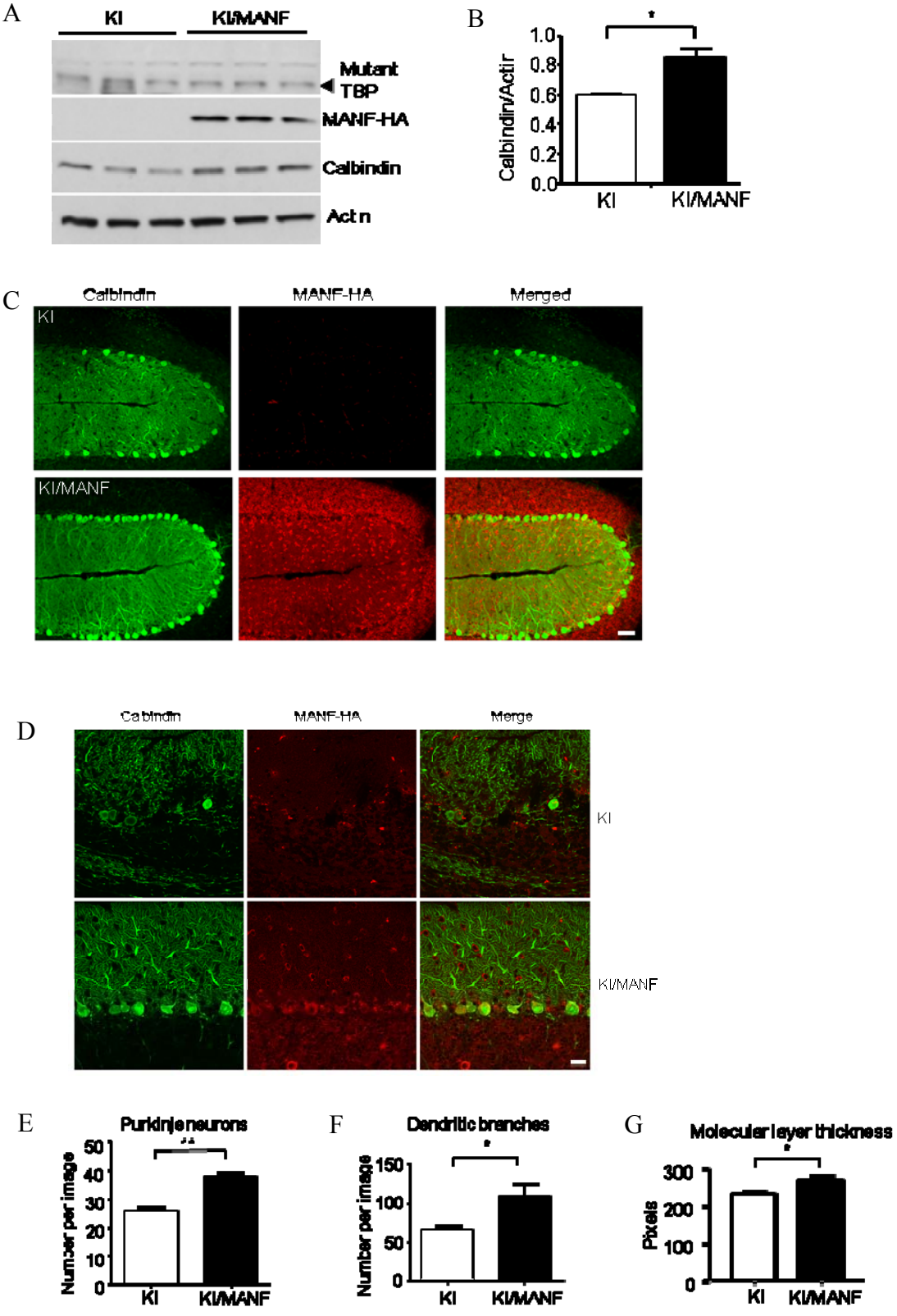
A
KI
KI/MANF
Mutant TBP
MANF-HA
Calbindin
Actin
B
Calbindin/Actin
1.0
0.8
0.6
0.4
0.2
0.0
KI
KI/MANF
C
Calbindin
MANF-HA
Merged
KI
KI/MANF
D
Calbindin
MANF-HA
Merge
KI
KI/MANF
E
Purkinje neurons
Number per image
50
40
30
20
10
0
KI
KI/MANF
F
Dendritic branches
Number per image
150
100
50
0
KI
KI/MANF
G
Molecular layer thickness
Pixels
300
200
100
0
KI
KI/MANF

Figure 3-13 Improvement of Purkinje cell survival in SCA17 KI mice with MANF overexpression.

(A) Western blotting analysis of mutant TBP labeled by 1C2 antibody, transgenic MANF labeled by anti-HA, and calbindin in the cerebellum of 6-month-old SCA17 KI and KI/MANF mice. Actin was used as a loading control. (B) The ratio of calbindin to actin is presented (*P<0.05). (C) Immunofluorescent staining images (10X by confocal microscope) of SCA17 KI and KI/MANF mouse cerebellum. Calbindin staining was used to reveal Purkinje neurons, and HA antibody was used to stain transgenic MANF. Scale bar: 50 μm. (D) High magnification images of the cerebellum sections of KI and KI/MANF mice at the age of 6 months. Scale bar: 20 μm. (E, F, G) Quantitative assessment of the number of Purkinje neurons labeled by anti-calbindin per image field, dendritic branches and thickness of molecular layer (10X, n=9, *P < 0.05, **P < 0.01). Data are represented as mean ± SEM.

Chapter 4

MANF alleviates SCA17 neuropathology through protein kinase C (PKC) signaling

This chapter includes work published as Su Yang, Shanshan Huang, Marta A. Gaertig, Xiao-Jiang Li, and Shihua Li (2014) *Neuron,* January 22; 81: 349-365. The majority of the work was done by Su Yang. Marta Gaertig helped with mouse breeding. Xiao-Jiang Li and Shihua Li helped with experimental design and data analysis. Xiao-Jiang Li edited the manuscript for publication.

4.1 Abstract

Despite strong evidence suggesting an important role of MANF for neuronal survival, the signaling pathways mediated by MANF remains elusive. We purified recombinant MANF from bacteria, and found elevated PKC phosphorylation when we treated PC12 cells with purified MANF protein. This result was further confirmed *in vivo*, as a significant reduction of PKC phsophorylation was found in the cerebellum of SCA17 KI mice. This reduction was ameliorated when MANF was overexpressed. In addition, manipulation of PKC signaling in mouse brain altered Purkinje cell survival and mouse behaviors. Taken together, these results indicate MANF potentially regulates neuronal activity through PKC signaling pathway.

4.2 Introduction

Classical neurotrophic factors (NTFs), such as NGF, BDNF and NT-3, regulate neuronal functions by binding to their respective receptors on the cell membrane. The binding of NTFs activates the intracellular kinase domain of the receptors, and triggers a series of kinase based reactions that eventually alter neuronal functioning. A similar scenario possibly applies to MANF, as previous studies suggest the addition of MANF protein promoted dopaminergic neuronal survival in both cell culture and rat brain (Petrova et al., 2003; Voutilainen et al., 2009). However, the mechanisms behind the neuronal survival promoting effects of MANF is still a mystery. The pursuit of answers to this question was partially hampered by the fact that MANF is localized in the ER, and possesses important functions inside cells. Nevertheless, a recent paper identified KDEL receptor as a potential binding partner of MANF (Henderson et al., 2013). KDEL

receptor is a seven-transmembrane-domain protein that is linked to the activation of several kinase mediated signaling cascades (Capitani and Sallese, 2009). These studies led us to explore potential signaling pathways that are regulated by MANF.

In this chapter, we purified recombinant MANF protein from bacteria, and applied the purified MANF to PC12 cell cultures. By checking the phosphorylation level of several key signaling molecules, we found PKC activity was greatly stimulated upon MANF treatment. The PKC family consists of at least 15 homologous serine/threonine kinases that play important roles in various cellular functions, such as cell cycle control, proliferation, differentiation, metastasis and apoptosis (Clemens et al., 1992; Griner and Kazanietz, 2007). Although predominantly studied in cancer, PKC is present at a high level in the brain, and is proposed to influence a broad spectrum of neuronal activities. Furthermore, reduced levels of PKC have been reported in various neurodegenerative diseases, including AD, PD and HD (Tanaka and Nishizuka, 1994). Interestingly, several studies found alteration of PKC signaling could lead to dysregulated Purkinje cell development (Gundlfinger et al., 2003; Metzger and Kapfhammer, 2000, 2003), suggesting PKC could play an important role in the maintenance of Purkinje cell survival as well. Indeed, we found a significant reduction of the active form of PKC in the cerebellum of SCA17 KI mice. This reduction was rescued by MANF overexpression. Moreover, manipulation of PKC signaling in mouse brain altered Purkinje cell survival and mouse behaviors. Therefore, we propose MANF could promote Purkinje cell survival by activating PKC signaling.

4.3 Materials and Methods

Antibodies and plasmids

Primary antibodies from commercial sources used include: Actin (Sigma, A5060), PKCγ (Santa Cruz, 211), and phosphorylated PKC (Cell Signaling, 9379). All secondary antibodies were purchased from Jackson Immunoresearch.

Viral vector and stereotaxic injection

Adenoviral PKCγ virus was obtained from Vector Biolabs. Method for stereotaxic injection is described in Chapter 3.

Phorbol 12-myristate 13-acetate (PMA) injection

For injection of PMA into the mice, PMA (Sigma, P8139) was dissolved in corn oil, and injected intraperitoneally into mice at the dose of 0.15 mg per 1kg body weight every 3 days.

Purification of recombinant MANF protein

Mouse MANF cDNA was cloned into pET-28a vector containing His tag. The vector was transformed into XL1-Blue competent cells, and MANF production was induced by incubating the cells with IPTG for 1 hour at 37℃. The cells were lysed in lysis buffer (5mM

imidazole, 500mM NaCl, 20mM Tris-HCl, pH 8.0, 20mM Betamercaptoethanol, 1mM PMSF) by sonication, and then mixed with Ni-NTA beads (QIAGEN) at 4℃ for 2 hours. The beads with lysate were loaded to Poly-Prep Chromatography column (BIO-RAD), and washed with washing buffer (15mM imidazole, 500mM NaCl, 20mM Tris-HCl, pH 8.0, 20mM Betamercaptoethanol, 0.1% NP40, 1mM PMSF) three times. MANF was finally eluted in elution buffer (400mM imidazole, 500mM NaCl, 20mM Tris-HCl, pH 8.0, 20mM Betamercaptoethanol, 0.1% NP40, 1mM PMSF), and concentrated using Amico Ultra-4 centrifugal filters (Millipore). MANF aliquots, dissolved in PBS, were kept at -80℃.

Statistical analysis

For mouse behavioral analysis, each group consisted of at least 6 animals. For western blotting analysis, immunostaining, or other biochemical assays, data were generated from 3 or more experiments, and the results were expressed as mean ± SEM. Statistical significances were calculated based on either t-test, one-way ANOVA or two-way ANOVA. A P-value of <0.05 was considered significant.

4.4 Results

MANF is proposed to have anti-apoptotic effects due to the resemblance of its C-terminal structure with the SAP domain of Ku70, a well known inhibitor of apoptosis (Hellman et al., 2011). Using immunostaining with an antibody to activated caspase-3, we

found a minimal level of activated caspase 3 in the cerebellum of SCA17 KI and KI/MANF mice (**Figure 4-1**), indicating that the primary cause of Purkinje neuron degeneration in SCA17 is not apoptosis.

Since MANF can also bind membrane receptors, which could potentially trigger intracellular signaling (Henderson et al., 2013), we produced His-tagged MANF in bacteria and purified this recombinant protein (**Figure 4-2A**), which was then applied to cultured PC12 cells (1.5 μg/ml) to identify intracellular signaling event that is likely to associate with the neuronal protective effect of MANF. Using antibodies to phosphorylated signaling proteins, we found that protein kinase C phosphorylation was increased by MANF (**Figure 4-2B, C**). To confirm whether this signaling change could also occur *in vivo*, we performed western blotting and immunohistochemical assays using wild type and SCA17 KI mouse cerebellum tissue. Indeed, a significant reduction in PKC phosphorylation was found in SCA17 KI mouse cerebellum tissue (**Figure 4-3A, B, C**). This reduction, however, could be attenuated by expression of transgenic MANF (**Figure 4-3A, B**).

It has also been reported that prolonged treatment with Phorbol 12-myristate 13-acetate (PMA), a PKC modulator, could reduce PKC expression and phosphorylation (Freisewinkel et al., 1991; Liu et al., 2000; Ohigashi et al., 1999; Reynolds et al., 1994). We intraperitoneally injected PMA into 3-month old WT and SCA17 KI mice (0.15 mg/kg, once every three days) for 24 days and found that this prolonged treatment indeed reduced phosphorylation of PKC (**Figure 4-4A**). More importantly, PMA injection worsened the motor impairment of SCA17 KI mice, manifested by a significant longer time for mice to finish the balance beam test (**Figure 4-4B**).

Reduction in PKC signaling has recently been found to affect dendritic branches and morphology of cerebellar Purkinje cells in the mouse brain (Thomanetz et al., 2013). It would be interesting to see if overexpression of PKC is able to reduce Purkinje cell pathology in SCA17 KI mice. Thus, we injected adenoviral vector expressing PKCγ into the cerebellum of SCA17 KI mice at 5 months of age. Three weeks after injection, we observed a significant increase in the number of Purkinje cells and dendritic branches in the injected cerebellum of SCA17 KI mice (**Figure 4-5A, B, C, D**). These findings identified PKC as a downstream component of MANF mediated signaling pathway, and also highlighted the importance of PKC phosphorylation on the survival of adult Purkinje cells in SCA17.

4.5 Discussion

The signaling pathways mediated by MANF remain largely unclear. Using recombined MANF in PC12 cells, we found that MANF increased PKC phosphorylation. This finding led us to uncover the significant reduction of PKC phosphorylation in the cerebellum in SCA17 KI mice. Importantly, transgenic MANF can alleviate the reduction in PKC phosphorylation in SCA17 KI mouse cerebellum. Several studies indicate PKC activity modulates Purkinje cell maturation, and reduction or absence of PKC signaling leads to abnormal Purkinje cell dendritic morphology and dysfunction during early development (Gundlfinger et al., 2003; Metzger and Kapfhammer, 2000, 2003; Schrenk et al., 2002; Thomanetz et al., 2013). PKC has complex effects, which are cell-type dependent and different in developing neurons and adult neurons. It would be more important to understand whether and how PKC function is involved in the survival of Purkinje neurons in adult mice,

as SCA17 neuropathology occurs in adult neurons and loss of PKC signaling has been found in the Purkinje cells of SCA1 mouse model (Skinner et al., 2001). In addition, PKCγ null mice displayed impaired motor coordination (Chen et al., 1995). The importance of studying the role of PKC in adult neurons is also underscored by the fact that mutations in PKCγ can cause spinocerebellar ataxia-14, another age-dependent ataxia disease that is also characterized by cerebellar Purkinje cell degeneration (Chen et al., 2003; Shuvaev et al., 2011). Thus, decreased PKC activity mediated by loss of MANF could contribute to the late onset of Purkinje cell degeneration in SCA17.

Figure 4-1

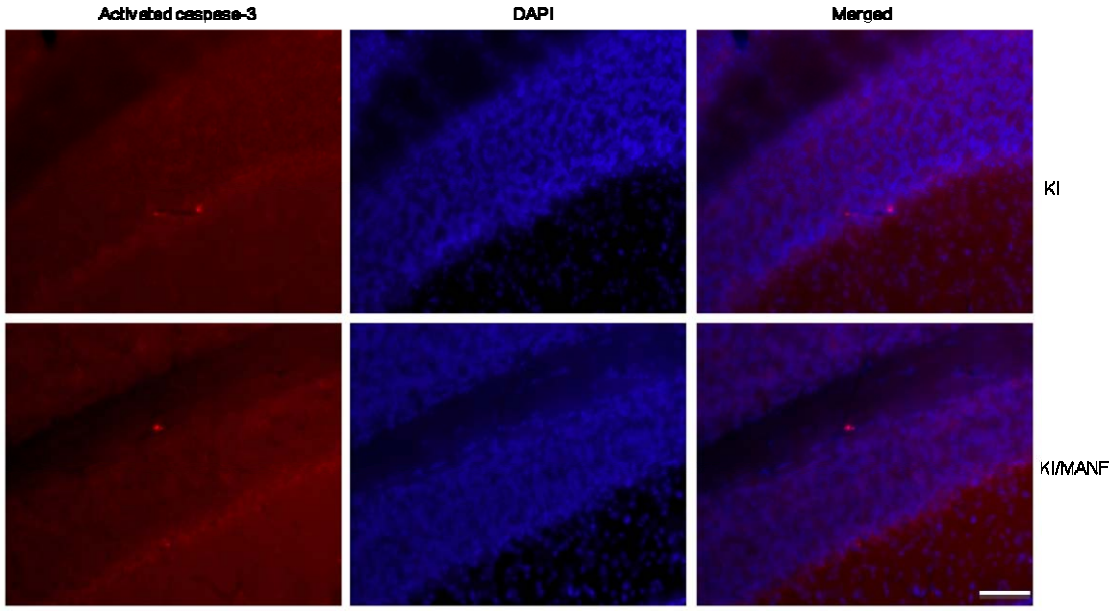

Figure 4-1 Low levels of activiated caspase-3 in the cerebellum of SCA17 KI and KI/MANF mice.

No significant difference was seen between SCA17 KI and KI/MANF cerebellar tissues. Scale bar: 20 μm.

Figure 4-2

A

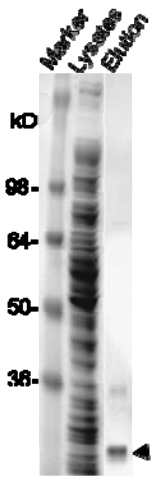

B

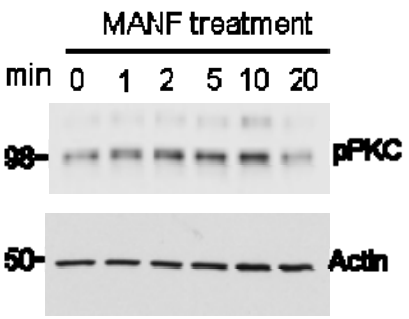

C

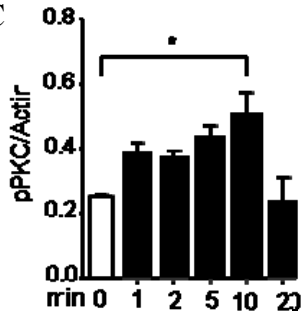

Figure 4-2 Purified MANF protein activates PKC signaling in PC12 cell culture.

(A) Coomassie staining of SDS gel containing total bacterial lysates and eluted His-MANF (arrowhead). (B) The purified His-MANF was applied to PC12 cells and the PC12 cell lysates were subjected to western blotting with an antibody to phosphor-PKC (pPKC). Actin was used as a loading control. (C) The ratios of pPKC to actin are shown (*$P< 0.05$). Data are represented as mean ± SEM.

Figure 4-3

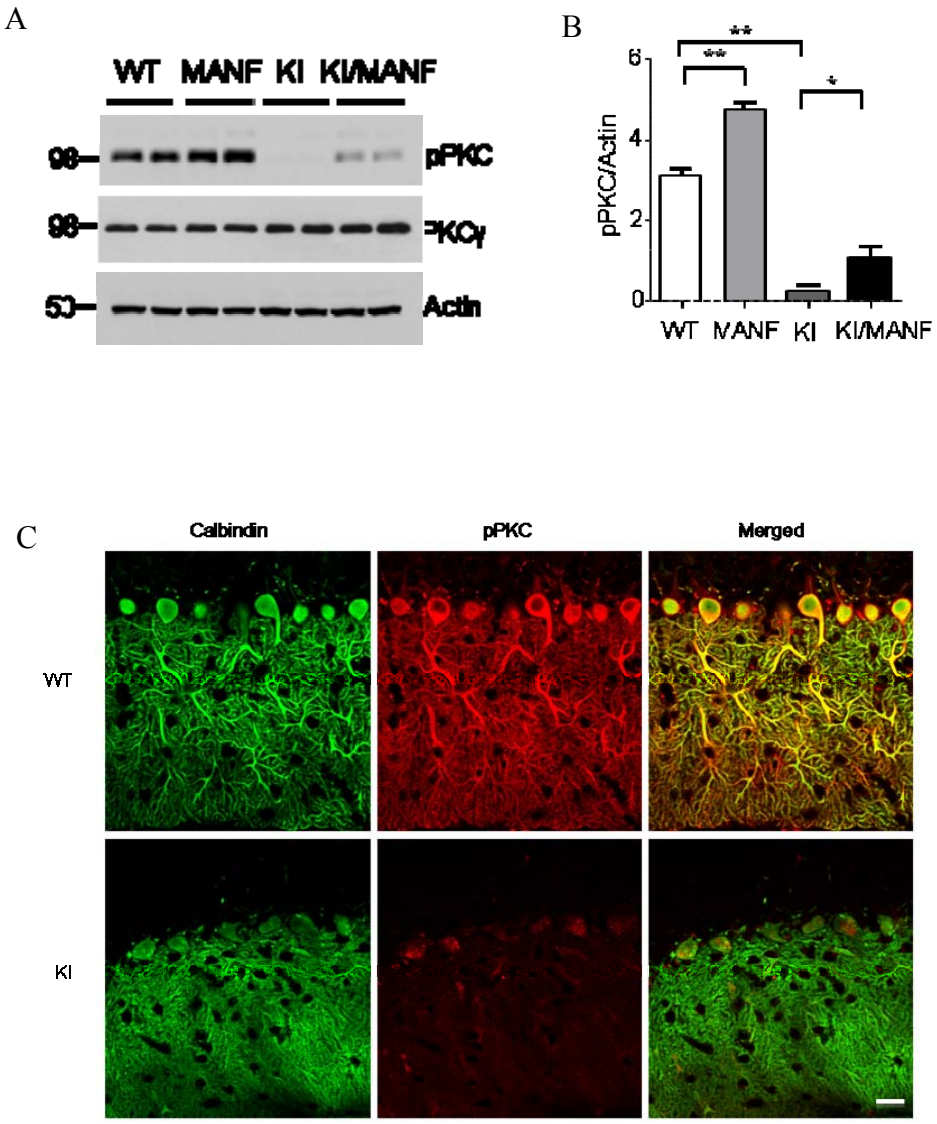
A
WT MANF KI KI/MANF
98
pPKC
98
PKCγ
50
Actin
B
pPKC/Actin
6
4
2
0
**
**
*
WT MANF KI KI/MANF
C
Calbindin
pPKC
Merged
WT
KI

Figure 4-3 Reduction of phosphorylated PKC in the cerebellum of SCA17 KI mice.

(A) Western blotting analysis of phosphor-PKC (pPKC) in the cerebellum of mice with different genotypes. (B) The ratios of pPKC to actin are show (*$P < 0.05$, **$P < 0.01$). (C) Immunofluorescent staining images (40X by confocal microscope) of WT and TBP105Q inducible KI cerebellum. Calbindin antibody was used to reveal Purkinje cells, and pPKC antibody was used to stain phosphorylated PKC. Scale bar: 20 μm. Data are represented as mean ± SEM.

Figure 4-4

A

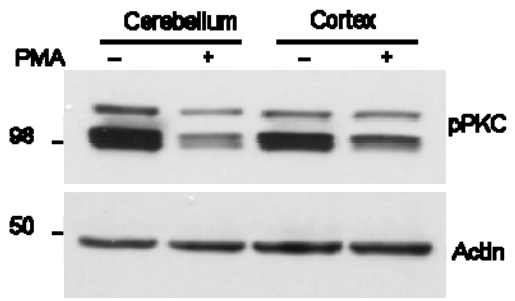
Cerebellum
Cortex
PMA
–
+
–
+
98
pPKC
50
Actin

B

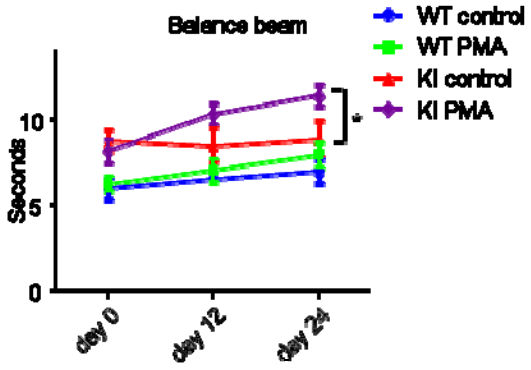
Balance beam
WT control
WT PMA
KI control
KI PMA
Seconds
10
5
0
day 0
day 12
day 24
*

Figure 4-4 Inhibition of PKC signaling exacerbated motor impairment in SCA17 KI mice.

(A) Western blotting analysis of the brain lysates from WT mice that were injected with (+) or without (-) the PKC phosphorylation modulator PMA. (B) Balance beam test of WT and SCA17 KI mice before PMA injection and 12 or 24 days after the first PMA injection. Mice injected with corn oil only were used as a control (n=6 per group, $*P < 0.05$). Data are represented as mean ± SEM.

Figure 4-5

A

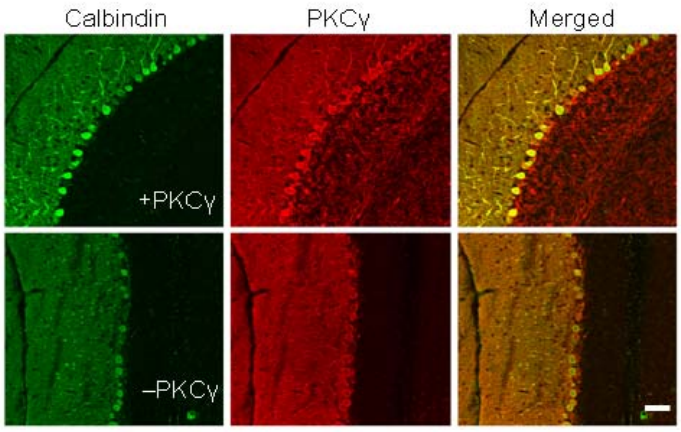

B

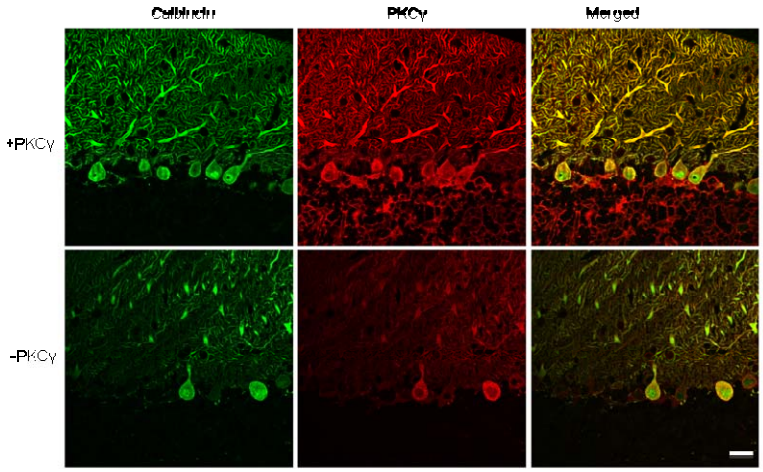

C

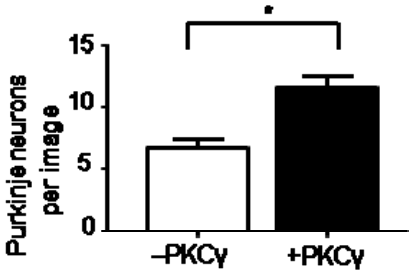

D

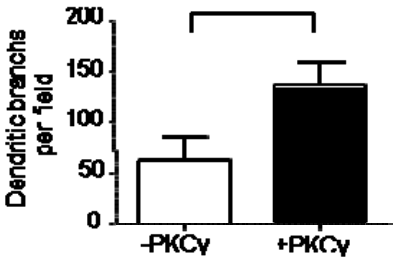

Figure 4-5 Overexpression of PKCγ ameliorated Purkinje cell degeneration in the cerebellum of SCA17 KI mice.

(A) Immunofluorescent staining images of Purkinje neuron of SCA17 KI cerebellum injected with (+) or without (–) PKCγ adenovirus. Calbindin staining was used to reveal Purkinje neurons, and PKCγ antibody was used to detect viral PKCγ. Scale bar; 50 μm (B) Immunofluorescent staining images (40X by confocal microscope) of SCA17 KI mouse cerebellum that was injected with (+) or without (–) adenoviral PKCγ. Scale bar: 20 μm. (C) Quantitative analysis of the number of Purkinje cells and (D) their branches in KI mice with or without viral PKCγ virus injection (20X, n=9, $*P < 0.05$). Data are represented as mean ± SEM.

Chapter 5

Conclusions and Future directions

5.1 Summary and conclusions

In this study, we aimed to understand two major questions in polyQ disease research: what is/are the mechanism(s) behind the age-dependent onset of polyQ diseases, and what is/are the mechanism(s) explaining the region-specific pathology in polyQ diseases. Two possibilities could explain the late-onset nature of polyQ diseases: one is that during aging, the long duration of protein expression allows misfolded proteins to accumulate and become toxic over time; the other is that aged neurons are more vulnerable to toxicity caused by misfolded proteins, when compared with neurons at an early stage. By inducing mutant TBP expression at differently aged TBP105Q inducible knock in mice, we found 14-month old mice displayed earlier onset of SCA17 symptoms than 3-month old mice, which correlated well with a higher level of mutant TBP in 14-month old mouse brains, despite the fact that both age groups of mice expressed mutant TBP for the same length of time. We also identified the chaperone system, especially one chaperone molecule Hsc70, as a target negatively affected by the natural aging process. Overexpression of Hsc70 improved mutant TBP functioning and ameliorated SCA17 pathology. Therefore, our data supports the latter possibility that age related decline of chaperone activity renders neurons more vulnerable to insults caused by misfolded proteins.

Moreover, we identified the decrease of MANF as a potential mechanism contributing to the region-specific neurodegeneration in SCA17. MANF is a neurotrophic factor enriched in the Purkinje cell layer of the cerebellum, and this enrichment is lost in the presence of mutant TBP. Mutant TBP reduced MANF expression by impairing the functions of XBP1s, a transcription factor involved in the regulation of MANF

transcription. Overexpression of MANF by means of virus infection or transgenic approach ameliorated toxicity caused by mutant TBP, possibly through PKC signaling pathway.

Taken together, we propose the following model that explains the age-dependent, region-specific neurodegeneration in SCA17 (**Figure 5-1**). During aging, the function of the chaperone system gradually declines, which leads to the accumulation of mutant TBP over time. As the total level of TBP is strictly regulated in the cells, mutant TBP accumulation simultaneously results in a reduced wild-type TBP level. Therefore, the toxicity of mutant TBP could be explained from two aspects: one is gain of toxic functions, meaning mutant TBP directly affects the functions of other proteins, possibly by sequestering them from their functional locations; the other one is loss of endogenous functions, which is exemplified by our study that mutant TBP cannot efficiently facilitate XBP1s-mediated transcriptional activities. Both mechanisms could contribute to the reduced level of MANF, a neurotrophic factor enriched in the Purkinje cells. MANF regulates PKC signaling *in vitro*, and reduction of PKC phosphorylation is found in the cerebellum of TBP105Q knock-in mice, which potentially leads to cerebellum specific degeneration in SCA17.

Our findings may have broad therapeutic implications for age-dependent neurodegenerative diseases. First, we identified Hsc70 as a molecular chaperone whose activity is impaired by aging. Overexpression of Hsc70 ameliorated mutant TBP caused toxicity both *in vitro* and *in vivo*, highlighting the importance of Hsc70 in determining SCA17 disease progression. Hsp70, a homologue of Hsc70, has been extensively studied in the polyQ diseases. A plethora of studies indicating Hsp70 overexpression affords

protection against toxicity mediated by mutant polyQ proteins, yet discrepancies exist in terms of protective mechanisms and extent of protection (Cummings et al., 1998; Hansson et al., 2003; McLear et al., 2008; Stenoien et al., 1999; Zhou et al., 2001), which could possibly be due to the fact that different organisms and different methods for Hsp70 overexpression were used in these studies. Hsc70 and Hsp70 share 84% amino acid identity (Chappell et al., 1986), and most of their functions are analogous. However, only Hsc70 is involved in chaperone mediated autophagy (He and Klionsky, 2009), and maintains protein/DNA transcriptional complex (Gehring, 2004; Li et al., 2008). More importantly, in contrast to stress induced Hsp70, Hsc70 is constitutively and abundantly expressed, constituting 1-2% of total cellular proteins (Newmyer and Schmid, 2001). Therefore, compared with Hsp70, Hsc70 could be more relevant to the pathogenesis of polyQ diseases, and overexpression of Hsc70 could be more efficacious to treat polyQ diseases.

Second, we identified MANF as a new target and PKC phosphorylation as its downstream signaling for SCA17 therapy. MANF is uniquely enriched in the Purkinje cell layer, and mutant TBP specifically decreased MANF in the cerebellum. MANF overexpression dramatically improved Purkinje cell survival in the presence of mutant TBP. It should be noted that MANF overexpression did not completely abolish mutant TBP toxicity in SCA17 KI mice. One possible explanation is that mutant TBP could also impair other tissues, such muscle (unpublished data), and transgenic MANF is only expressed in the brain. Neurotrophic factors have long been proposed as a potential treatment for neurodegenerative diseases, yet most clinical trials showed somewhat disappointing results (Bloch et al., 2004; Ochs et al., 2000). However, several technical

challenges remain unsolved before denying the therapeutic potentials of neurotrophic factors: for example, how to effectively deliver the neurotrophic factors to the target site; how to keep the neurotrophic factors active over a long period of time; what are the optimum doses for treatment. The activity of MANF in PD and SCA17 mouse models clearly warrants future development of MANF in treating neurodegenerative diseases. Because decreased levels in MANF occur in old neurons, their function can be improved into old age, which would be more economical than other preventative therapeutics that need to begin in earlier life. As Purkinje neuron degeneration is also prominent in other types of SCAs (Koeppen, 2005), the identification of MANF also provides a potential target for the treatment of specific neurodegeneration in these diseases.

5.2 Remaining questions and Future directions

The use of mouse genetics fundamentally changed our approach to study polyQ diseases. Since the generation of the first genetic HD mouse model (R6/2 mice) in 1996 (Mangiarini et al., 1996), a myriad of mouse models have been produced. These mouse models differ in their disease context (which polyQ protein encoding gene is mutated), expression profile (mutant polyQ protein is expressed all over the body, only in the brain, or restricted to specific types of cells) and expression level (mutant polyQ protein is overexpressed or expressed at endogenous levels), which allowed for detailed investigation of the pathogenic pathways mediated by expanded polyQ proteins. We believe further studying our TBP105Q knock-in mouse model could not only help elucidate SCA17 pathogenesis, but have broad implications for other polyQ diseases as well. This claim is rooted in several facts: (1) the use of Cre-loxP system enables easy

and flexible manipulation of mutant TBP expression in selected sets of cell populations; (2) mutant TBP is expressed endogenously, which faithfully recapitulates the physiological conditions in SCA17; (3) obvious and relevant disease phenotypes are observed in TBP 105Q knock-in mice, which facilitate mechanistic study and drug screening. Therefore, there is still a lot of meaningful work that could be done using TBP105Q knock-in mouse model.

Other protective mechanisms mediated by MANF

Our study identified PKC signaling as a downstream pathway mediated by MANF, and overexpression of MANF could rescue reduced PKC phosphorylation found in the cerebellum of SCA17 KI mice. However, this pathway alone may not be sufficient to explain the protective mechanisms by MANF, since only a modest increase of PKC signaling was found in KI/MANF mice (**Figure 4-3A**). Given the fact that the definitive receptor for MANF is still unknown, an important future goal is to make use of our bacterial recombinant MANF to further explore MANF mediated signaling pathways. However, a caveat of using bacterial MANF is possible differences in posttranslational modifications, compared with mammalian MANF. In addition, during export out of ER, an N-terminal signal peptide is cleaved off from the mature MANF protein, which is still present in bacterial MANF. Alternatively, MANF could be enriched from culture medium of mammalian cells transfected with MANF construct.

A major distinction between MANF and other classical neurotrophic factors is its capacity to function inside the cells. As MANF is induced upon ER stress, it would be

interesting to investigate if ER stress occurs in the presence of mutant TBP, and whether MANF overexpression alleviates ER stress in SCA17 mouse models.

Moreover, massive Purkinje cell degeneration is also characterized in other SCAs. Could MANF overexpression act as a universal protective mechanism that ameliorates symptoms in other SCA mouse models? We could cross MANF transgenic mice with SCA1 transgenic mice (Burright et al., 1995) or SCA3 transgenic mice (Chou et al., 2008) to see if any behavior improvements exist. One long-term goal is to translate bench work into clinical trials to see if boosting MANF function could be used as a therapy to treat SCAs patients.

Altered protein-protein interaction by mutant TBP

TBP is a general transcription factor that plays critical roles in the transcription of genes with or without TATA-box. However, expanded polyQ in TBP does not lead to global transcriptional dysregulation, which is suggested by the microarray result from mutant TBP transgenic mouse tissues (Friedman et al., 2007). Therefore, instead of causing transcriptional defects directly, mutant TBP is likely to alter the transcription of a subset of genes by affecting other specific transcription factors. Indeed, in our study, we found reduced association between mutant TBP and XBP1s, a transcription factor involved in ER stress response. Could mutant TBP affect some other transcription factors in a similar manner? To accomplish this, we could perform TBP pull-down followed by mass spectrometry (MS) analysis to look for changes in interaction partners between wild type and mutant TBP. Both the materials (TBP13Q and TBP105Q stable cell lines) and

antibody (EM192) for pull-down are readily available, and any potential target from MS result could be confirmed using SCA17 KI mouse tissues.

Non-motor symptoms in SCA17

Beside motor deficiencies such as ataxia and parkinsonism, SCA17 patients also display non-motor symptoms, including dementia, psychiatric abnormalities and seizure (Koide et al., 1999; Manto, 2005; Nakamura et al., 2001). In agreement with this phenomenon, radiological evaluation of patient brains reveals global cerebral atrophy (Cho et al., 2007; Rolfs et al., 2003). However, current research of SCA17 animal models mainly focuses on cerebellum degeneration and motor symptoms, as the large cell body and elaborated dendritic structures makes Purkinje cell an ideal target to study. Nonetheless, the non-motor symptoms represent an important aspect of SCA17 pathology, and similar symptoms occur in patients with other polyQ diseases, such as HD (Stevanin and Brice, 2008; Toyoshima et al., 2004). Therefore, understanding the mechanisms causing non-motor symptoms in SCA17 could be informative to other polyQ diseases as well. We could cross our floxed TBP105Q KI mice with CamKII-Cre transgenic mice to specifically express mutant TBP in the forebrain, such as cortex, striatum and hippocampus. We could analyze non-motor symptoms in CamKII-Cre/TBP105Q KI mice by performing a battery of standard tests, such as Morris water maze test, forced swimming test and fear conditioning test. Abnormal performances in certain tests will give us a general idea about which brain region is affected by mutant TBP expression, allowing us to further investigate the pathological mechanisms in that brain region.

Metabolic abnormalities mediated by MANF overexpression

Our observation of MANF transgenic mice revealed an unexpected finding that these transgenic mice become significantly obese with an average body weight about twice as much as their wild type littermates. This phenotype is unlikely to be due to the disruption of certain genes by random insertion of the transgene, as multiple lines of MANF transgenic mice showed increased body weight, and the extent of body weight increase correlated well with the level of MANF overexpression. Give that MANF is only overexpressed in the central nervous system, an interesting hypothesis is that MANF could function in the brain to regulate energy metabolism. Within the brain, the hypothalamus is the center for controlling metabolic processes. Several signaling molecules, including insulin, leptin and BDNF, regulate food intake through hypothalamus (Bruning et al., 2000; Lebrun et al., 2006; Sahu, 2003), provide the rationale that MANF could function as another signaling molecule to modify hypothalamic activities. To confirm our hypothesis, we can inject MANF lentivirus into the hypothalamus of wild type mice to see if hypothalamic overexpression of MANF leads to obesity. Again, we need to gather more information about MANF mediated signaling pathways, and check if these pathways overlap with pathways previously known to regulate hypothalamic activity. Elucidating the role of MANF on metabolic regulation could be a new direction in studying metabolic disorders, and draw more attention to study this poorly understood neurotrophic factor.

Figure 5-1

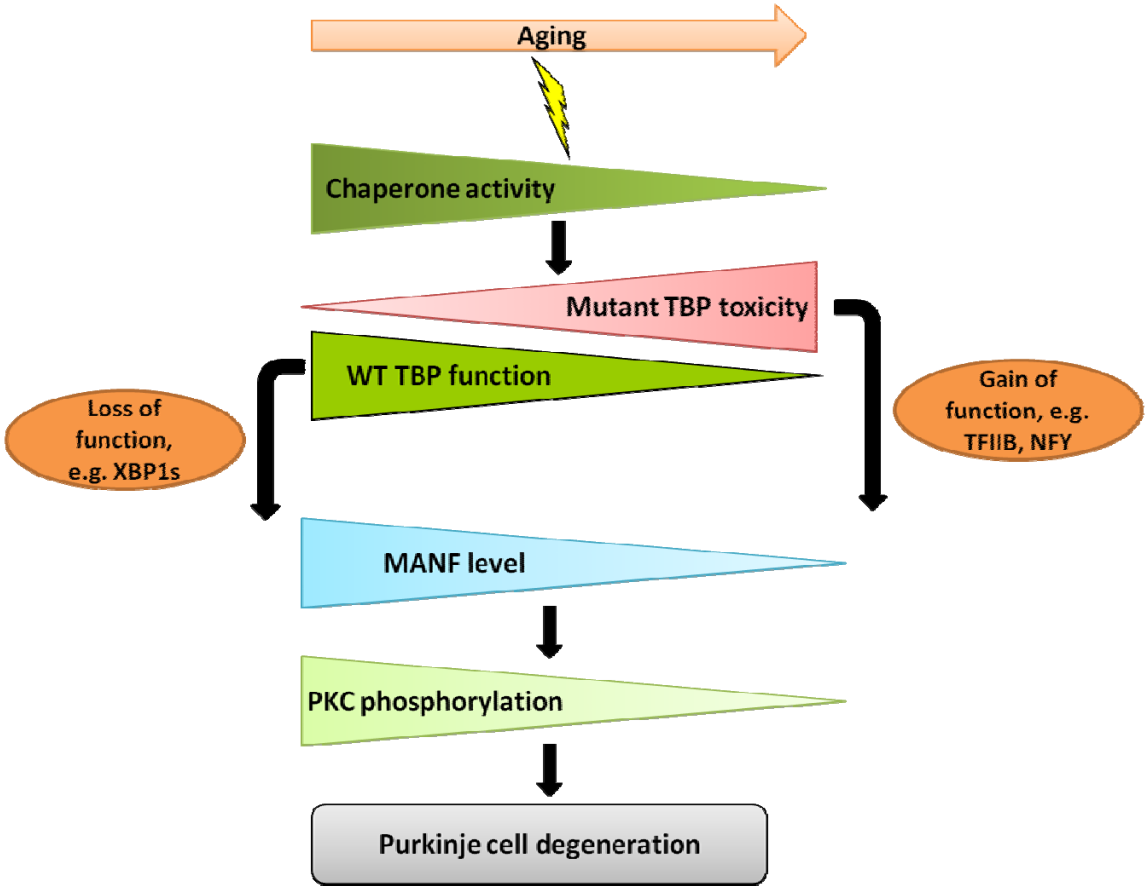
Aging
Chaperone activity
Mutant TBP toxicity
WT TBP function
Loss of function, e.g. XBP1s
Gain of function, e.g. TFIIB, NFY
MANF level
PKC phosphorylation
Purkinje cell degeneration

Figure 5-1 Proposed model for the age-related, region-specific neurodegeneration in SCA17.

Aging causes gradual decline of chaperone functioning, which leads to the accumulation of mutant TBP over time. Since the total level of TBP is strictly regulated, mutant TBP accumulation simultaneously results in a reduced wild-type (WT) TBP level. Mutant TBP could directly affects the functions of other proteins (such as TFIIB and NFY) in a gain-of-function manner. On the other hand, a reduction of WT TBP may not be able to provide sufficient support to transcription mediated by other transcription factors (such as XBP1s). Both mechanisms could contribute to a reduced level of MANF, a neurotrophic factor enriched in the Purkinje cells. MANF regulates PKC signaling, and decreased MANF reduces PKC phosphorylation, which potentially leads to cerebellum specific degeneration in SCA17.

References

Afanas'ev, I. (2010). Signaling and Damaging Functions of Free Radicals in Aging-Free Radical Theory, Hormesis, and TOR. Aging Dis *1*, 75-88.

Airaksinen, M.S., and Saarma, M. (2002). The GDNF family: signalling, biological functions and therapeutic value. Nat Rev Neurosci *3*, 383-394.

Akerfelt, M., Morimoto, R.I., and Sistonen, L. (2010). Heat shock factors: integrators of cell stress, development and lifespan. Nat Rev Mol Cell Biol *11*, 545-555.

Bauer, P.O., Goswami, A., Wong, H.K., Okuno, M., Kurosawa, M., Yamada, M., Miyazaki, H., Matsumoto, G., Kino, Y., Nagai, Y.*, et al.* (2010). Harnessing chaperone-mediated autophagy for the selective degradation of mutant huntingtin protein. Nat Biotechnol *28*, 256-263.

Bauer, S., Kerr, B.J., and Patterson, P.H. (2007). The neuropoietic cytokine family in development, plasticity, disease and injury. Nat Rev Neurosci *8*, 221-232.

Blennow, K., de Leon, M.J., and Zetterberg, H. (2006). Alzheimer's disease. Lancet *368*, 387-403.

Bloch, J., Bachoud-Levi, A.C., Deglon, N., Lefaucheur, J.P., Winkel, L., Palfi, S., Nguyen, J.P., Bourdet, C., Gaura, V., Remy, P.*, et al.* (2004). Neuroprotective gene therapy for Huntington's disease, using polymer-encapsulated cells engineered to secrete human ciliary neurotrophic factor: results of a phase I study. Hum Gene Ther *15*, 968-975.

Bowman, A.B., Lam, Y.C., Jafar-Nejad, P., Chen, H.K., Richman, R., Samaco, R.C., Fryer, J.D., Kahle, J.J., Orr, H.T., and Zoghbi, H.Y. (2007). Duplication of Atxn1l suppresses SCA1 neuropathology by decreasing incorporation of polyglutamine-expanded ataxin-1 into native complexes. Nat Genet *39*, 373-379.

Brown, I.R. (2007). Heat shock proteins and protection of the nervous system. Ann N Y Acad Sci *1113*, 147-158.

Bruni, A.C., Takahashi-Fujigasaki, J., Maltecca, F., Foncin, J.F., Servadio, A., Casari, G., D'Adamo, P., Maletta, R., Curcio, S.A., De Michele, G.*, et al.* (2004). Behavioral disorder, dementia, ataxia, and rigidity in a large family with TATA box-binding protein mutation. Arch Neurol *61*, 1314-1320.

Bruning, J.C., Gautam, D., Burks, D.J., Gillette, J., Schubert, M., Orban, P.C., Klein, R., Krone, W., Muller-Wieland, D., and Kahn, C.R. (2000). Role of brain insulin receptor in control of body weight and reproduction. Science *289*, 2122-2125.

Brusco, A., Gellera, C., Cagnoli, C., Saluto, A., Castucci, A., Michielotto, C., Fetoni, V., Mariotti, C., Migone, N., Di Donato, S.*, et al.* (2004). Molecular genetics of hereditary spinocerebellar ataxia: mutation analysis of spinocerebellar ataxia genes and CAG/CTG repeat expansion detection in 225 Italian families. Arch Neurol *61*, 727-733.

Burley, S.K., and Roeder, R.G. (1996). Biochemistry and structural biology of transcription factor IID (TFIID). Annu Rev Biochem *65*, 769-799.

Burright, E.N., Clark, H.B., Servadio, A., Matilla, T., Feddersen, R.M., Yunis, W.S., Duvick, L.A., Zoghbi, H.Y., and Orr, H.T. (1995). SCA1 transgenic mice: a model for neurodegeneration caused by an expanded CAG trinucleotide repeat. Cell *82*, 937-948.

Butler, J.E., and Kadonaga, J.T. (2002). The RNA polymerase II core promoter: a key component in the regulation of gene expression. Genes Dev *16*, 2583-2592.

Canals, J.M., Pineda, J.R., Torres-Peraza, J.F., Bosch, M., Martin-Ibanez, R., Munoz, M.T., Mengod, G., Ernfors, P., and Alberch, J. (2004). Brain-derived neurotrophic factor regulates the onset and severity of motor dysfunction associated with enkephalinergic neuronal degeneration in Huntington's disease. J Neurosci *24*, 7727-7739.

Capitani, M., and Sallese, M. (2009). The KDEL receptor: new functions for an old protein. FEBS Lett *583*, 3863-3871.

Cattaneo, E., Zuccato, C., and Tartari, M. (2005). Normal huntingtin function: an alternative approach to Huntington's disease. Nat Rev Neurosci *6*, 919-930.

Chan, H.Y., Warrick, J.M., Gray-Board, G.L., Paulson, H.L., and Bonini, N.M. (2000). Mechanisms of chaperone suppression of polyglutamine disease: selectivity, synergy and modulation of protein solubility in Drosophila. Hum Mol Genet *9*, 2811-2820.

Chang, Y.C., Lin, C.Y., Hsu, C.M., Lin, H.C., Chen, Y.H., Lee-Chen, G.J., Su, M.T., Ro, L.S., Chen, C.M., and Hsieh-Li, H.M. (2011). Neuroprotective effects of granulocyte-colony stimulating factor in a novel transgenic mouse model of SCA17. J Neurochem *118*, 288-303.

Chappell, T.G., Welch, W.J., Schlossman, D.M., Palter, K.B., Schlesinger, M.J., and Rothman, J.E. (1986). Uncoating ATPase is a member of the 70 kilodalton family of stress proteins. Cell *45*, 3-13.

Chen, C., Kano, M., Abeliovich, A., Chen, L., Bao, S., Kim, J.J., Hashimoto, K., Thompson, R.F., and Tonegawa, S. (1995). Impaired motor coordination correlates with persistent multiple climbing fiber innervation in PKC gamma mutant mice. Cell *83*, 1233-1242.

Chen, D.H., Brkanac, Z., Verlinde, C.L., Tan, X.J., Bylenok, L., Nochlin, D., Matsushita, M., Lipe, H., Wolff, J., Fernandez, M.*, et al.* (2003). Missense mutations in the regulatory domain of PKC gamma: a new mechanism for dominant nonepisodic cerebellar ataxia. Am J Hum Genet *72*, 839-849.

Chen, S., Ferrone, F.A., and Wetzel, R. (2002). Huntington's disease age-of-onset linked to polyglutamine aggregation nucleation. Proc Natl Acad Sci U S A *99*, 11884-11889.

Chiang, H.L., Terlecky, S.R., Plant, C.P., and Dice, J.F. (1989). A role for a 70-kilodalton heat shock protein in lysosomal degradation of intracellular proteins. Science *246*, 382-385.

Cho, S.R., Benraiss, A., Chmielnicki, E., Samdani, A., Economides, A., and Goldman, S.A. (2007). Induction of neostriatal neurogenesis slows disease progression in a transgenic murine model of Huntington disease. J Clin Invest *117*, 2889-2902.

Chou, A.H., Yeh, T.H., Ouyang, P., Chen, Y.L., Chen, S.Y., and Wang, H.L. (2008). Polyglutamine-expanded ataxin-3 causes cerebellar dysfunction of SCA3 transgenic mice by inducing transcriptional dysregulation. Neurobiol Dis *31*, 89-101.

Clemens, M.J., Trayner, I., and Menaya, J. (1992). The role of protein kinase C isoenzymes in the regulation of cell proliferation and differentiation. J Cell Sci *103 (Pt 4)*, 881-887.

Colin, E., Zala, D., Liot, G., Rangone, H., Borrell-Pages, M., Li, X.J., Saudou, F., and Humbert, S. (2008). Huntingtin phosphorylation acts as a molecular switch for anterograde/retrograde transport in neurons. EMBO J *27*, 2124-2134.

Collier, T.J., Kanaan, N.M., and Kordower, J.H. (2011). Ageing as a primary risk factor for Parkinson's disease: evidence from studies of non-human primates. Nat Rev Neurosci *12*, 359-366.

Craig, K., Keers, S.M., Walls, T.J., Curtis, A., and Chinnery, P.F. (2005). Minimum prevalence of spinocerebellar ataxia 17 in the north east of England. J Neurol Sci *239*, 105-109.

Cummings, C.J., Mancini, M.A., Antalffy, B., DeFranco, D.B., Orr, H.T., and Zoghbi, H.Y. (1998). Chaperone suppression of aggregation and altered subcellular proteasome localization imply protein misfolding in SCA1. Nat Genet *19*, 148-154.

Cummings, C.J., Sun, Y., Opal, P., Antalffy, B., Mestril, R., Orr, H.T., Dillmann, W.H., and Zoghbi, H.Y. (2001). Over-expression of inducible HSP70 chaperone suppresses neuropathology and improves motor function in SCA1 mice. Human molecular genetics *10*, 1511-1518.

Cvetanovic, M., Patel, J.M., Marti, H.H., Kini, A.R., and Opal, P. (2011). Vascular endothelial growth factor ameliorates the ataxic phenotype in a mouse model of spinocerebellar ataxia type 1. Nat Med *17*, 1445-1447.

Damiano, M., Galvan, L., Deglon, N., and Brouillet, E. (2010). Mitochondria in Huntington's disease. Biochim Biophys Acta *1802*, 52-61.

DiFiglia, M., Sapp, E., Chase, K.O., Davies, S.W., Bates, G.P., Vonsattel, J.P., and Aronin, N. (1997). Aggregation of huntingtin in neuronal intranuclear inclusions and dystrophic neurites in brain. Science *277*, 1990-1993.

Duan, W., Guo, Z., Jiang, H., Ware, M., Li, X.J., and Mattson, M.P. (2003). Dietary restriction normalizes glucose metabolism and BDNF levels, slows disease progression, and increases survival in huntingtin mutant mice. Proc Natl Acad Sci U S A *100*, 2911-2916.

Duyao, M., Ambrose, C., Myers, R., Novelletto, A., Persichetti, F., Frontali, M., Folstein, S., Ross, C., Franz, M., Abbott, M.*, et al.* (1993). Trinucleotide repeat length instability and age of onset in Huntington's disease. Nat Genet *4*, 387-392.

Evron, E., Cairns, P., Halachmi, N., Ahrendt, S.A., Reed, A.L., and Sidransky, D. (1997). Normal polymorphism in the incomplete trinucleotide repeat of the arginine-rich protein gene. Cancer Res *57*, 2888-2889.

Federico, A., Cardaioli, E., Da Pozzo, P., Formichi, P., Gallus, G.N., and Radi, E. (2012). Mitochondria, oxidative stress and neurodegeneration. J Neurol Sci.

Freisewinkel, I., Riethmacher, D., and Stabel, S. (1991). Downregulation of protein kinase C-gamma is independent of a functional kinase domain. FEBS Lett *280*, 262-266.

Friedman, M.J., Li, S., and Li, X.J. (2009). Activation of gene transcription by heat shock protein 27 may contribute to its neuronal protection. J Biol Chem *284*, 27944-27951.

Friedman, M.J., Shah, A.G., Fang, Z.H., Ward, E.G., Warren, S.T., Li, S., and Li, X.J. (2007). Polyglutamine domain modulates the TBP-TFIIB interaction: implications for its normal function and neurodegeneration. Nat Neurosci *10*, 1519-1528.

Friedman, M.J., Wang, C.E., Li, X.J., and Li, S. (2008). Polyglutamine expansion reduces the association of TATA-binding protein with DNA and induces DNA binding-independent neurotoxicity. J Biol Chem *283*, 8283-8290.

Fusco, F.R., Chen, Q., Lamoreaux, W.J., Figueredo-Cardenas, G., Jiao, Y., Coffman, J.A., Surmeier, D.J., Honig, M.G., Carlock, L.R., and Reiner, A. (1999). Cellular localization of huntingtin in striatal and cortical neurons in rats: lack of correlation with neuronal vulnerability in Huntington's disease. J Neurosci *19*, 1189-1202.

Gandhi, S., and Abramov, A.Y. (2012). Mechanism of oxidative stress in neurodegeneration. Oxid Med Cell Longev *2012*, 428010.

Gauthier, L.R., Charrin, B.C., Borrell-Pages, M., Dompierre, J.P., Rangone, H., Cordelieres, F.P., De Mey, J., MacDonald, M.E., Lessmann, V., Humbert, S.*, et al.* (2004). Huntingtin controls neurotrophic support and survival of neurons by enhancing BDNF vesicular transport along microtubules. Cell *118*, 127-138.

Gehring, U. (2004). Biological activities of HAP46/BAG-1. The HAP46/BAG-1 protein: regulator of HSP70 chaperones, DNA-binding protein and stimulator of transcription. EMBO Rep *5*, 148-153.

Gestwicki, J.E., and Garza, D. (2012). Protein quality control in neurodegenerative disease. Prog Mol Biol Transl Sci *107*, 327-353.

Gharami, K., Xie, Y., An, J.J., Tonegawa, S., and Xu, B. (2008). Brain-derived neurotrophic factor over-expression in the forebrain ameliorates Huntington's disease phenotypes in mice. J Neurochem *105*, 369-379.

Gidalevitz, T., Ben-Zvi, A., Ho, K.H., Brignull, H.R., and Morimoto, R.I. (2006). Progressive disruption of cellular protein folding in models of polyglutamine diseases. Science *311*, 1471-1474.

Gostout, B., Liu, Q., and Sommer, S.S. (1993). "Cryptic" repeating triplets of purines and pyrimidines (cRRY(i)) are frequent and polymorphic: analysis of coding cRRY(i) in the proopiomelanocortin (POMC) and TATA-binding protein (TBP) genes. Am J Hum Genet *52*, 1182-1190.

Griner, E.M., and Kazanietz, M.G. (2007). Protein kinase C and other diacylglycerol effectors in cancer. Nat Rev Cancer *7*, 281-294.

Gundlfinger, A., Kapfhammer, J.P., Kruse, F., Leitges, M., and Metzger, F. (2003). Different regulation of Purkinje cell dendritic development in cerebellar slice cultures by protein kinase Calpha and -beta. J Neurobiol *57*, 95-109.

Gutekunst, C.A., Li, S.H., Yi, H., Mulroy, J.S., Kuemmerle, S., Jones, R., Rye, D., Ferrante, R.J., Hersch, S.M., and Li, X.J. (1999). Nuclear and neuropil aggregates in Huntington's disease: relationship to neuropathology. J Neurosci *19*, 2522-2534.

Hansson, O., Nylandsted, J., Castilho, R.F., Leist, M., Jaattela, M., and Brundin, P. (2003). Overexpression of heat shock protein 70 in R6/2 Huntington's disease mice has only modest effects on disease progression. Brain Res *970*, 47-57.

He, C., and Klionsky, D.J. (2009). Regulation mechanisms and signaling pathways of autophagy. Annu Rev Genet *43*, 67-93.

Helenius, K., Yang, Y., Tselykh, T.V., Pessa, H.K., Frilander, M.J., and Makela, T.P. (2011). Requirement of TFIIH kinase subunit Mat1 for RNA Pol II C-terminal domain Ser5 phosphorylation, transcription and mRNA turnover. Nucleic Acids Res *39*, 5025-5035.

Hellman, M., Arumae, U., Yu, L.Y., Lindholm, P., Peranen, J., Saarma, M., and Permi, P. (2011). Mesencephalic astrocyte-derived neurotrophic factor (MANF) has a unique mechanism to rescue apoptotic neurons. J Biol Chem *286*, 2675-2680.

Helmlinger, D., Bonnet, J., Mandel, J.L., Trottier, Y., and Devys, D. (2004). Hsp70 and Hsp40 chaperones do not modulate retinal phenotype in SCA7 mice. J Biol Chem *279*, 55969-55977.

Henderson, M.J., Richie, C.T., Airavaara, M., Wang, Y., and Harvey, B.K. (2013). Mesencephalic astrocyte-derived neurotrophic factor (MANF) secretion and cell surface binding are modulated by KDEL receptors. J Biol Chem *288*, 4209-4225.

Hernandez, N. (1993). TBP, a universal eukaryotic transcription factor? Genes Dev *7*, 1291-1308.

Hetz, C. (2012). The unfolded protein response: controlling cell fate decisions under ER stress and beyond. Nat Rev Mol Cell Biol *13*, 89-102.

Hobbs, N.K., Bondareva, A.A., Barnett, S., Capecchi, M.R., and Schmidt, E.E. (2002). Removing the vertebrate-specific TBP N terminus disrupts placental beta2m-dependent interactions with the maternal immune system. Cell *110*, 43-54.

Holmberg, C.I., Staniszewski, K.E., Mensah, K.N., Matouschek, A., and Morimoto, R.I. (2004). Inefficient degradation of truncated polyglutamine proteins by the proteasome. EMBO J *23*, 4307-4318.

Huang, C.C., Faber, P.W., Persichetti, F., Mittal, V., Vonsattel, J.P., MacDonald, M.E., and Gusella, J.F. (1998). Amyloid formation by mutant huntingtin: threshold, progressivity and recruitment of normal polyglutamine proteins. Somat Cell Mol Genet *24*, 217-233.

Huang, E.J., and Reichardt, L.F. (2001). Neurotrophins: roles in neuronal development and function. Annu Rev Neurosci *24*, 677-736.

Huang, S., Ling, J.J., Yang, S., Li, X.J., and Li, S. (2011). Neuronal expression of TATA box-binding protein containing expanded polyglutamine in knock-in mice reduces chaperone protein response by impairing the function of nuclear factor-Y transcription factor. Brain *134*, 1943-1958.

Humbert, S., Bryson, E.A., Cordelieres, F.P., Connors, N.C., Datta, S.R., Finkbeiner, S., Greenberg, M.E., and Saudou, F. (2002). The IGF-1/Akt pathway is neuroprotective in Huntington's disease and involves Huntingtin phosphorylation by Akt. Dev Cell *2*, 831-837.

Jana, N.R., Tanaka, M., Wang, G., and Nukina, N. (2000). Polyglutamine length-dependent interaction of Hsp40 and Hsp70 family chaperones with truncated N-terminal huntingtin: their role in suppression of aggregation and cellular toxicity. Hum Mol Genet *9*, 2009-2018.

Jorgensen, N.D., Andresen, J.M., Pitt, J.E., Swenson, M.A., Zoghbi, H.Y., and Orr, H.T. (2007). Hsp70/Hsc70 regulates the effect phosphorylation has on stabilizing ataxin-1. J Neurochem *102*, 2040-2048.

Kalchman, M.A., Graham, R.K., Xia, G., Koide, H.B., Hodgson, J.G., Graham, K.C., Goldberg, Y.P., Gietz, R.D., Pickart, C.M., and Hayden, M.R. (1996). Huntingtin is ubiquitinated and interacts with a specific ubiquitin-conjugating enzyme. J Biol Chem *271*, 19385-19394.

Kampinga, H.H., and Craig, E.A. (2010). The HSP70 chaperone machinery: J proteins as drivers of functional specificity. Nat Rev Mol Cell Biol *11*, 579-592.

Kegel, K.B., Kim, M., Sapp, E., McIntyre, C., Castano, J.G., Aronin, N., and DiFiglia, M. (2000). Huntingtin expression stimulates endosomal-lysosomal activity, endosome tubulation, and autophagy. J Neurosci *20*, 7268-7278.

Keller, J.N., Hanni, K.B., and Markesbery, W.R. (2000a). Possible involvement of proteasome inhibition in aging: implications for oxidative stress. Mech Ageing Dev *113*, 61-70.

Keller, J.N., Huang, F.F., and Markesbery, W.R. (2000b). Decreased levels of proteasome activity and proteasome expression in aging spinal cord. Neuroscience *98*, 149-156.

Kelp, A., Koeppen, A.H., Petrasch-Parwez, E., Calaminus, C., Bauer, C., Portal, E., Yu-Taeger, L., Pichler, B., Bauer, P., Riess, O.*, et al.* (2013). A novel transgenic rat model for spinocerebellar ataxia type 17 recapitulates neuropathological changes and supplies in vivo imaging biomarkers. J Neurosci *33*, 9068-9081.

Kim, J.L., Nikolov, D.B., and Burley, S.K. (1993). Co-crystal structure of TBP recognizing the minor groove of a TATA element. Nature *365*, 520-527.

Kim, Y.E., Hipp, M.S., Bracher, A., Hayer-Hartl, M., and Hartl, F.U. (2013). Molecular chaperone functions in protein folding and proteostasis. Annu Rev Biochem *82*, 323-355.

Koeppen, A.H. (2005). The pathogenesis of spinocerebellar ataxia. Cerebellum *4*, 62-73.

Koga, H., Martinez-Vicente, M., Arias, E., Kaushik, S., Sulzer, D., and Cuervo, A.M. (2011). Constitutive upregulation of chaperone-mediated autophagy in Huntington's disease. J Neurosci *31*, 18492-18505.

Koide, R., Kobayashi, S., Shimohata, T., Ikeuchi, T., Maruyama, M., Saito, M., Yamada, M., Takahashi, H., and Tsuji, S. (1999). A neurological disease caused by an expanded CAG trinucleotide repeat in the TATA-binding protein gene: a new polyglutamine disease? Hum Mol Genet *8*, 2047-2053.

Komander, D., and Rape, M. (2012). The ubiquitin code. Annu Rev Biochem *81*, 203-229.

Lebrun, B., Bariohay, B., Moyse, E., and Jean, A. (2006). Brain-derived neurotrophic factor (BDNF) and food intake regulation: a minireview. Auton Neurosci *126-127*, 30-38.

Lee, A.H., Iwakoshi, N.N., and Glimcher, L.H. (2003). XBP-1 regulates a subset of endoplasmic reticulum resident chaperone genes in the unfolded protein response. Mol Cell Biol *23*, 7448-7459.

Lee, J., Hwang, Y.J., Kim, K.Y., Kowall, N.W., and Ryu, H. (2013). Epigenetic mechanisms of neurodegeneration in Huntington's disease. Neurotherapeutics *10*, 664-676.

Lee, L.C., Chen, C.M., Wang, H.C., Hsieh, H.H., Chiu, I.S., Su, M.T., Hsieh-Li, H.M., Wu, C.H., Lee, G.C., Lee-Chen, G.J.*, et al.* (2012). Role of the CCAAT-binding protein NFY in SCA17 pathogenesis. PLoS One *7*, e35302.

Lee, T.I., and Young, R.A. (2000). Transcription of eukaryotic protein-coding genes. Annu Rev Genet *34*, 77-137.

Levi-Montalcini, R. (1987). The nerve growth factor 35 years later. Science *237*, 1154-1162.

Levine, B., and Kroemer, G. (2008). Autophagy in the pathogenesis of disease. Cell *132*, 27-42.

Li, L., Johnson, L.A., Dai-Ju, J.Q., and Sandri-Goldin, R.M. (2008). Hsc70 focus formation at the periphery of HSV-1 transcription sites requires ICP27. PLoS One *3*, e1491.

Li, X.J., and Li, S. (2011a). Proteasomal dysfunction in aging and Huntington disease. Neurobiol Dis *43*, 4-8.

Li, X.J., and Li, S. (2011b). Proteasomal dysfunction in aging and Huntington disease. Neurobiol Dis *43*, 4-8.

Lieberman, A.P., Harmison, G., Strand, A.D., Olson, J.M., and Fischbeck, K.H. (2002). Altered transcriptional regulation in cells expressing the expanded polyglutamine androgen receptor. Hum Mol Genet *11*, 1967-1976.

Lim, J., Crespo-Barreto, J., Jafar-Nejad, P., Bowman, A.B., Richman, R., Hill, D.E., Orr, H.T., and Zoghbi, H.Y. (2008). Opposing effects of polyglutamine expansion on native protein complexes contribute to SCA1. Nature *452*, 713-718.

Lindholm, P., and Saarma, M. (2010). Novel CDNF/MANF family of neurotrophic factors. Dev Neurobiol *70*, 360-371.

Liu, K., Hsiung, S., Adlersberg, M., Sacktor, T., Gershon, M.D., and Tamir, H. (2000). Ca(2+)-evoked serotonin secretion by parafollicular cells: roles in signal transduction of phosphatidylinositol 3'-kinase, and the gamma and zeta isoforms of protein kinase C. J Neurosci *20*, 1365-1373.

Liu, T., Daniels, C.K., and Cao, S. (2012). Comprehensive review on the HSC70 functions, interactions with related molecules and involvement in clinical diseases and therapeutic potential. Pharmacol Ther *136*, 354-374.

Lopez-Otin, C., Blasco, M.A., Partridge, L., Serrano, M., and Kroemer, G. (2013). The hallmarks of aging. Cell *153*, 1194-1217.

Luthi-Carter, R., Hanson, S.A., Strand, A.D., Bergstrom, D.A., Chun, W., Peters, N.L., Woods, A.M., Chan, E.Y., Kooperberg, C., Krainc, D*., et al.* (2002). Dysregulation of gene expression in the R6/2 model of polyglutamine disease: parallel changes in muscle and brain. Hum Mol Genet *11*, 1911-1926.

Maltecca, F., Filla, A., Castaldo, I., Coppola, G., Fragassi, N.A., Carella, M., Bruni, A., Cocozza, S., Casari, G., Servadio, A*., et al.* (2003). Intergenerational instability and marked anticipation in SCA-17. Neurology *61*, 1441-1443.

Mangiarini, L., Sathasivam, K., Seller, M., Cozens, B., Harper, A., Hetherington, C., Lawton, M., Trottier, Y., Lehrach, H., Davies, S.W*., et al.* (1996). Exon 1 of the HD gene with an

expanded CAG repeat is sufficient to cause a progressive neurological phenotype in transgenic mice. Cell *87*, 493-506.

Manto, M.U. (2005). The wide spectrum of spinocerebellar ataxias (SCAs). Cerebellum *4*, 2-6.

Marsh, J.L., Walker, H., Theisen, H., Zhu, Y.Z., Fielder, T., Purcell, J., and Thompson, L.M. (2000). Expanded polyglutamine peptides alone are intrinsically cytotoxic and cause neurodegeneration in Drosophila. Hum Mol Genet *9*, 13-25.

Martianov, I., Viville, S., and Davidson, I. (2002). RNA polymerase II transcription in murine cells lacking the TATA binding protein. Science *298*, 1036-1039.

McLear, J.A., Lebrecht, D., Messer, A., and Wolfgang, W.J. (2008). Combinational approach of intrabody with enhanced Hsp70 expression addresses multiple pathologies in a fly model of Huntington's disease. FASEB J *22*, 2003-2011.

McMurray, C.T. (2010). Mechanisms of trinucleotide repeat instability during human development. Nat Rev Genet *11*, 786-799.

Metzger, F., and Kapfhammer, J.P. (2000). Protein kinase C activity modulates dendritic differentiation of rat Purkinje cells in cerebellar slice cultures. Eur J Neurosci *12*, 1993-2005.

Metzger, F., and Kapfhammer, J.P. (2003). Protein kinase C: its role in activity-dependent Purkinje cell dendritic development and plasticity. Cerebellum *2*, 206-214.

Mizobuchi, N., Hoseki, J., Kubota, H., Toyokuni, S., Nozaki, J., Naitoh, M., Koizumi, A., and Nagata, K. (2007). ARMET is a soluble ER protein induced by the unfolded protein response via ERSE-II element. Cell Struct Funct *32*, 41-50.

Mizushima, N. (2007). Autophagy: process and function. Genes Dev *21*, 2861-2873.

Moller, T. (2010). Neuroinflammation in Huntington's disease. J Neural Transm *117*, 1001-1008.

Nagai, Y., Inui, T., Popiel, H.A., Fujikake, N., Hasegawa, K., Urade, Y., Goto, Y., Naiki, H., and Toda, T. (2007). A toxic monomeric conformer of the polyglutamine protein. Nat Struct Mol Biol *14*, 332-340.

Nagaoka, U., Kim, K., Jana, N.R., Doi, H., Maruyama, M., Mitsui, K., Oyama, F., and Nukina, N. (2004). Increased expression of p62 in expanded polyglutamine-expressing cells and its association with polyglutamine inclusions. J Neurochem *91*, 57-68.

Nakamura, K., Jeong, S.Y., Uchihara, T., Anno, M., Nagashima, K., Nagashima, T., Ikeda, S., Tsuji, S., and Kanazawa, I. (2001). SCA17, a novel autosomal dominant cerebellar ataxia caused by an expanded polyglutamine in TATA-binding protein. Hum Mol Genet *10*, 1441-1448.

Nascimento-Ferreira, I., Santos-Ferreira, T., Sousa-Ferreira, L., Auregan, G., Onofre, I., Alves, S., Dufour, N., Colomer Gould, V.F., Koeppen, A., Deglon, N.*, et al.* (2011). Overexpression of the autophagic beclin-1 protein clears mutant ataxin-3 and alleviates Machado-Joseph disease. Brain *134*, 1400-1415.

Nedelsky, N.B., Pennuto, M., Smith, R.B., Palazzolo, I., Moore, J., Nie, Z., Neale, G., and Taylor, J.P. (2010). Native functions of the androgen receptor are essential to pathogenesis in a Drosophila model of spinobulbar muscular atrophy. Neuron *67*, 936-952.

Newmyer, S.L., and Schmid, S.L. (2001). Dominant-interfering Hsc70 mutants disrupt multiple stages of the clathrin-coated vesicle cycle in vivo. J Cell Biol *152*, 607-620.

Nikolov, D.B., and Burley, S.K. (1994). 2.1 A resolution refined structure of a TATA box-binding protein (TBP). Nat Struct Biol *1*, 621-637.

Niyaz, Y., Zeiner, M., and Gehring, U. (2001). Transcriptional activation by the human Hsp70-associating protein Hap50. J Cell Sci *114*, 1839-1845.

Novoselova, T.V., Margulis, B.A., Novoselov, S.S., Sapozhnikov, A.M., van der Spuy, J., Cheetham, M.E., and Guzhova, I.V. (2005). Treatment with extracellular HSP70/HSC70 protein can reduce polyglutamine toxicity and aggregation. J Neurochem *94*, 597-606.

Ochs, G., Penn, R.D., York, M., Giess, R., Beck, M., Tonn, J., Haigh, J., Malta, E., Traub, M., Sendtner, M.*, et al.* (2000). A phase I/II trial of recombinant methionyl human brain derived neurotrophic factor administered by intrathecal infusion to patients with amyotrophic lateral sclerosis. Amyotrophic lateral sclerosis and other motor neuron disorders : official publication of the World Federation of Neurology, Research Group on Motor Neuron Diseases *1*, 201-206.

Ohigashi, T., Mallia, C.S., McGary, E., Scandurro, A.B., Rondon, I., Fisher, J.W., and Beckman, B.S. (1999). Protein kinase C alpha protein expression is necessary for sustained erythropoietin production in human hepatocellular carcinoma (Hep3B) cells exposed to hypoxia. Biochim Biophys Acta *1450*, 109-118.

Orr, H.T., and Zoghbi, H.Y. (2007). Trinucleotide repeat disorders. Annu Rev Neurosci *30*, 575-621.

Palgi, M., Lindstrom, R., Peranen, J., Piepponen, T.P., Saarma, M., and Heino, T.I. (2009). Evidence that DmMANF is an invertebrate neurotrophic factor supporting dopaminergic neurons. Proc Natl Acad Sci U S A *106*, 2429-2434.

Parkash, V., Lindholm, P., Peranen, J., Kalkkinen, N., Oksanen, E., Saarma, M., Leppanen, V.M., and Goldman, A. (2009). The structure of the conserved neurotrophic factors MANF and CDNF explains why they are bifunctional. Protein engineering, design & selection : PEDS *22*, 233-241.

Passos, J.F., and von Zglinicki, T. (2005). Mitochondria, telomeres and cell senescence. Exp Gerontol *40*, 466-472.

Perez-Navarro, E., Canudas, A.M., Akerund, P., Alberch, J., and Arenas, E. (2000). Brain-derived neurotrophic factor, neurotrophin-3, and neurotrophin-4/5 prevent the death of striatal projection neurons in a rodent model of Huntington's disease. J Neurochem *75*, 2190-2199.

Perletti, L., Dantonel, J.C., and Davidson, I. (1999). The TATA-binding protein and its associated factors are differentially expressed in adult mouse tissues. J Biol Chem *274*, 15301-15304.

Perutz, M.F., Johnson, T., Suzuki, M., and Finch, J.T. (1994). Glutamine repeats as polar zippers: their possible role in inherited neurodegenerative diseases. Proc Natl Acad Sci U S A *91*, 5355-5358.

Petrova, P., Raibekas, A., Pevsner, J., Vigo, N., Anafi, M., Moore, M.K., Peaire, A.E., Shridhar, V., Smith, D.I., Kelly, J.*, et al.* (2003). MANF: a new mesencephalic, astrocyte-derived neurotrophic factor with selectivity for dopaminergic neurons. J Mol Neurosci *20*, 173-188.

Pugh, B.F. (2000). Control of gene expression through regulation of the TATA-binding protein. Gene *255*, 1-14.

Qin, Z.H., Wang, Y., Kegel, K.B., Kazantsev, A., Apostol, B.L., Thompson, L.M., Yoder, J., Aronin, N., and DiFiglia, M. (2003). Autophagy regulates the processing of amino terminal huntingtin fragments. Hum Mol Genet *12*, 3231-3244.

Ravikumar, B., Vacher, C., Berger, Z., Davies, J.E., Luo, S., Oroz, L.G., Scaravilli, F., Easton, D.F., Duden, R., O'Kane, C.J.*, et al.* (2004). Inhibition of mTOR induces autophagy and reduces toxicity of polyglutamine expansions in fly and mouse models of Huntington disease. Nat Genet *36*, 585-595.

Reid, S.J., Rees, M.I., van Roon-Mom, W.M., Jones, A.L., MacDonald, M.E., Sutherland, G., During, M.J., Faull, R.L., Owen, M.J., Dragunow, M.*, et al.* (2003). Molecular investigation of TBP allele length: a SCA17 cellular model and population study. Neurobiol Dis *13*, 37-45.

Ren, J., Jegga, A.G., Zhang, M., Deng, J., Liu, J., Gordon, C.B., Aronow, B.J., Lu, L.J., Zhang, B., and Ma, J. (2011). A Drosophila model of the neurodegenerative disease SCA17 reveals a role of RBP-J/Su(H) in modulating the pathological outcome. Hum Mol Genet *20*, 3424-3436.

Reynolds, N.J., Baldassare, J.J., Henderson, P.A., Shuler, J.L., Ballas, L.M., Burns, D.J., Moomaw, C.R., and Fisher, G.J. (1994). Translocation and downregulation of protein kinase C isoenzymes-alpha and -epsilon by phorbol ester and bryostatin-1 in human keratinocytes and fibroblasts. J Invest Dermatol *103*, 364-369.

Rolfs, A., Koeppen, A.H., Bauer, I., Bauer, P., Buhlmann, S., Topka, H., Schols, L., and Riess, O. (2003). Clinical features and neuropathology of autosomal dominant spinocerebellar ataxia (SCA17). Ann Neurol *54*, 367-375.

Rubinsztein, D.C., Leggo, J., Crow, T.J., DeLisi, L.E., Walsh, C., Jain, S., and Paykel, E.S. (1996). Analysis of polyglutamine-coding repeats in the TATA-binding protein in different human populations and in patients with schizophrenia and bipolar affective disorder. Am J Med Genet *67*, 495-498.

Sahu, A. (2003). Leptin signaling in the hypothalamus: emphasis on energy homeostasis and leptin resistance. Front Neuroendocrinol *24*, 225-253.

Sapp, E., Schwarz, C., Chase, K., Bhide, P.G., Young, A.B., Penney, J., Vonsattel, J.P., Aronin, N., and DiFiglia, M. (1997). Huntingtin localization in brains of normal and Huntington's disease patients. Ann Neurol *42*, 604-612.

Scherzinger, E., Lurz, R., Turmaine, M., Mangiarini, L., Hollenbach, B., Hasenbank, R., Bates, G.P., Davies, S.W., Lehrach, H., and Wanker, E.E. (1997). Huntingtin-encoded polyglutamine expansions form amyloid-like protein aggregates in vitro and in vivo. Cell *90*, 549-558.

Schmidt, E.E., Bondareva, A.A., Radke, J.R., and Capecchi, M.R. (2003). Fundamental cellular processes do not require vertebrate-specific sequences within the TATA-binding protein. J Biol Chem *278*, 6168-6174.

Schrenk, K., Kapfhammer, J.P., and Metzger, F. (2002). Altered dendritic development of cerebellar Purkinje cells in slice cultures from protein kinase Cgamma-deficient mice. Neuroscience *110*, 675-689.

Serizawa, H., Makela, T.P., Conaway, J.W., Conaway, R.C., Weinberg, R.A., and Young, R.A. (1995). Association of Cdk-activating kinase subunits with transcription factor TFIIH. Nature *374*, 280-282.

Shah, A.G., Friedman, M.J., Huang, S., Roberts, M., Li, X.J., and Li, S. (2009). Transcriptional dysregulation of TrkA associates with neurodegeneration in spinocerebellar ataxia type 17. Hum Mol Genet *18*, 4141-4152.

Shridhar, R., Shridhar, V., Rivard, S., Siegfried, J.M., Pietraszkiewicz, H., Ensley, J., Pauley, R., Grignon, D., Sakr, W., Miller, O.J.*, et al.* (1996a). Mutations in the arginine-rich protein gene, in lung, breast, and prostate cancers, and in squamous cell carcinoma of the head and neck. Cancer Res *56*, 5576-5578.

Shridhar, V., Rivard, S., Shridhar, R., Mullins, C., Bostick, L., Sakr, W., Grignon, D., Miller, O.J., and Smith, D.I. (1996b). A gene from human chromosomal band 3p21.1 encodes a highly conserved arginine-rich protein and is mutated in renal cell carcinomas. Oncogene *12*, 1931-1939.

Shridhar, V., Rivard, S., Wang, X., Shridhar, R., Paisley, C., Mullins, C., Beirnat, L., Dugan, M., Sarkar, F., Miller, O.J.*, et al.* (1997). Mutations in the arginine-rich protein gene (ARP) in pancreatic cancer. Oncogene *14*, 2213-2216.

Shuvaev, A.N., Horiuchi, H., Seki, T., Goenawan, H., Irie, T., Iizuka, A., Sakai, N., and Hirai, H. (2011). Mutant PKCgamma in spinocerebellar ataxia type 14 disrupts synapse elimination and long-term depression in Purkinje cells in vivo. J Neurosci *31*, 14324-14334.

Skinner, P.J., Vierra-Green, C.A., Clark, H.B., Zoghbi, H.Y., and Orr, H.T. (2001). Altered trafficking of membrane proteins in purkinje cells of SCA1 transgenic mice. Am J Pathol *159*, 905-913.

Song, W., Chen, J., Petrilli, A., Liot, G., Klinglmayr, E., Zhou, Y., Poquiz, P., Tjong, J., Pouladi, M.A., Hayden, M.R.*, et al.* (2011). Mutant huntingtin binds the mitochondrial fission GTPase dynamin-related protein-1 and increases its enzymatic activity. Nat Med *17*, 377-382.

Stenoien, D.L., Cummings, C.J., Adams, H.P., Mancini, M.G., Patel, K., DeMartino, G.N., Marcelli, M., Weigel, N.L., and Mancini, M.A. (1999). Polyglutamine-expanded androgen receptors form aggregates that sequester heat shock proteins, proteasome components and SRC-1, and are suppressed by the HDJ-2 chaperone. Hum Mol Genet *8*, 731-741.

Stevanin, G., and Brice, A. (2008). Spinocerebellar ataxia 17 (SCA17) and Huntington's disease-like 4 (HDL4). Cerebellum *7*, 170-178.

Suzuki, Y., Tsunoda, T., Sese, J., Taira, H., Mizushima-Sugano, J., Hata, H., Ota, T., Isogai, T., Tanaka, T., Nakamura, Y.*, et al.* (2001). Identification and characterization of the potential promoter regions of 1031 kinds of human genes. Genome Res *11*, 677-684.

Takahashi, M., Ishikawa, K., Sato, N., Obayashi, M., Niimi, Y., Ishiguro, T., Yamada, M., Toyoshima, Y., Takahashi, H., Kato, T.*, et al.* (2012). Reduced brain-derived neurotrophic

factor (BDNF) mRNA expression and presence of BDNF-immunoreactive granules in the spinocerebellar ataxia type 6 (SCA6) cerebellum. Neuropathology *32*, 595-603.

Takahashi, T., Kikuchi, S., Katada, S., Nagai, Y., Nishizawa, M., and Onodera, O. (2008). Soluble polyglutamine oligomers formed prior to inclusion body formation are cytotoxic. Hum Mol Genet *17*, 345-356.

Tanaka, C., and Nishizuka, Y. (1994). The protein kinase C family for neuronal signaling. Annu Rev Neurosci *17*, 551-567.

Tanaka, H., Shimada, Y., Harada, H., Shinoda, M., Hatooka, S., Imamura, M., and Ishizaki, K. (2000). Polymorphic variation of the ARP gene on 3p21 in Japanese esophageal cancer patients. Oncol Rep *7*, 591-593.

Tasset, I., Sanchez-Lopez, F., Aguera, E., Fernandez-Bolanos, R., Sanchez, F.M., Cruz-Guerrero, A., Gascon-Luna, F., and Tunez, I. (2012). NGF and nitrosative stress in patients with Huntington's disease. J Neurol Sci *315*, 133-136.

Thomanetz, V., Angliker, N., Cloetta, D., Lustenberger, R.M., Schweighauser, M., Oliveri, F., Suzuki, N., and Ruegg, M.A. (2013). Ablation of the mTORC2 component rictor in brain or Purkinje cells affects size and neuron morphology. J Cell Biol *201*, 293-308.

Thompson, L.M., Aiken, C.T., Kaltenbach, L.S., Agrawal, N., Illes, K., Khoshnan, A., Martinez-Vincente, M., Arrasate, M., O'Rourke, J.G., Khashwji, H.*, et al.* (2009). IKK phosphorylates Huntingtin and targets it for degradation by the proteasome and lysosome. J Cell Biol *187*, 1083-1099.

Thulasiraman, V., and Matts, R.L. (1998). Luciferase renaturation assays of chaperones and chaperone antagonists. Methods Mol Biol *102*, 129-141.

Toyoshima, Y., Yamada, M., Onodera, O., Shimohata, M., Inenaga, C., Fujita, N., Morita, M., Tsuji, S., and Takahashi, H. (2004). SCA17 homozygote showing Huntington's disease-like phenotype. Ann Neurol *55*, 281-286.

Tsuji, S. (2004). Spinocerebellar ataxia type 17: latest member of polyglutamine disease group highlights unanswered questions. Arch Neurol *61*, 183-184.

Tydlacka, S., Wang, C.E., Wang, X., Li, S., and Li, X.J. (2008). Differential activities of the ubiquitin-proteasome system in neurons versus glia may account for the preferential accumulation of misfolded proteins in neurons. J Neurosci *28*, 13285-13295.

Vacher, C., Garcia-Oroz, L., and Rubinsztein, D.C. (2005). Overexpression of yeast hsp104 reduces polyglutamine aggregation and prolongs survival of a transgenic mouse model of Huntington's disease. Hum Mol Genet *14*, 3425-3433.

Vonsattel, J.P., Myers, R.H., Stevens, T.J., Ferrante, R.J., Bird, E.D., and Richardson, E.P., Jr. (1985). Neuropathological classification of Huntington's disease. J Neuropathol Exp Neurol *44*, 559-577.

Voutilainen, M.H., Back, S., Porsti, E., Toppinen, L., Lindgren, L., Lindholm, P., Peranen, J., Saarma, M., and Tuominen, R.K. (2009). Mesencephalic astrocyte-derived neurotrophic factor is neurorestorative in rat model of Parkinson's disease. J Neurosci *29*, 9651-9659.

Wang, H.L., Yeh, T.H., Chou, A.H., Kuo, Y.L., Luo, L.J., He, C.Y., Huang, P.C., and Li, A.H. (2006). Polyglutamine-expanded ataxin-7 activates mitochondrial apoptotic pathway of cerebellar neurons by upregulating Bax and downregulating Bcl-x(L). Cell Signal *18*, 541-552.

Wang, J., Wang, C.E., Orr, A., Tydlacka, S., Li, S.H., and Li, X.J. (2008). Impaired ubiquitin-proteasome system activity in the synapses of Huntington's disease mice. J Cell Biol *180*, 1177-1189.

Wexler, N.S., Lorimer, J., Porter, J., Gomez, F., Moskowitz, C., Shackell, E., Marder, K., Penchaszadeh, G., Roberts, S.A., Gayan, J.*, et al.* (2004). Venezuelan kindreds reveal that genetic and environmental factors modulate Huntington's disease age of onset. Proc Natl Acad Sci U S A *101*, 3498-3503.

Wu, Y.R., Lin, H.Y., Chen, C.M., Gwinn-Hardy, K., Ro, L.S., Wang, Y.C., Li, S.H., Hwang, J.C., Fang, K., Hsieh-Li, H.M.*, et al.* (2004). Genetic testing in spinocerebellar ataxia in Taiwan: expansions of trinucleotide repeats in SCA8 and SCA17 are associated with typical Parkinson's disease. Clin Genet *65*, 209-214.

Wyttenbach, A., Carmichael, J., Swartz, J., Furlong, R.A., Narain, Y., Rankin, J., and Rubinsztein, D.C. (2000). Effects of heat shock, heat shock protein 40 (HDJ-2), and proteasome inhibition on protein aggregation in cellular models of Huntington's disease. Proc Natl Acad Sci U S A *97*, 2898-2903.

Yoshida, H., Matsui, T., Yamamoto, A., Okada, T., and Mori, K. (2001). XBP1 mRNA is induced by ATF6 and spliced by IRE1 in response to ER stress to produce a highly active transcription factor. Cell *107*, 881-891.

Yu, Y.C., Kuo, C.L., Cheng, W.L., Liu, C.S., and Hsieh, M. (2009). Decreased antioxidant enzyme activity and increased mitochondrial DNA damage in cellular models of Machado-Joseph disease. J Neurosci Res *87*, 1884-1891.

Zeiner, M., Niyaz, Y., and Gehring, U. (1999). The hsp70-associating protein Hap46 binds to DNA and stimulates transcription. Proc Natl Acad Sci U S A *96*, 10194-10199.

Zhang, Y., Li, M., Drozda, M., Chen, M., Ren, S., Mejia Sanchez, R.O., Leavitt, B.R., Cattaneo, E., Ferrante, R.J., Hayden, M.R.*, et al.* (2003). Depletion of wild-type huntingtin in mouse models of neurologic diseases. J Neurochem *87*, 101-106.

Zhou, H., Li, S.H., and Li, X.J. (2001). Chaperone suppression of cellular toxicity of huntingtin is independent of polyglutamine aggregation. J Biol Chem *276*, 48417-48424.

Zuccato, C., and Cattaneo, E. (2007). Role of brain-derived neurotrophic factor in Huntington's disease. Prog Neurobiol *81*, 294-330.

Zuccato, C., Ciammola, A., Rigamonti, D., Leavitt, B.R., Goffredo, D., Conti, L., MacDonald, M.E., Friedlander, R.M., Silani, V., Hayden, M.R.*, et al.* (2001). Loss of huntingtin-mediated BDNF gene transcription in Huntington's disease. Science *293*, 493-498.

Zuccato, C., Tartari, M., Crotti, A., Goffredo, D., Valenza, M., Conti, L., Cataudella, T., Leavitt, B.R., Hayden, M.R., Timmusk, T.*, et al.* (2003). Huntingtin interacts with REST/NRSF to modulate the transcription of NRSE-controlled neuronal genes. Nat Genet *35*, 76-83.